

**DEVELOPMENT OF A GENE-KNOCKDOWN APPROACH
BASED ON siRNA/GOLD NANOPARTICLES FOR BREAST
CANCER THERAPY**

**MEME KANSERİ TEDAVİSİ İÇİN siRNA/ALTIN
NANOPARTİKÜL BAZLI GEN SUSTURMA YAKLAŞIMININ
GELİŞTİRİLMESİ**

REZA SHAHBAZI

PROF. DR. KEZBAN ULUBAYRAM
Supervisor

Submitted to Graduate School of Science and Engineering of Hacettepe University
as a Partial Fulfillment to the Requirements
for the Award of the Degree of Doctor of Philosophy
in Nanotechnology and Nanomedicine

2017

This work named “**Development of a Gene-Knockdown Approach Based on siRNA/Gold Nanoparticles for Breast Cancer Therapy**” by **REZA SHAHBAZI** has been approved as a thesis for the Degree of **DOCTOR OF PHILOSOPHY IN NANOTECHNOLOGY AND NANOMEDICINE** by the below mentioned Examining Committee Members.

Prof. Dr. Çetin KOCAEFE
Head

Prof. Dr. Kezban ULUBAYRAM
Supervisor

Assoc. Prof. Dr. Mustafa TÜRK
Member

Assoc. Prof. Dr. Pınar Yılıör HURİ
Member

Assoc. Prof. Dr. Eda Ayşe AKSOY
Member

This thesis has been approved as a thesis for the Degree of **DOCTOR OF PHILOSOPHY IN NANOTECHNOLOGY AND NANOMEDICINE** by Board of Directors of the Institute for Graduate School of Science and Engineering.

Prof. Dr. Menemşe GÜMÜŞDERELİOĞLU
Director of the Institute of
Graduate School of Science and Engineering

YAYINLAMA VE FİKRİ MÜLKİYET HAKLARI BEYANI

Enstitü tarafından onaylanan lisansüstü tezimin/raporumun tamamını veya herhangi bir kısmını, basılı (kağıt) ve elektronik formatta arşivleme ve aşağıda verilen koşullarla kullanıma açma iznini Hacettepe üniversitesine verdiğimi bildiririm. Bu izinle Üniversiteye verilen kullanım hakları dışındaki tüm fikri mülkiyet haklarım bende kalacak, tezimin tamamının ya da bir bölümünün gelecekteki çalışmalarda (makale, kitap, lisans ve patent vb.) kullanım hakları bana ait olacaktır.

Tezin kendi orijinal çalışmam olduğunu, başkalarının haklarını ihlal etmediğimi ve tezimin tek yetkili sahibi olduğumu beyan ve taahhüt ederim. Tezimde yer alan telif hakkı bulunan ve sahiplerinden yazılı izin alınarak kullanması zorunlu metinlerin yazılı izin alarak kullandığımı ve istenildiğinde suretlerini Üniversiteye teslim etmeyi taahhüt ederim.

- Tezimin/Raporumun tamamı dünya çapında erişime açılabilir ve bir kısmı veya tamamının fotokopisi alınabilir.

(Bu seçenekle teziniz arama motorlarında indekslenebilecek, daha sonra tezinizin erişim statüsünün değiştirilmesini talep etmeniz ve kütüphane bu talebinizi yerine getirirse bile, tezinin arama motorlarının önbelleklerinde kalmaya devam edebilecektir.)

- Tezimin/Raporumun 02/02/2020 tarihine kadar erişime açılmasını ve fotokopi alınmasını (İç Kapak, Özet, İçindekiler ve Kaynakça hariç) istemiyorum.

(Bu sürenin sonunda uzatma için başvuruda bulunmadığım takdirde, tezimin/raporumun tamamı her yerden erişime açılabilir, kaynak gösterilmek şartıyla bir kısmı ve ya tamamının fotokopisi alınabilir)

- Tezimin/Raporumun tarihine kadar erişime açılmasını istemiyorum, ancak kaynak gösterilmek şartıyla bir kısmı veya tamamının fotokopisinin alınmasını onaylıyorum.

- Serbest Seçenek/Yazarın Seçimi

08 / 02 / 2017

(İmza)

Reza Shahbazi

*Dedicated to My Brilliant and
Outrageously Loving and Supportive
Wife, Safa*

ETHICS

In this thesis study, prepared in accordance with the spelling rules of Institute of Graduate Studies in Science of Hacettepe University,

I declare that

- all the information and documents have been obtained in the base of the academic rules
- all audio-visual and written information and results have been presented according to the rules of scientific ethics
- in case of using others works, related studies have been cited in accordance with the scientific standards
- all cited studies have been fully referenced
- I did not do any distortion in the data set
- and any part of this thesis has not been presented as another thesis study at this or any other university.

02/02/2017



REZA SHAHBAZI

ABSTRACT

DEVELOPMENT OF A GENE-KNOCKDOWN APPROACH BASED ON siRNA/GOLD NANOPARTICLES FOR BREAST CANCER THERAPY

Reza Shahbazi

Doctor of Philosophy, Department of Nanotechnology and Nanomedicine

Supervisor: Prof. Dr. Kezban Ulubayram

Co-supervisor: Assoc. Prof. Dr. Bülent Özpolat

February 2017, 122 pages

Breast cancer is considered to be one of the leading causes of death in the 21st century and has claimed the lives of many people. As one of its subtypes, triple-negative breast cancer (TNBC) is a devastating disease, owing to the aggressive course, early metastasis, drug resistance, and poor clinical outcome and patient survival. Recently, different gene therapy approaches such as the use of siRNAs have brought hope for the treatment of TNBC. Although siRNA-based therapeutics offer tremendous potential as targeted therapies, their low transfection efficiency, and *in vivo* degradation by serum endo and exo-nucleases have prevented their delivery into tumors and made that an important obstacle for their translation into the clinic. So, the development of safe and effective delivery systems with robust target knockdown is of paramount importance. To address this problem, in this thesis it was aimed to develop a novel gold nanoparticle/siRNA based nanotherapeutic for gene knockdown approach in triple negative breast cancer.

In the first and second sections of this thesis, it was aimed to develop gold nanoparticle based delivery vehicles and evaluate their cellular biodistribution. In this regard, highly stable and monodisperse polyethylenimine (PEI) functionalized gold nanoparticles were synthesized by a new method of surface modification. For the first time in literature, it was found that PEI functionalized gold nanoparticles in

the size range of 45-82 nm, can enter to the cell nucleolus even in postmitotic dorsal root ganglion (DRG) neurons which are known to be very difficult cell types to transfect. It was shown that PEI functionalization increased the uptake rate of gold nanoparticles and delayed the fast excretion rate. Also, it was observed that PEI functionalization increased the emission signal intensity of gold nanoparticles. With a great potential for theranostic applications, the cellular biodistribution of nanoparticles was clearly visualized under both confocal and two-photon microscopes.

In the third section, it was aimed to develop a siRNA therapeutic for TNBC therapy based on PEI-functionalized gold nanoparticles. With this purpose, eukaryotic elongation factor 2 kinase (eEF-2K) was chosen as the therapeutic target and conjugated with nanoparticles. Prepared siRNA therapeutic was highly monodisperse (PDI of 0.1) and stable. It was shown that this siRNA therapeutic was highly effective for eEF-2K gene down-regulation in vitro and in vivo and showed remarkable antitumor efficacy that was associated with eEF-2K knockdown, inhibition of Src and MAPK-ERK signaling pathways in a TNBC orthotopic tumor model. A significant tumor inhibition (~90%) was achieved by only one intravenous injection of siRNA therapeutic per week at a relatively low dose of 8 µg/mouse (0.3 mg/kg), which is below the limit of any potential toxicity. Finally, siRNA therapeutic conjugated with doxorubicin was developed for combinational therapy approach which decreased the cell viability significantly in compare to sole doxorubicin chemotherapeutic drug.

In conclusion, a potent theranostic gold nanoparticle based gene delivery vehicle was developed and used in the preparation of eEF-2K siRNA based therapeutics. It was concluded that prepared eEF-2K siRNA therapeutics are promising for TNBC treatment and imaging.

Keywords: PEI-functionalized gold nanoparticles, nucleolus, eEF-2K, siRNA, nanotherapeutics, triple-negative breast cancer, theranostics

ÖZET

MEME KANSERİ TEDAVİSİ İÇİN siRNA/ALTIN NANOPARTİKÜL BAZLI GEN SUSTURMA YAKLAŞIMININ GELİŞTİRİLMESİ

Reza Shahbazi

Doktora, Nanoteknoloji ve Nanotıp Bölümü

Tez Danışmanı: Prof. Dr. Kezban Ulubayram

Yardımcı Danışman: Doç. Dr. Bülent Özpolat

Şubat 2017, 122 sayfa

Meme kanseri, 21. yüzyılda önde gelen ölüm nedenlerinden biri olarak kabul edilmekte olup birçok kişinin yaşamını yitirmesine neden olmaktadır. Meme kanserinin alt tiplerinden biri olarak bilinen üçlü negatif meme kanseri (ÜNMK), agresif seyir, erken metastaz, ilaç direnci, zayıf klinik sonuç ve düşük hayatta kalma oranı nedeniyle yıkıcı bir hastalık olarak bilinmektedir. Son zamanlarda, siRNA'ların kullanımı gibi farklı gen tedavisi yaklaşımları ÜNMK'nın tedavisi için umut vaat etmektedir. siRNA temelli terapötikler hedefe yönelik terapiler olarak büyük bir potansiyel sunmakla birlikte düşük transfeksiyon verimliliği ve *in vivo* şartlarında serum endo ve ekso-nükleazlar tarafından bozunmaları, siRNA'ların tümöre taşınmasını önlemekte ve kliniğe translasyonunda büyük engel teşkil etmektedir. Bu nedenle güçlü hedef gen susturmasına sahip olan güvenli ve etkin taşıma sistemlerinin geliştirilmesi büyük önem taşımaktadır. Bu sorunu çözmek için, bu tez kapsamında üçlü negatif meme kanserinde gen susturma yaklaşımı için yeni bir siRNA/altın nanopartikül bazlı nanoterapötiklerin geliştirilmesi amaçlanmıştır.

Tezin, birinci ve ikinci bölümlerinde altın nanopartikül bazlı gen taşıma araçlarının geliştirilmesi ve hücrel dağılımlarının değerlendirilmesi hedeflenmiştir. Bu amaçla son derece kararlı ve monodispers polietilenimin (PEI) ile fonksiyonlaştırılmış altın nanopartiküller yeni bir yüzey modifikasyonu yöntemi ile sentezlenmiştir. Literatürde bir ilk olarak, 45-82 nm boyut aralığında PEI ile fonksiyonlaştırılmış altın

nanopartiküllerin, transfeksiyonu çok zor olduğu bilinen postmitotik dorsal kök gangliyon (DKG) nöronlarında hücre çekirdeğine girdiği açıklanmıştır. Ayrıca, PEI ile fonksiyonlaştırmanın altın nanopartiküllerin hücre alımını arttırdığı ve atılım hızını geciktirdiği gösterilmiştir. Ayrıca, PEI ile fonksiyonlaştırılan altın nanopartiküllerin emisyon sinyal yoğunluğunu artırdığı izlenmiştir. Teranostik uygulamalar için büyük potansiyele sahip olan bu nanopartiküllerin hücresel dağılımı hem konfokal hem de çift fotonlu mikroskoplar altında açıkça görüntülenmiştir.

Üçüncü bölümde, ÜNМК tedavisi için PEI ile fonksiyonlaştırılmış altın nanopartikül ile siRNA terapötiklerin geliştirilmesi amaçlanmıştır. Bu amaçla, ökaryotik uzama faktörü 2 kinaz (eEF-2K) terapötik hedef olarak seçilmiş ve altın nanopartiküllerle konjuge edilmiştir. Hazırlanan siRNA terapötiklerin oldukça monodispers (PDI=0,1) ve kararlı olduğu izlenmiştir. Bu siRNA terapötiklerin, *in vitro* ve *in vivo* şartlarda gen susturma için son derece etkili olduğu ve ÜNМК ortotopik tümör modelinde eEF-2K'yı susturma, Src inhibisyonu ve MAPK-ERK sinyal yollarıyla ilişkili olarak dikkate değer antitümör etkinliğine sahip olduğu gösterilmiştir. Haftalık tek bir intravenöz enjeksiyonuyla fare başına 8 mikrogram (0,3 mg/kg) olan düşük bir dozda anlamlı tümör inhibisyonu (~%90) sağlanmış olup, bu doz potansiyel toksisite dozunun altındadır. Son olarak doksorubisin ile konjuge edilmiş siRNA terapötikler kombinasyon tedavi yaklaşımı için geliştirilmiş ve bunların tek başına doxorubisin ile karşılaştırıldığında hücre canlılığını önemli ölçüde azalttığı gözlenmiştir.

Sonuç olarak, etkili teranostik altın nanopartikül bazlı gen taşıma aracı geliştirilerek, eEF-2K siRNA terapötiklerin hazırlanmasında kullanılmıştır. Hazırlanan eEF-2K siRNA terapötiklerin ÜNМК tedavisinde ve görüntülemeye umut verici olduğu sonucuna varılmıştır.

Anahtar Kelimeler: PEI ile fonksiyonlaştırılmış altın nanopartiküller, çekirdekçik, eEF-2K, siRNA, nanoterapötikler, üçlü negatif meme kanseri, teranostik

ACKNOWLEDGEMENTS

First and foremost, I would like to express my special gratitude to my supervisor Prof. Dr. Kezban Ulubayram for her continuous support during my Ph.D. study and related research and also for her contributions of time, immense knowledge, and funding.

I would also like to express my sincere gratitude to my co-supervisor Assoc. Prof. Dr. Bülent Özpolat for all his invaluable guidance and support specially during the in vivo studies. Without his precious support, it would not be possible to conduct this research.

For this dissertation, I would like to thank the rest of my thesis committee: Assoc. Prof. Dr. Mustafa Türk, and Assoc. Prof. Dr. Eda Ayşe Aksoy for their insightful comments and encouragement.

I gratefully acknowledge The Scientific and Technological Research Council of Turkey (TUBITAK) and BİDEB for 2215 “Graduate Scholarship Programme for International Students”. This funding had a great impact on doing all my research during Ph.D.

I am very much thankful to Assoc. Prof. Dr. Hakan Eroğlu and Assoc. Prof. Dr. İpek Eroğlu for being so helpful and supportive.

I am deeply grateful to Özlem Yurtalan, our lab’s secretary, for all her support and motivation and specially the joy which she brought to our research environment.

My time at Hacettepe University was made delightful in large part because of my precious friends that became a part of my life. I am grateful (In no particular order) to Semih Çalamak, Şükrü Öztürk, İlyas Özçiçek, Merve Gültekinoglu, Gülce Taşkor, Minela Arslan, Halime Serinçay, Betül Süyümbike Yağcı, Gülseher Manap, Hacer Aksel.

Most of all, I would like to thank my loving, supportive, encouraging, and patient wife Safa, whose faithful support is so appreciated. Lastly, I would like to thank my family for all their love and encouragement. For my parents who raised me with a love of science and supported me in all my pursuits. Thank you.

TABLE OF CONTENTS

ABSTRACT	i
ÖZET	iii
ACKNOWLEDGEMENTS	v
TABLE OF CONTENTS	vi
LIST OF TABLES	xi
LIST OF FIGURES	xii
ABBREVIATIONS	xvi
1. INTRODUCTION	1
1.1. General Information	1
1.2. Breast Cancer Statistics and Its Subtypes	2
1.2.1. Luminal Tumors	3
1.2.2. HER2 Over-Expression Tumors.....	3
1.2.3. Basal Tumors.....	4
1.3. Triple Negative Breast Cancer and Its Biology.....	4
1.3.1. Approved Strategies for Triple Negative Breast Cancer Therapy	5
1.3.2. Elongation Factor 2 Kinase as a Novel Target for TNBC Therapy.....	6
1.4. Oligonucleotide-Based Therapeutics in Gene Therapy.....	6
1.4.1. Morpholino Oligonucleotides.....	7
1.4.2. siRNAs.....	7
1.4.3. miRNAs.....	8
1.4.4. shRNAs.....	8
1.4.5. Hurdles in Front of Oligonucleotide-Based Cancer Therapeutics	9
1.5. Viral and Non-Viral Gene Delivery Vehicles.....	9

1.5.1. Viral Delivery Vehicles	9
1.5.1.1. Retroviral vectors.....	9
1.5.1.2. Adenoviral vectors	10
1.5.1.3. Adeno-associated vectors	10
1.5.1.4. Helper-dependent adenoviral vector.....	10
1.5.1.5. Hybrid adenoviral vectors	11
1.5.1.6. Herpes simplex virus	11
1.5.1.7. Lentiviruses	11
1.5.1.8. Poxvirus vectors	12
1.5.1.9. Epstein–Barr virus	12
1.5.2. Non-Viral Delivery Vehicles	12
1.5.2.1. Naked DNA.....	12
1.5.2.2. DNA particle bombardment by gene gun.....	12
1.5.2.3. Electroporation	12
1.5.2.4. Hydrodynamic.....	13
1.5.2.5. Ultrasound	13
1.5.2.6. Magnetofection	13
1.5.2.7. Cationic liposomes	13
1.5.2.8. Cationic polymers	13
1.5.2.9. Lipid–polymer systems.....	14
1.6. Nanoparticles as Robust Gene Delivery Vehicles	14
1.7. Gold Nanoparticles for the Delivery of Oligonucleotide Based Therapeutics	15
1.8. Review of the Published Literature in Cancer Gene Therapy	17
1.9. Aim of the Thesis	18
2. MATERIALS AND METHODS.....	20

2.1. Materials	20
2.2. Methods	22
2.2.1. Synthesis of Gold Nanoparticles and PEI Modification	22
2.2.1.1. Synthesis of seed gold nanoparticles	22
2.2.1.2. Growth of seed nanoparticles by seeding-growth method	23
2.2.1.3. Surface modification of synthesized gold nanoparticles	23
2.2.2. Cellular Biodistribution of Gold Nanoparticles	24
2.2.2.1. Isolation of DRG sensory neurons and cell culture studies.....	24
2.2.2.2. Determination of the cellular uptake by ICP-MS analysis	25
2.2.2.3. Imaging the cellular biodistribution of gold nanoparticles by confocal microscope	25
2.2.2.4. Imaging of the nanoparticle incubated cells by two-photon microscope	25
2.2.2.5. Toxicity studies of gold nanoparticles	26
2.2.2.6. Immunocytochemical studies.....	26
2.2.3. <i>In Vitro</i> and <i>In Vivo</i> Gene Delivery Studies	27
2.2.3.1. Determination of optimal siRNA conjugation ratio	27
2.2.3.2. siRNA design and <i>in vitro</i> gene-knockdown studies	27
2.2.3.3. Development of orthotopic xenograft tumor model in mice.....	28
2.2.3.4. Injection of prepared nano-formulation and tumor analysis	28
2.2.4. Development of Doxorubicin and eEF-2K siRNA Conjugated Gold Nanoparticles for Combinational Therapy Approach	29
2.2.4.1. Preparation of doxorubicin and eEF-2K siRNA conjugated gold nanoparticles	29
2.2.4.2. In vitro evaluation of the doxorubicin conjugated gold nanoparticles in MDA-MB-231 cells.....	29

2.2.4.3. In vitro evaluation of the doxorubicin and eEF-2K siRNA conjugated gold nanoparticles in MDA-MB-231 and MDA-MB-436 cells	30
2.2.5. Statistical Analysis	30
3. RESULTS AND DISCUSSION.....	31
3.1. Synthesis of Gold Nanoparticles	31
3.1.1. Determining the Optimal Synthesis Method.....	31
3.2. Surface Modification of Gold Nanoparticles with Polyethylenimine.....	34
3.2.1. Synthesis of Citrate Capped Gold Nanoparticles in Different Size Ranges	34
3.2.2. Polyethylenimine Modification of Gold Nanoparticles in Different Size Ranges	37
3.3. Cellular Biodistribution and Imaging Potential of Gold Nanoparticles.....	40
3.3.1. Effect of Gold Nanoparticles on Cell Morphology.....	40
3.3.2. Effect of Gold Nanoparticles on Cell Viability	42
3.3.3. Effect of Gold Nanoparticles on Neural Cell Skeleton.....	45
3.3.4. Cellular Uptake of Gold nanoparticles.....	47
3.3.5. Imaging the Cellular Biodistribution of Gold Nanoparticles by Confocal Microscope	48
3.3.6. Nucleolar Localization of PEI-Functionalized Gold Nanoparticles	52
3.3.7. Imaging Gold Nanoparticle Incubated Cells by IR Irradiation.....	55
3.3.8. Potential Mechanism for Nucleolar Localization	58
3.4. Gene-Knockdown Studies by siRNA/Gold Nanotherapeutics for Triple Negative Breast Cancer Therapy.....	59
3.4.1. Properties of PEI-Functionalized Gold Nanoparticles as eEF-2K siRNA Carriers	59
3.4.2. Conjugation of eEF-2K siRNA to PEI-Functionalized Gold Nanoparticles	62
3.4.3. <i>In Vitro</i> Down-Regulation of eEF-2K by AuNP-PEI/eEF-2K siRNA.....	67

3.4.4. Effective <i>In Vivo</i> Target Knockdown and Growth Inhibition in a TNBC Tumor Model.....	68
3.5. Doxorubicin Conjugated siRNA Therapeutics for Combinational Therapy .	71
3.5.1. Characterization of Doxorubicin and eEF-2K siRNA Conjugated Gold Nanoparticles.....	71
3.5.2. Effect of Doxorubicin Conjugated Gold Nanoparticles on the Cell Viability of MDA-MB-231 Cells.....	74
3.5.3. Effect of Combinational Therapy with Doxorubicin and eEF-2K siRNA Conjugated Gold Nanoparticles on the Cell Viability of MDA-MB-231 Cells	75
CONCLUSION	78
REFERENCES.....	80
CURRICULUM VITAE	99
APPENDIX 1	101

LIST OF TABLES

Table 1. Properties of synthesized gold nanoparticle groups.....	34
Table 2. Uptake amounts of gold nanoparticles (%) in DRG neurons.....	47
Table 3. Effect of different AuNP-PEI:siRNA ratios on size, polydispersity index (PDI), and zeta potential values.	66

LIST OF FIGURES

Figure 1. Intrinsic and molecular subtypes of breast cancer [8].....	3
Figure 2. Oligonucleotide delivery by nanoparticles and active or passive targeting [47].	15
Figure 3. Tumor targeting and concomitant imaging “Theranostic Approach” [47].	16
Figure 4. Schematic representation of the aim of the study.....	19
Figure 5. Mechanism of synthesizing gold nanoparticles [129].....	31
Figure 6. Characteristics of synthesized gold nanoparticles. A) Nanoparticles synthesized with conventional Turkevich method. B) Nanoparticles synthesized with modified Turkevich method.	32
Figure 7. Characteristics of synthesized larger gold nanoparticles. A) Nanoparticles synthesized with conventional Turkevich method. B) Nanoparticles synthesized with the seeding-growth method.	33
Figure 8. Characteristics of synthesized gold nanoparticles. A) Size distribution of the nanoparticles showing the shifts in size after PEI modification B) UV-visible spectrum of nanoparticles showing the shifts in the spectrum after PEI modification.	35
Figure 9. Transmission electron microscope (TEM) and scanning electron microscope (SEM) images of gold nanoparticles showing the morphology, size and PEI coating. A) AuNP ₁₉ (Seed gold nanoparticles). B) PEI/AuNP ₂₃ nanoparticles. C) AuNP ₄₅ nanoparticles. D) PEI/AuNP ₄₈ nanoparticles. E) AuNP ₇₆ nanoparticles. F) PEI/AuNP ₈₂ nanoparticles.	36
Figure 10. Seeding-growth and functionalization of gold nanoparticles surface with PEI.	38
Figure 11. Hoffman modulation contrast microscope images of the DRG neurons before and after incubation with different gold nanoparticle groups. Yellow arrows are showing the nanoparticle aggregates.....	41

Figure 12. Cell viability studies showing the effect of gold nanoparticles on cells at different concentrations and time intervals. A) 0.5 µg/mL. B) 5 µg/mL. C) 50 µg/mL. Samples are labelled as; (A) AuNP₁₉, (B) PEI/AuNP₂₃, (C) AuNP₄₅, (D) PEI/AuNP₄₈, (E) AuNP₇₆, (F) PEI/AuNP₈₂. 43

Figure 13. Toxicity of citrate capped and PEI-functionalized gold nanoparticles on L929 fibroblast cells. A) Cell viability by the treatment with 51 nm citrate capped gold nanoparticles. B) Cell viability for 54 nm PEI-functionalized gold nanoparticles. DMSO was used as a positive control for cell viability..... 44

Figure 14. Effect of citrate capped and PEI-functionalized gold nanoparticles on DRG neural cell skeleton. A1-A3) Control. B1-B3) AuNP₁₉ nanoparticles. C1-C3) PEI/AuNP₂₃ nanoparticles. D1-D3) AuNP₄₅ nanoparticles. E1-E3) PEI/AuNP₄₈ nanoparticles. F1-F3) AuNP₇₆ nanoparticles. G1-G3) PEI/AuNP₈₂ nanoparticles. Images were taken by using 40x objective..... 46

Figure 15. Imaging gold nanoparticles incubated cells with laser scanning confocal microscope. (a1, a2) Control. (b1, b2) AuNP₁₉. (c1, c2) PEI/AuNP₂₃. (d1, d2) AuNP₄₅. (e1-e4) PEI/AuNP₄₈. (f1, f2) AuNP₇₆. (g1-g4) PEI/AuNP₈₂. Images in T-PMT mode have a gray background..... 49

Figure 16. Times series mode imaging of the PEI/AuNP₄₈ nanoparticles. Images were taken by using 40x objective and they were taken with 5 min intervals. 51

Figure 17. Nucleolar localization of PEI-functionalized gold nanoparticles. A) Tile scan mode. B) Maximum intensity projection mode. C) Magnified confocal image. 52

Figure 18. Washing and re-incubation of the cells with PEI-functionalized gold nanoparticles. A) DRG cells after 24 h of incubation with PEI/AuNP₄₈ nanoparticles. B) Re-incubation of the cells with PEI/AuNP₄₈ nanoparticles. C) DRG cells after 24 h of incubation with PEI/AuNP₈₂. D) Re-incubation of the cells with PEI/AuNP₈₂ nanoparticles. Excreted nanoparticle aggregates are shown with red arrows. Images were taken by using 40x objective..... 53

Figure 19. Cellular biodistribution of unfunctionalized citrate capped gold nanoparticles and PEI-functionalized gold nanoparticles. 54

Figure 20. Imaging the cells incubated with PEI/AuNP ₈₂ nanoparticles under the two-photon microscope. A1, A2) 3D and maximum intensity projection images (magnification: 20x). B1, B2) 63x magnification. C1, C2) Single cell imaging with two-photon and T-PMT modes (magnification:63x).....	57
Figure 21. Schematic representation of AuNP-PEI and eEF-2K siRNA conjugation.	59
Figure 22. Characterization of synthesized AuNP-PEI nanoparticles. A) Size distribution of synthesized nanoparticles. B) LSPR peak reveals shifts indicating an increase in size and surface modification of AuNP-PEI.....	60
Figure 23. Transmission electron microscope (TEM) and scanning electron microscope (SEM) images of synthesized gold nanoparticles. A, B) TEM images of synthesized seed gold nanoparticles. C) TEM image of AuNPs after seeding-growth step. D) SEM image of PEI-functionalized gold nanoparticles (AuNP-PEI).....	61
Figure 24. Analysis of various AuNP-PEI:siRNA conjugation ratios and stability tests. A) Gel electrophoresis analysis of different AuNP-PEI:eEF-2K siRNA conjugation ratios. B) Stability of various AuNP-PEI:siRNA ratios over 1 h period. C) Re-dispersing of the precipitated nanoparticles by shaking them. Positive control is only siRNA alone without AuNP-PEI nanoparticles. Negative control consists of AuNP-PEI nanoparticles without any siRNA conjugation.	63
Figure 25. UV-visible spectrophotometric analysis of the various AuNP-PEI:siRNA ratios.	64
Figure 26. LSPR peaks of various AuNP-PEI:siRNA ratios.....	64
Figure 27. Size distribution of AuNP-PEI/eEF-2K siRNA nanoparticles at different ratios.	65
Figure 28. Zeta potential values of synthesized nanoparticles and prepared nano-formulations at different ratios.	67
Figure 29. AuNP-PEI/eEF-2K siRNA nano-formulation effectively downregulates eEF-2K in MDA-MB-231 TNBC cells and inhibits phosphorylation of its downstream target EF2 <i>in vitro</i>	68

Figure 30. *In vivo* gene knockdown studies by systemically (intravenously, n=5) injected AuNP-PEI/eEF-2K siRNA nano-formulation shows effective eEF-2K downregulation along with the inhibition of EF2 phosphorylation. 69

Figure 31. Inhibition of tumor growth was observed during the 4 weeks of intravenous treatment with AuNP-PEI/eEF-2K siRNA nano-formulation (once-a-week injection with 8 µg of siRNA per mouse, n=5) in the MDA-MB-231 TNBC orthotopic xenograft tumor model. A and B indicate treatment with AuNP-PEI/control-siRNA and AuNP-PEI/eEF-2K-siRNA, respectively. 70

Figure 32. Preparation steps of the doxorubicin and eEF-2K siRNA conjugated gold nanoparticles (AuNP-DOX-eEF-2K siRNA) as combinational nanotherapeutics.. 72

Figure 33. Size distribution graph of; A) citrate capped gold nanoparticles and B) Doxorubicin and eEF-2K siRNA conjugated gold nanoparticles..... 73

Figure 34. Cell viability assay showing the concentration dependent decrease of the cell viability in MDA-MB-231 cells after doxorubicin treatment. The IC₅₀ value of doxorubicin was found to be 0.2 µM after 48 h..... 74

Figure 35. Cell viability assay showing the effect of doxorubicin conjugated gold nanoparticles (AuNP-PEG-PEI-DOX) and unconjugated doxorubicin (DOX) on MDA-MB-231 cells after 72 h. 75

Figure 36. MTS assay comparing the effect of combinational nanotherapeutics (AuNP-DOX-eEF-2K siRNA) and doxorubicin conjugated gold nanoparticles (AuNP-DOX) on; A) MDA-MB-436 cells, and B) MDA-MB-231 cells..... 77

ABBREVIATIONS

Abbreviations

ER	Estrogen
PR	Progesterone
TNBC	Triple Negative Breast Cancer
CAV	Caveolin
PARP	Poly (ADP-Ribose) Polymerase
BLBC	Basal-Like Breast Cancer
eEF-2K	Elongation Factor 2 Kinase
RISC	RNA-Inducing Silencing Complex
RES	Reticuloendothelial System
EPR	Enhanced Permeability and Retention
AAV	Adeno-Associated Vectors
HdAd	Helper-Dependent Adenoviral Vectors
HSV	Herpes Simplex Virus
DISC	Disabled Infectious Single Copy
PLL	Poly-L-Lysine
HFV	Human Foamy Virus
MNPs	Magnetic Nanoparticles
CT	Computed Tomography
MUA	11-Mercaptoundecanoic Acid
AuNPs	Gold Nanoparticles
PLK1	Polo-Like Kinase 1
H ₄ AuCl ₄ ·3H ₂ O	Hydrogen Tetrachloroaurate (III) Trihydrate
TEM	Transmission Electron Microscope

SEM	Scanning Electron Microscope
ICP-MS	Inductively Coupled Plasma Mass Spectrometry
PEI	Polyethylenimine
DRG	Dorsal Root Ganglion
LSCM	Laser Scanning Confocal Microscope
DMSO	Dimethyl Sulfoxide
PDI	Polydispersity Index
HAuCl ₄	Chloroauric Acid
NaBH ₄	Sodium Borohydride
ICC	Immunocytochemistry
LSPR	Localized Surface Plasmon Resonance
AuNP-PEI	PEI-Functionalized Gold Nanoparticles
OD	Optical Density
DGCR8	DiGeorge syndrome critical region 8

1. INTRODUCTION

1.1. General Information

Cancer is one of the leading problems of every nation and society that is growing every minute and needs to be addressed before turning into a global threat for the human race. Cancer is known by the uncontrolled growth of the cells and its spread to the nearby tissues and organs. Different factors play a key role in the transformation of healthy cells to rogue cells that can proliferate in an uncontrolled manner and migrate to other tissues and localize. These factors range from tobacco, organisms, unhealthy diet, to internal factors like; genetic mutations, hormonal factors and immune conditions. These factors may act alone or in combination with other factors but something which is very important is that the early signs of being cancer show itself ten or more years after. It should be noticed that it can be prevented in most cases by changing the way of life [1].

Between all the reported cases of cancer, breast cancer is the most frequent reported type of cancer in women and is ranked as the second cause of death in women. It is mostly recognized with painless lumps or masses in the breast but it can show itself with less frequent symptoms such as; irritation, redness and scaliness of the breast skin, swelling, thickening, distortion, sensitivity, nipple deformities, or continuous discharge. Pain is the less frequent symptom but benign types may cause painful breast [1, 2].

Breast cancer is a heterogeneous disease and categorized in different subtypes which will be discussed later on. Taking into account the heterogeneous state of the disease, many factors together determine the progression of the disease. According to the size and spread of the tumor different treatment approaches are chosen which will be discussed in the context. However, with all the breakthroughs made in recent years, breast cancer is still a serious disease threatening the life of women and men especially if not diagnosed early on. In the meantime, triple negative breast cancer which is the main subject of this study is known to be more aggressive than the other types and it is associated with the least favorable survival rate. Therefore,

developing a new therapeutic formulation based on gene knockdown was aimed in this study to achieve a more effective treatment.

1.2. Breast Cancer Statistics and Its Subtypes

According to the published data by American Cancer Society [1] it is estimated that about 246,660 women and 2,600 men will be diagnosed with invasive breast cancer in 2016. It was reported that during the 10-year period from 2003 to 2012 the incidence of breast cancer in white women was stable and increased by 0.3% for black women. It is estimated that 40,890 lives (40,450 women, 440 men) will be lost to breast cancer in 2016 and it is the second cause of death by cancer in women. Because of the improvements in early diagnosis and emergence of new therapies, death rate decreased to 1.9% in white women and 1.4% in black women which in total the death rate declined 36% between the years 1989 to 2012. It is to say that 249,000 lives were saved thanks to the breakthroughs in cancer diagnosis and treatment. These results are heartwarming and show that death by cancer is having a downward trend and with the introduction of new formulations breast cancer could be a history one day.

It is known that breast cancer has different forms that are associated with different histopathological and biological features which respond differently to treatments. Therefore, determining the accurate subtype is very important before making any decision and it is fundamental to prescribe a certain and efficient treatment method [3]. Conventionally, pathological features such as; the grade and size of the tumor, the involvement of lymph nodes along with immunohistochemistry markers like; ER, PR and HER2 have been used to determine a treatment path for breast cancer patients [4]. However, in recent years, gene expression analysis have shown that tumor related molecular factors are more important than anatomical factors in determining a guaranteed therapeutic approach [5].

There are many subtyping studies in the literature that have mentioned different genes and subtyped breast cancer into different groups, but all of the more or less accord with the classification proposed by Sørlie et al. [6-8]. They classified the breast cancer tumors into 5 major classes named; luminal A, luminal B, HER2 over-expression, basal and normal-like tumors (Figure 1).

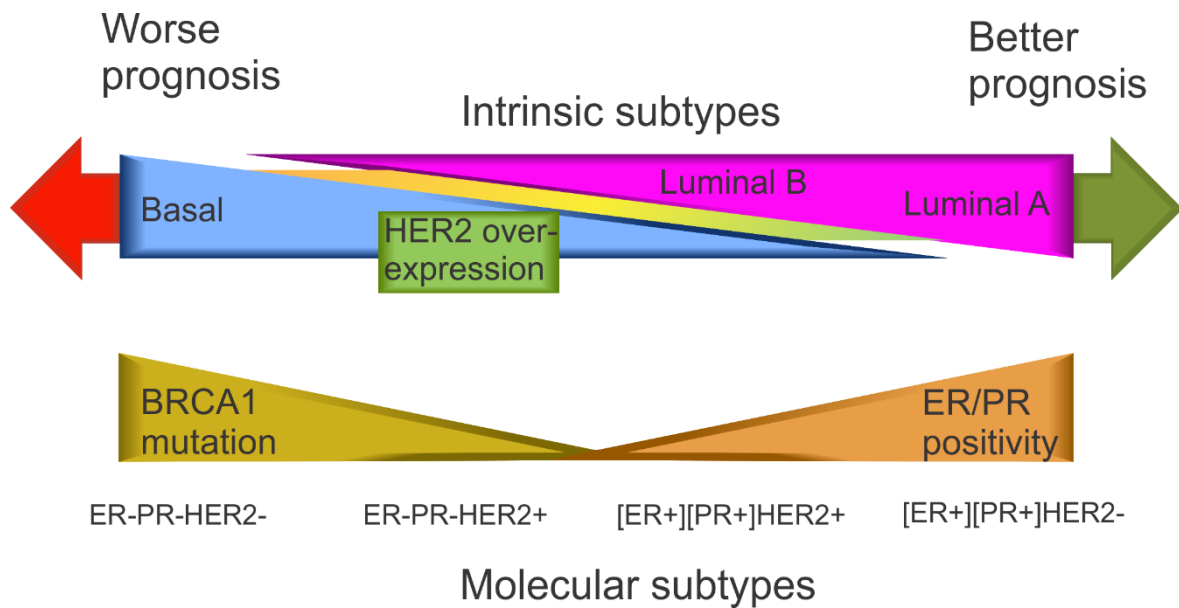


Figure 1. Intrinsic and molecular subtypes of breast cancer [8].

1.2.1. Luminal Tumors

Luminal tumors express hormone receptors and have two subtypes, luminal A and luminal B. Luminal A tumors are associated with the positive expression of estrogen and progesterone (ER+, PR+) and negative expression of HER2 (HER2-). On the other hand, all the markers are positively expressed in luminal B tumors (ER+, PR+, HER2+) [9]. It should be noticed that this classification is not always applicable for all the tumors, for example, HER2 positivity is not valid for all the luminal B subtypes. In compared to luminal B tumors, ER related genes are highly expressed in luminal A tumors and proliferative genes have a low expression [10]. In this respect, most of the breast cancer tumors are luminal A tumors but the grade of the luminal B tumors is higher and they have worst prognosis and high recurrence. Luminal tumors respond better to hormone therapy than conventional chemotherapy [8, 11].

1.2.2. HER2 Over-Expression Tumors

These tumors are characterized by negative expressions of both ER and PR, and positive expression of HER2 (ER-, PR-, HER2+). HER2 over expression tumors are associated with poor prognosis, due to their early relapse. Targeted therapies based on anti-HER2 monoclonal antibody is available for HER2 over expression tumors but not all the tumors respond to the existing targeted therapies and resistance can become an issue [4, 8].

1.2.3. Basal Tumors

Basal tumors are characterized by the negative expressions of all the ER, PR and HER2 markers (ER-, PR-, HER2-). With the negative expression of all the markers, they are called triple negative tumors. They have an expression profile like basal epithelial cells of other parts of the body and normal breast myoepithelial cells [6, 8]. Like HER2 over-expression tumors, triple negative tumors are probable to be of grade 3 tumors [7, 12]. Triple negative tumors account for 60%-90% of the basal tumors and they are very important to be diagnosed early due to their aggressiveness and lack of targeted systemic therapy [13]. High waist to hip ratio, high parity, lack of breast feeding and earlier menarche are among the risk factors for triple negative breast cancer [14].

Triple negative tumors have a high risk of local and regional relapse and lower survival rate. These tumors have a tendency of metastasizing to visceral organs (except bone) and they are not likely to involve lymph nodes [14]. They have a rapid growth rate and size of the basal tumors tend to be larger than the other subtypes with approximately 2 cm in average [15]. Negative status of important markers (ER-, PR-, HER2-) makes conventional chemotherapies the only treatment of choice and poor prognosis of the disease is due to the relatively few treatment options [11].

1.3. Triple Negative Breast Cancer and Its Biology

It should be noticed that only 70% of triple negative breast cancers (TNBCs) are basal like and the remainder have different biological features that are distinct [16]. So, it can be concluded that TNBCs are not single subtyped tumors but they are heterogeneous entities [17]. Together with the negative expression of breast cancer markers (ER-, PR-, HER2-), basal cytokeratins (especially cytokeratin 5, 14 and 17) and the EGFR HER1 which are associated with poor prognosis are positively expressed in TNBC [18, 19]. Also, TNBCs are more probable to express myoepithelial markers, like caveolins (CAV) 1 and 2, c-kit and P-cadherin [20]. On the other hand, they are less probable to express epithelial markers, like E-cadherin [17, 21]. Likewise, Ki67 and TOP2A genes which are associated with proliferation are highly expressed in TNBC. TNBCs contain high cyclin E expression and low cyclin D1 expression [22].

It has been reported that approximately 50% of TNBCs have aberrant p53 and also expression of p63 which is a homolog of p53 [20, 23]. It is known that decreased expression of Rb1 which is a tumor-suppressor gene, leads to the upregulation of cyclin-dependent kinase inhibitor p16 [24]. All these features contribute to the poor prognosis of TNBC [25]. Most of the TNBCs contain BRCA1 mutation which interferes with DNA repair mechanism by homologous recombination and makes the cells susceptible to chemotherapy and agents that target DNA repair by poly (ADP-ribose) polymerase (PARP) inhibition [17, 26-28].

1.3.1. Approved Strategies for Triple Negative Breast Cancer Therapy

Due to the ineffective hormonal and HER2 targeted therapies, chemotherapy is the mainstay for TNBC therapy. Anthracycline- based or anthracycline and taxane-based chemotherapy regimens are effective on TNBC or basal-like breast cancer (BLBC) [29]. However, if the pathologic complete response (pCR) is not achieved it will result in even a worse overall survival. Some studies have reported different gene expression profile after treating the different subtypes. For instance, upon *in vitro* treatment with 5-fluorouracil and doxorubicin, for the luminal subtype variety of genes related with both cell cycle and proliferation are repressed, however for BLBC subtype only genes related with differentiation are repressed [17, 30]. TNBCs do not show high sensitivity for taxanes as in the advanced form of disease overall survival for patients treated with paclitaxel was lower [31]. In the meantime, some studies have mentioned that TNBC cells respond better to antimetabolites like cyclophosphamide, methotrexate and 5-fluorouracil (CMF) than other tumor types but it is not as strong as the effect of anthracyclines and taxanes [32]. It has been reported that BRCA1 mutation increases the sensitivity to DNA crosslinker therapeutics and sensitizes the cancer cells to compounds like platinum [33].

Other therapeutic drugs such as; PARP inhibitors, angiogenesis inhibitors, EGFR inhibitors and Src inhibitors are currently being investigated in phase I or II clinical trials [17]. Knowing the strong and weak points of existing drugs, it is urgently needed to develop new formulations for TNBC therapy.

1.3.2. Elongation Factor 2 Kinase as a Novel Target for TNBC Therapy

In recent years, eukaryotic elongation factor 2 kinase (eEF-2K) has garnered interest as a potential cancer-therapeutic target [34, 35]. eEF-2K is a Ca^{2+} and calmodulin dependent protein kinase that specially phosphorylates eEF-2, an abundant protein that facilitates the translocation of peptidyl tRNA from the ribosomal A-site to the P-site. In vitro, phosphorylation of eEF-2 by eEF-2K inhibits its activity and protein synthesis is arrested [36]. eEF-2 phosphorylation is increased in intact cells by a variety of treatments that increase the levels of intracellular Ca^{2+} and this is associated with inhibition of protein synthesis [37]. Higher activity of eEF-2K has been correlated with a higher proliferation rate in C6 glioma cells and breast cancer cells [38], even though, depending upon the cell type, high eEF-2K activity is not always proportional to high mitotic frequency. Changes in the level of eEF-2 phosphorylation or eEF-2K levels also accompany cell cycle progression, cellular differentiation, and oogenesis [39]. eEF-2K is highly up-regulated in TNBC cell and tumors and remarkably associated with poor survival in TNBC patients. eEF-2K promotes cell proliferation, invasion/metastasis, angiogenesis and drug resistance by inducing the activity of PI3K/AKT, Src/FAK/Paxillin, cyclinD1, c-myc and VEGF [35]. eEF-2K is regulated by the mTOR and MAPK pathways [40, 41]. Mitogens constitutively activate eEF-2K in human breast cancer and constitutively activated eEF-2K in human breast cancer has been linked to cell proliferation [42]. Glioblastoma and breast cancer cells also employ eEF-2K as a survival pathway by regulating autophagy in stress, nutrient/growth factor deprivation, and hypoxia [43, 44]. Additionally, eEF-2K has been implicated in ageing [45]. The AMPK, mTOR, p38, MAK, p70, S6 kinase pathways in part regulate eEF-2K activity via phosphorylation [41], the cdc2-cyclin B complex [46] and an additional unknown kinase [40].

With its known high expression in many tumors as well as TNBC, eEF-2K is considered as a great target for gene therapy studies.

1.4. Oligonucleotide-Based Therapeutics in Gene Therapy

Oligonucleotides based therapeutics are known to be more specific for cancer treatment compared with other conventional chemotherapeutics which mostly target both healthy and unhealthy cells. Oligonucleotides based therapeutics are more

target specific and act on highly expressed oncogenes or their regulatory pathways, and exert their therapeutic effect by downregulating these molecular pathways [47]. In recent years, different potential oligonucleotide based therapeutics such as; morpholino oligonucleotides, siRNAs, miRNAs and shRNAs have been developed and investigated.

1.4.1. Morpholino Oligonucleotides

Morpholino oligonucleotides are made of nonionic DNA analogs which their backbone has been altered and are considered to be one of the most powerful tools for gene downregulation [47-50]. Morpholino oligonucleotides downregulate their targets by attaching to their targets by Watson-Crick base-pairing. Their name is coined from the morpholino ring which is interconnected to four genetic bases (adenine, cytosine, guanine, and thymine). Normally, long 25-base structures are necessary for antisense gene downregulation. Due to their strong backbone structure, they are highly resistant to degradation by serum endo and exo-nucleases and are considered to be good candidates for in vivo gene downregulation studies. Moreover, they do not have negative groups in their backbone which inhibit their nonselective interaction with cellular proteins [47, 49, 51].

1.4.2. siRNAs

Recently, gene therapy has proved that it is a reliable approach for cancer treatment and one of the popular approaches is the use of siRNAs. Gene knockdown by siRNAs is a great approach to study and regulate different pathways that play a key role in cancer cell survival and proliferation. Gene knockdown by siRNAs was first reported by Fire, et al. in a roundworm called *Caenorhabditis Elegans* and they showed the high potency of double-stranded RNA for gene knockdown studies [52]. Elbashir, et al. proved the gene knockdown potency of siRNAs by using synthetic short RNA duplexes in mammalian cells [53]. siRNAs are regarded as powerful means of gene inhibition as they can inhibit every single protein of interest regardless of its localization within the cells [54]. siRNAs are noncoding RNAs generally with 20 to 25 base-pair and are produced biologically via cleavage by dicer enzyme, nuclease activity of RNase III, or chemical synthesis. Dicer cleaves the long double stranded RNAs into short duplex RNAs that are loaded into Argonaute and passenger strand gets removed and by means of RNA-inducing silencing

complex (RISC) specific mRNA strands are recognized and slicing happens [55]. The reason for the overwhelming interest on siRNAs is that RNAi pathway is very good for target identification and allows rapid progression from target selection to preclinical trials. Furthermore, this strategy has offered great potential in terms of targeting undruggable targets [47, 56].

1.4.3. miRNAs

Taking advantage of miRNAs is another strategy for the silencing of target mRNAs. Like siRNAs, miRNAs are double-stranded RNA molecules with 20 to 24 nucleotides, endogenous RNA molecules but they have the ability to control the expression of more than one mRNA and they play a major role in regulating gene expression [57-60]. The mechanism of gene silencing starts with the transcription of miRNAs by RNA polymerase II or III and primary miRNAs are produced in the nucleus. After that double stranded RNAs get recognized by the protein called DiGeorge syndrome critical region 8 (DGCR8) being processed by RNase III Drosha and the double-stranded RNA-binding domain protein, a long nucleotide is generated. After more processing, it is transported to the cytoplasm where it forms an active complex with RISC with the purpose of mRNA degradation [47].

As mentioned before miRNAs have a great potential of binding to thousands of mRNAs, making them wonderful assets in controlling tumor suppressor genes or oncogenes (oncomirs) [59, 61].

1.4.4. shRNAs

shRNAs are a different of type gene silencing approach but with a similar functional outcome as siRNAs. After being synthesized in the cell nucleus shRNAs are transported to the cytoplasm and show their effect via binding to RISC complex [62]. Newly transcribed shRNAs have a hairpin-like stem-loop structure called pri-shRNA and get processed by Drosha enzyme and the protein DGCR8 and pre-shRNA is produced and transported to the cytoplasm by the protein called Exportin-5 [63, 64]. The loop of pre-shRNA is sliced later by RNase III complex, composed of Dicer and TAR RNA binding protein/PKR activating protein and double stranded RNA with 2-nucleotide 3' overhangs is associated with Argonaute 2 protein-containing RISC complex for following gene knockdown [47, 65-70].

1.4.5. Hurdles in Front of Oligonucleotide-Based Cancer Therapeutics

In spite of the immense interest in translating siRNA-based therapeutics as a therapeutic strategy, translation of these novel therapeutics into clinic has been hampered due to biological barriers and lack of safe and effective nano-delivery vehicles [71, 72]. siRNA is highly vulnerable to serum exo- and endonucleases, leading to a short half-life in serum. Because oligonucleotides are polyanions they do not easily cross cell membranes and, because this charge density leads to extensive hydration, they do not easily interact with albumin and other serum proteins, leading to rapid elimination by kidneys. The other barrier is the renal entrapment of siRNAs in reticuloendothelial system (RES) that exists in organs such as; liver, spleen, lung and bone marrow. Many delivery systems larger than ~20 nm and less than ~100 nm in diameter are optimal for preventing both renal and RES clearance and favorably improve the passive intra-tumoral delivery due to the absence of lymphatic drainage and leaky tumor vasculature which is called enhanced permeability and retention (EPR) [73]. Regarding the issues related with siRNAs, they need to be delivered by a perfectly designed and robust delivery vehicle capable of protecting siRNAs, targeting them to the tumor site and increasing their uptake by the cells.

1.5. Viral and Non-Viral Gene Delivery Vehicles

1.5.1. Viral Delivery Vehicles

Viral vectors such as; adenovirus (types 2 and 5), retrovirus, adeno-associated virus, pox virus, herpes virus, lentivirus and human foamy virus (HFV) are considered to be effective gene delivery vehicles [74, 75]. The genome of these viruses has been deranged by deleting some part of it but still there are very important problems such as; immunogenicity, toxin production, the insertional mutagenesis, and limited transgenic capacity size which need to be addressed [76, 77].

1.5.1.1. Retroviral vectors

Retroviral vectors are frequently used with the purpose of gene delivery in somatic and germline cells. In compare to adenoviral and lentiviral vectors, they can transfect non-dividing cells and they can pass through the nuclear pores which makes retroviruses proper candidates of in situ treatment [78, 79]. Retroviruses are

capable of linearly integrating into the host cell genome so they are good candidates for ex vivo delivery of somatic cells. For instance, they have been used for the gene therapy of X-SCID and regardless of achieving successful results, incidence of leukemia was reported in some patients which was due to the integration of retroviruses to the LMO2 gene and deranging its activation [80-82]. hyperlipidemia gene therapy and tumor vaccination. Nevertheless, low efficiency of retroviral vectors for *in vivo* delivery, immunogenic problems, and the insertional risks are among the most important limitations of these vectors [74, 78].

1.5.1.2. Adenoviral vectors

Adenoviruses type 2 and 5 are commonly used in gene transfection studies and are capable of transferring both dividing and non-dividing cells. They can be used as a gene delivery vector in many different tissue types as they have low host specificity [83]. In opposition to, retroviruses which integrate into the host genome, the gene expression provided by adenoviral vectors is short term. Due to the acute immunologic responses, the clinical application of adenoviral vectors is limited to tissues like; liver, lung or localized cancer gene therapy. Even though the risk of transfection with adenoviral vectors is rare and the genome of the virus does not integrate into the host genome, still in some occasions they have caused severe side effects or the death of the patient [84, 85].

1.5.1.3. Adeno-associated vectors

Adeno-associated vectors (AAV) share the features of adenoviral vectors, though they are safer than adenoviral vectors because of the deficiency in replication and pathogenicity [86]. AAVs are not generally associated with any disease and are considered to be safer. One of the important advantages of AAVs is their integration into a specific site on chromosome 19 which can result in the long-term expression of gene of interest *in vivo* with no noticeable side effects. However, limited transgene capacity and complicated process of vector production are limiting factors for their use in the clinic [74].

1.5.1.4. Helper-dependent adenoviral vector

“Gutless” or “guttled” helper-dependent adenoviral vectors (HdAd) are the last generation of adenovirus vectors which are considered to overcome the disadvantages of the first-generation vectors like; limited packaging capacity (8 kb

v.s. 38 kb), immunogenicity, and toxicity [83]. In this system, the helper vector, which has a conditional gene defect in the packaging domain, provides the required viral genes for replication and the second vector which contains the ends of the viral genome, therapeutic gene sequences, and the normal packaging recognition signal, facilitates the selective release from the cells [87]. In this way, this system is known to reduce the toxicity and extend the gene expression of up to 32 kb of DNA in host cells [74].

1.5.1.5. Hybrid adenoviral vectors

This type of vector is a hybrid of adenoviral vector with the high transduction efficiency and, adeno-associated and retroviruses with their long-term genome-integrating potential. These kinds of hybrid systems provide a table transduction [74, 88].

1.5.1.6. Herpes simplex virus

One of the recent viruses which has been introduced as a potent gene delivery vehicle is herpes simplex virus (HSV). It includes disabled infectious single copy (DISC) viruses, which have a defective glycoprotein H [74]. So, viral particles can infect the cells and they can replicate their own genome but they cannot produce infectious particles [89]. Due to their neuronotropic features these vectors have a great potential of gene delivery to nervous system tumors, and cancer cells [74, 90, 91].

1.5.1.7. Lentiviruses

Lentiviruses are actually a subclass of retroviruses but in compare to retroviruses which infect the dividing cells they can integrate to non-dividing cells. Due to their tropism to neural stem cells they are good candidates for safe ex vivo gene transfer in central nervous system with no major immune responses. The advantages of lentiviral vectors are; low immunogenicity, high-efficiency transfection, long-term stable expression of a transgene, and the ability to carry larger transgenes [74, 92, 93].

1.5.1.8. Poxvirus vectors

This type of vector is good for high-level expression of transgenes in the cytoplasm. The specific feature of this virus is its stable insertion capacity (more than 25 KB). Poxvirus vectors have been used in different types of cancer such as; colorectal cancer, prostate cancer, lung cancer and breast cancer [94]. Poxviruses have a complex structure and they are associated with some cytopathic effects [74].

1.5.1.9. Epstein–Barr virus

Epstein–Barr virus is used as a vector for the expression of large DNA fragments. Due to its localization in the nucleus of the host cell it is suitable for long-term retaining in the cell [95]. Due to its B-cell tropism it has been tested for immune therapy of cancer [96]. Generally, because of their carcinogenic properties and problems with their long-term maintenance, the use of viral vectors is limited in gene therapy [74].

1.5.2. Non-Viral Delivery Vehicles

1.5.2.1. Naked DNA

It is possible to transfer naked genes between 2-19 kb to thymus, skin, cardiac muscle, liver cells, and skeletal muscle [97]. Even though, this method is considered to be a safe and simple method, it is only recommended in DNA vaccination applications and its efficiency is very low for other gene therapy applications [74].

1.5.2.2. DNA particle bombardment by gene gun

As an alternative technique to naked DNA application, particle bombardment by gene gun which is a modified form “biolistic” technique has been introduced. In this method plasmid DNA coated gold or tungsten particles with the size of 1-3 μm get accelerated by pressurized gas to very high speeds so they can penetrate to the cells [98]. This method is used for DNA-based immunization or vaccination in mucosa, skin, or surgically exposed tissue [74, 99].

1.5.2.3. Electroporation

In this method, the cell membrane is destabilized with a pair of electrodes inserted into the target tissue which enables the DNA molecules to penetrate into the cytoplasm and nucleoplasm of the cell. Unfortunately, the transgene can only

integrate to 0.01% of the cells. The most important problems are; the need for surgical procedure to place the electrodes into the tissue and also the applied high voltage can damage the cells and affect the stability of DNA [74, 100].

1.5.2.4. Hydrodynamic

This is a simple method with high efficiency for intracellular delivery of water-soluble molecules or particles to internal organs [101]. The in vivo efficiency of this method is higher than other non-viral delivery systems. However, it has only been successfully tested in small animals not in human [74].

1.5.2.5. Ultrasound

Due to the fact that ultrasound waves can cause nanometric pores in the cell membrane, it has been used to facilitate the uptake of DNA particles. However, the concentration of the plasmid DNA is very important. The only limitation of this method is its very low efficiency, especially in vivo [74, 102].

1.5.2.6. Magnetofection

This is an efficient transfection method which concentrates the oligonucleotide containing particles to the cells. Here the magnetic force helps to concentrate the particles in the area so nearly 100% of the cells can get in contact with the oligonucleotides in a very significant dose. This method has been successfully tested on a broad range of cell lines with siRNA, DNA, dsRNA, mRNA, shRNA, etc [74, 103].

1.5.2.7. Cationic liposomes

Cationic liposomes with the ability of capturing and delivering negatively charged nucleic acids have very unique characteristics like; incorporation of hydrophilic or hydrophobic drugs, no activation of immune system, low toxicity, and targeted delivery to the site of action [104]. However, the rapid degradation of liposomes by the reticuloendothelial system and the inability to sustain the delivery over a prolonged period of time are two major drawbacks which are addressed by the modification of the surface of liposomes with polyethylene glycol (PEG) [74, 105].

1.5.2.8. Cationic polymers

Poly-L-lysine (PLL) is one of the widely studied cationic polymers. The molecular weight of the cationic polymer is very important in gene delivery studies and as the

molecular weight increase the net positive charge of the polymer increases and along with that more stable complexes are formed. Also the length of the polymer is another important factor and as the length of the polymer increases its gene delivery efficiency, and toxicity increases as well [106]. The efficiency of gene delivery with PLL is low and to increase that it should be conjugated to other agents. Also, it has been mentioned that the conjugation of the PEG to cationic polymer can avoid the binding of plasma protein and increase its circulation of half-life [107]. Polyethylenimine (PEI) is another important cationic polymer which is synthesized in both linear (LPEI) and branched (BPEI) forms. It has been stated that in compare to branched form, the linear form of PEI has low toxicity and high gene delivery efficiency [108]. PEI forms toroidal polyplex particles, which are stable to aggregation and it has a strong buffering capacity [109]. However, PEI is non-biodegradable and in high concentrations it can cause serious toxicity in vivo. It is known that the PEI of 25 k for BPEI and 22 k for LPEI are the optimal molecular weights for gene delivery studies [110]. It should be noticed, in regard to cationic polymers, toxicity and transfection efficiency are two most important factors [74].

1.5.2.9. Lipid–polymer systems

These are three-part systems which in the first part DNA is pre-condensed with polycations and then it is coated with anionic liposomes, cationic liposomes, or amphiphilic polymers either containing helper lipids or not [74, 111].

1.6. Nanoparticles as Robust Gene Delivery Vehicles

Many transfection facilitating techniques such as; biological (viral vectors), chemical (cationic polymers and lipids) and physical (micro injection, biolistic particle delivery, electroporation, and laser-based transfection) methods have been introduced to address transfection problem and increase the internalization efficiency [112]. However, viral vectors are known to be immunogenic and cause toxicity, and also for chemical methods the main problem is associated with their toxicity. In this regard, nanoparticulate carrier systems such as; gold nanoparticles [113], silica nanoparticles, magnetic nanoparticles (MNPs), polymeric nanoparticles [114-116], have been proposed. Generally, it has been shown that these nanoparticle systems can improve the siRNA transfection when modified with cationic moieties and they can be targeted by active or passive targeting methods (Figure 2). Nevertheless,

there are some toxicity issues that are related with these nanoparticle systems or the use of different cationic structures. In the meantime, only liposomes which are lipid-based nanoparticles have been safely used in different clinical trials and there are many formulations [115]. Yet, there are many disadvantages such as; low solubility, short half-life, oxidation and hydrolysis, production cost and low stability that limit their use [117].

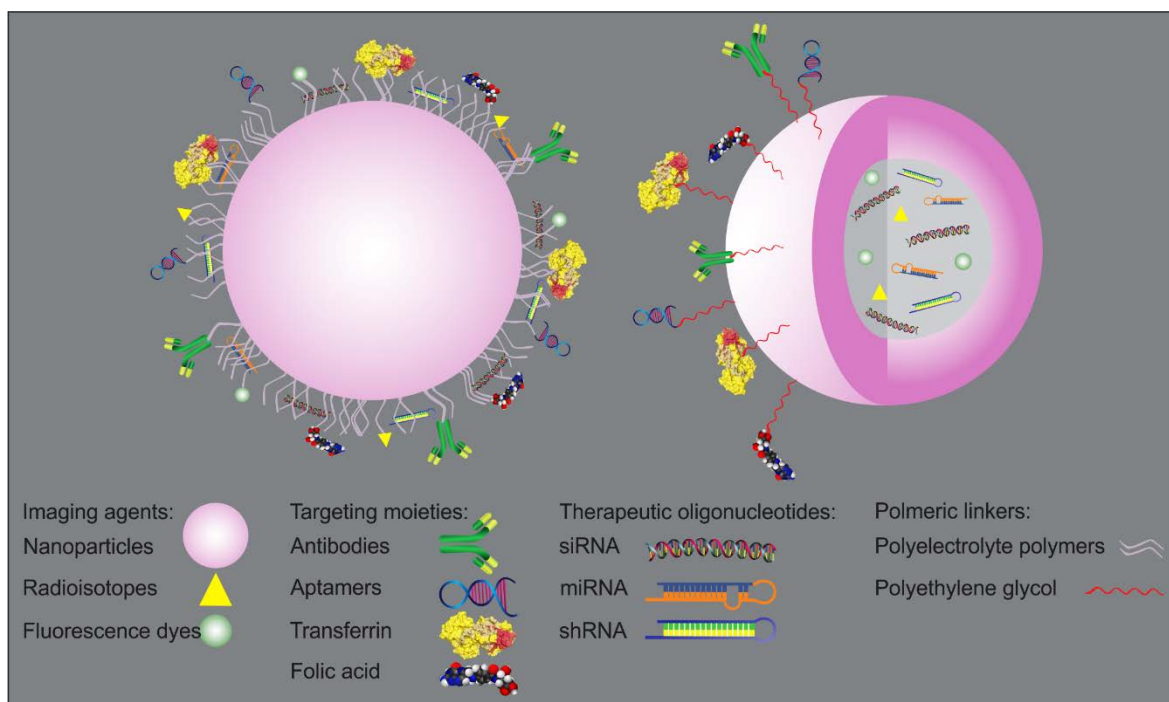


Figure 2. Oligonucleotide delivery by nanoparticles and active or passive targeting [47].

1.7. Gold Nanoparticles for the Delivery of Oligonucleotide Based Therapeutics

Gold nanoparticles are considered as outstanding siRNA delivery systems owing to their easy synthesis, amenable modification and bio-conjugation, and rational stability and biocompatibility [73, 118]. Also, gold nanoparticles can be synthesized in different size ranges which facilitates their passive targeting to the tumor site. Another important aspect of using gold nanoparticles is their in vivo imaging by computed tomography (CT) or imaging systems based on the infrared light (Figure 3). This approach which provides both therapy and diagnosis is called

“Theranostics” [47]. siRNAs can be delivered by gold nanoparticles either through covalent attachment to the gold surface via the thiol linkage known as polyvalent structure or directly conjugation by the means of cationic moieties [119]. However, there are some problems such as; aggregation upon polyelectrolyte addition, the amount and molecular weight of polyelectrolyte, toxicity, polydispersity, designing of the nanoparticle surface and size effect that prevent their entrance into the clinic. Finally, one of the most important factors is the size of gold nanoparticles. As it is known small sized nanoparticles (<5nm) are eliminated by kidneys, nanoparticles with size range of 10-20 nm tend to accumulate mostly in the liver and larger nanoparticles (100-200 nm) accumulate in both liver and spleen [71]. All the PEI coated gold nanoparticles which have been used for siRNA transfection were in the size range of 5-30 nm which is not an optimal size range for targeted cancer therapy. However, nanoparticles within the 60 nm diameter range are optimal for targeting of the tumors [120].

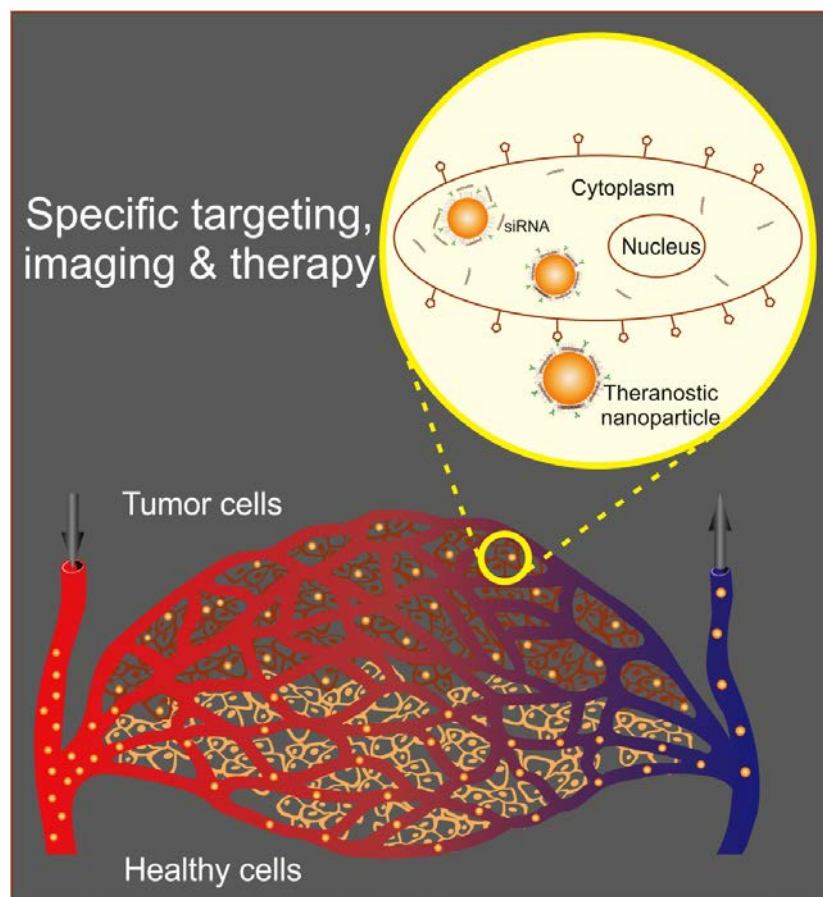


Figure 3. Tumor targeting and concomitant imaging “Theranostic Approach” [47].

1.8. Review of the Published Literature in Cancer Gene Therapy

Giljohann, et al. [121] have studied about gene knockdown using polyvalent siRNA-gold nanoparticle conjugates. They showed their resistance to nuclease degradation and high cellular uptake as a result of their oligonucleotide functionalization. They proved that dense surface functionalization of oligonucleotides increases the stability and efficacy of the bound RNA. They conducted protein knockdown studies in HeLa cells using a transfected luciferase plasmid as a target for this model system. Quantification of luciferase expression revealed that the nanoparticle agents down-regulate firefly luciferase in a dose and time dependent manner. Interestingly, the results of three independent experiments with the RNA-Au NPs showed knockdown that exceeds that of the free RNA 4 days after treatment.

Tekedereli, et al. [35] have studied the potential knockdown of eEF2-K using liposomal siRNA in triple negative breast cancer along Doxorubicin treatment. For the first time, they found that eEF2-K play an important role in breast cancer proliferation and metastasis and it was shown that eEF-2K down-modulation in vitro results in a decrease in the expression of c-Myc and cyclin D1 with a concomitant increase in the expression of p27Kip1. A decrease in the basal activity of c-Src (phospho-Tyr-416), focal adhesion kinase (phospho-Tyr-397), and Akt (phospho-Ser-473) also proved following eEF-2K down regulation in MDA-MB-231 cells. Also from their proposed data it is obvious that targeting results in a substantial decrease in eEF2 phosphorylation in the tumors, and leads to the inhibition of tumor growth, the induction of apoptosis and the sensitization of tumors to the chemotherapy agent doxorubicin.

Guo, et al. [122] developed charge-reversal functional gold nanoparticles (siRNA/PEI/PAH-Cit/PEI/MUA-AuNPs) by layer-by-layer technique and studied the delivery of both siRNA and plasmid DNA into cancer cells. They achieved successful downregulation of lamin A/C which is an important nuclear envelope protein and reported that the gene downregulation efficiency was better than commercially available Lipofectamine 2000. It was found that the charge reversion in the acidic environment of cancer cells causes the escape of gold complexes from endosome/lysosome and facilitates the release of functional nucleic acids into the cytoplasm.

Elbakry, et al. [123] developed a layer by layer technique and studied the gene silencing of EGFP. In this technique, the surface of gold nanoparticles was coated with 11-mercaptoundecanoic acid (MUA) to stabilize the nanoparticles and facilitate the capture of PEI with a molecular weight of 25000. In the next step, PEI was added and following that siRNA was conjugated to the nanoparticles. In the final step, another PEI layer was added to the nanoparticle solution as a final layer. They reported successful EGFP silencing and showed that in spite of the high toxicity of free PEI, PEI/siRNA/PEI-AuNPs had no serious toxicity. They concluded that in this approach higher siRNA concentration may be necessary due to the high stability of LbL-coated AuNPs and low siRNA release.

Song, et al. [124] PEI-capped gold nanoparticles using PEI as both the reductant and stabilizer. In order to prepare the nanoparticles, they mixed PEI and chloroauric acid and stirred at room temperature for 24 h. PEI-capped AuNPs/siRNA were used in order to target endogenous cell-cycle kinase, an oncogene polo-like kinase 1 (PLK1). They reported that significant gene knockdown was achieved by these nanoparticles and cell apoptosis was enhanced. Results were reported to be better than free PEI without any cellular toxicity. They concluded that PEI-capped AuNPs are suitable carriers for intracellular siRNA delivery.

1.9. Aim of the Thesis

With regard to the highly aggressive state of the triple negative breast cancer and very low survival rate, it was mainly aimed in this thesis to develop a novel siRNA/gold nanoparticle based nanotherapeutics for gene knockdown approach in triple negative breast cancer. eEF-2K has been proved to be highly expressed in TNBC tumors so it was aimed to specifically target this gene by siRNA therapeutics. In order to deliver siRNAs with high efficiency very good gene delivery vehicles are needed so another aim of the study was to develop a highly monodisperse and stable gold nanoparticles based gene delivery vehicle. Cellular uptake and distribution of gold nanoparticles are very important factors that can affect the final result of the gene delivery so it was aimed to study the cellular uptake and distribution of the gold nanoparticles. As theranostic approach is considered to be a next generation technology in personalized medicine, it was aimed to develop a theranostic nanotherapeutics capable of both therapy and diagnosis. After developing a theranostic potent gene delivery vehicle, it was aimed to develop eEF-

2K siRNA conjugated nanotherapeutics and assess their capability at *in vitro* and *in vivo* eEF-2K gene down-regulation (Figure 4). As in recent years, the importance of combinational therapy approaches has been proved, the final aim of this thesis was to develop a combinational nanotherapeutics bearing both eEF-2K siRNA and doxorubicin chemotherapeutic for more effective results in TNBC therapy.

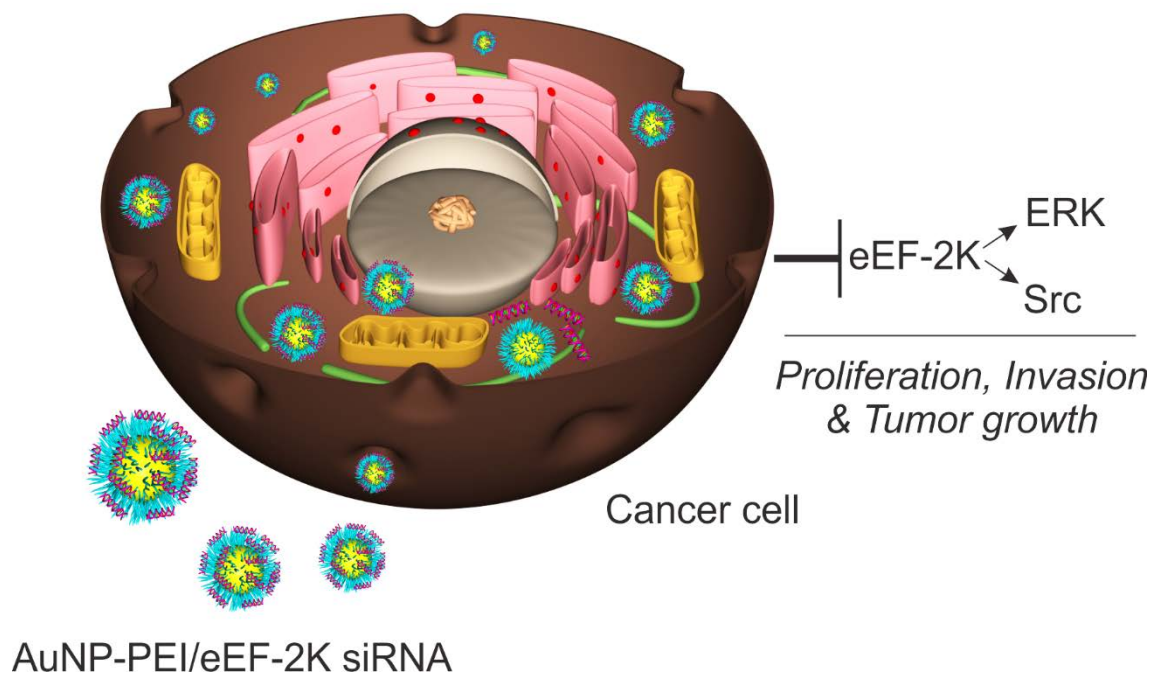


Figure 4. Schematic representation of the aim of the study.

2. MATERIALS AND METHODS

2.1. Materials

Trisodium citrate dehydrate solution - (Sigma-Aldrich)

Hydrogen tetrachloroaurate(III) trihydrate - (Sigma-Aldrich)

Hydroquinone - (Sigma-Aldrich)

Polyethyleneimine 2000 MW - (Sigma-Aldrich)

Dulbecco's Modified Eagle Medium - (Thermo Fisher Scientific)

L-glutamine - (Thermo Fisher Scientific)

Penicillin streptomycin - (Thermo Fisher Scientific)

MTT Formazan - (Sigma-Aldrich)

Dimethyl sulfoxide - (Sigma-Aldrich)

Agarose gel - (Sigma-Aldrich)

Ethidium bromide - (Sigma-Aldrich)

eEF-2K siRNA - (Sigma-Aldrich)

Doxorubicin - (Sigma-Aldrich)

control siRNA - (Sigma-Aldrich)

Bradford assay - (Bio-Rad)

Phosphate buffered saline - (Sigma-Aldrich)

eEF-2K antibody - (Thermo Fisher Scientific)

p-EF2 (Thr-56) antibody - (Thermo Fisher Scientific)

EF2 antibody - (Thermo Fisher Scientific)

p-Src (Tyr-416) antibody - (Thermo Fisher Scientific)

Src, p-p38 antibody - (Thermo Fisher Scientific)

p-ERK antibody - (Thermo Fisher Scientific)

Anti-rabbit/anti-mouse secondary antibody - (Amersham Life Science)

ChemiGlow detection reagents - (Alpha Innotech)

Anti- β -actin primary antibody - (Sigma Chemical)

Donkey anti-mouse secondary antibody - (Sigma Chemical)

RPMI 1640 cell culture medium - (Gibco)

Ketalar - (Pfizer)

Neurobasal A medium (NBA) - (Gibco)

GlutaMAX™ - (Gibco)

B-27 Supplements - (Gibco)

Fetal bovine serum - (Gibco)

Goat Serum - (Gibco)

Antibiotic-Antimycotic Solution - (Sigma)

Collagenase Type IV - (Sigma)

Hanks' Balanced Salt solution - (Sigma)

DNase I - (Sigma)

Percoll® - (Sigma)

Trypsin - (Sigma)

Trypsin Inhibitor - (Sigma)

Poly-L-Lysine - (Sigma)

Laminin - (Sigma)

Propidium iodide - (Sigma)

Bovine Serum Albumin - (Sigma)

Sodium azide - (Sigma-Aldrich)

TWEEN® 20 - (Sigma)

Triton™ X-100 - (Sigma)

DAPI - (Sigma)

Ethanol - (Sigma)

Dimethyl ether (DME) - (Sigma)

Paraformaldehyde (Sigma)

Mouse Anti-beta III Tubulin antibody (Abcam)

Chicken polyclonal Anti-200 kD Neurofilament Heavy antibody (Abcam)

Alexa Fluor[®] 488 Goat Anti-Mouse IgG H&L (Abcam)

Alexa Fluor[®] 594 Goat Anti-Chicken IgG (Abcam)

MitoTracker[®] Red (Abcam)

2.2. Methods

2.2.1. Synthesis of Gold Nanoparticles and PEI Modification

2.2.1.1. Synthesis of seed gold nanoparticles

Turkevich method of synthesizing gold nanoparticles was used to prepare seed gold nanoparticles and it was modified in order to synthesize highly monodisperse seed gold nanoparticles [125, 126]. A 3.33% stock solution of trisodium citrate dehydrate was prepared and 1 mL of it was added to hydrogen tetrachloroaurate (III) trihydrate ($\text{HAuCl}_4 \cdot 3\text{H}_2\text{O}$) solution (0.25 mM, 100 mL) and stirred for 10 min under reflux system. It should be noticed to avoid that splashing of the solution while stirring because it can affect the polydispersity of the final nanoparticle product. Before doing any characterization, the solution was cooled to room temperature. Synthesized seed gold nanoparticles were used in the following growth step in order to synthesize the gold nanoparticles with the larger sizes. Transmission Electron Microscope (TEM) (FEI Tecnai G² Spirit BioTwin CTEM Microscope, USA) and Scanning Electron Microscope (SEM) (Zeiss Evo HD SEM 15 LS instrument, Germany) were used to characterized the shape and size of the nanoparticles. LSPR peak was obtained using a UV-visible spectrophotometer (Agilent 8453, USA). Hydrodynamic size and zeta potential measurements were performed by using the Zetasizer Nano ZS analyzer (Malvern[®] Instrument Ltd., England). Size and zeta potential measurements were performed in three repetitions each with 10 analyses, and the results were obtained as means \pm standard deviation.

2.2.1.2. Growth of seed nanoparticles by seeding-growth method

In this method of synthesis hydroquinone, which is a weak reducing agent, was used. Hydroquinone is not able to trigger the nucleation but it can facilitate the deposition of gold atoms on seed gold nanoparticles and based on the amount of seed, gold nanoparticles between 50 – 200 nm can be synthesized. So, the only variable here which determines the size of the final product is the amount of added seed gold nanoparticles.

Gold nanoparticles of different sizes were synthesized by using seed gold nanoparticles from the previous step and were grown by seeding-growth method [127]. $\text{HAuCl}_4 \cdot 3\text{H}_2\text{O}$ stock solution of 0.25 mM was prepared and predetermined amount of seed gold nanoparticles were added and stirred. As a stabilizing agent trisodium citrate dehydrate was used. A 15 mM stock solution of trisodium citrate dehydrate was prepared and was added to the mixture of $\text{HAuCl}_4 \cdot 3\text{H}_2\text{O}$ and seed gold nanoparticles in 0.15 mM concentration. At the final step, a 25 mM stock solution of hydroquinone was prepared and was quickly added to the mixture in 0.25 mM concentration and stirred for 10 min. The splashing of the solution should be avoided as it affects the polydispersity of the sample. Synthesized nanoparticles were characterized in terms of shape, size, LSPR peak, and zeta potential. The concentration of nanoparticles was determined by inductively coupled plasma mass spectrometry (ICP-MS) analysis (Perkin Elmer DRC II, USA).

2.2.1.3. Surface modification of synthesized gold nanoparticles

Polyethylenimine (PEI) (MW 2000 by LS) was used to modify the surface of AuNPs. A 2% stock solution of PEI was prepared and added in 0.005% (v/v %) concentration to a stirring solution of gold nanoparticles. Freshly synthesized gold nanoparticles were coated with PEI by stirring for 1 h with PEI solution. In the final step, PEI-coated gold nanoparticles were purified by centrifuging at 7000 g for 30 min and dispersing in 18.2 M Ω deionized water. AuNPs were characterized in terms of shape, size, LSPR peak, and zeta potential.

2.2.2. Cellular Biodistribution of Gold Nanoparticles

2.2.2.1. Isolation of DRG sensory neurons and cell culture studies

All animal procedures were performed by virtue of Medipol University Institutional Animal Care and Use Committee. A validated protocol by Demir *et al.* [128] was followed for the isolation of Dorsal Root Ganglion (DRG) sensory neurons. Balb-C mice were used to isolate DRG sensory neurons. 25 Balb-C mice (15 females and 10 males) were used in total. Pre-anesthetization was carried out by DME inhalation and following that anaesthetization was performed by I.P. injection of Ketamin (100 mg/kg).

Mice were decapitalized and after dissection of the dorsal root, DRGs were obtained under the stereo microscope (Zeiss, Germany). During the microdissection, DRGs were trimmed and placed in 4°C RPMI 1640 medium and following that, they were transferred to collagenase Type IV (100 U/mL) containing NBA culture medium (B-27 supplement (2/100 v/v), antibiotic/antimycotic (1/100 v/v) and GlutaMAX™ (1/100 v/v) comprising NBA medium and incubated for 40 min at 37°C, 5% CO₂. DRGs were washed three times and digested enzymatically for 15 min (37°C, 5% CO₂) in trypsin (1 mg/mL) containing NBA culture medium. In order to increase the isolation efficiency, the cells were triturated using different pipet tips (from 2 mm down). Cells were incubated with DNase (50 mg/mL) for 30 min and then they were centrifuged at 120 g for 3 min and dispersed in NBA culture medium containing both FBS (10% v/v) and trypsin inhibitor (700 mg/mL).

A percoll gradient (NBA culture medium and percoll) 60%, 35% and 10% (from bottom to top, respectively) was prepared and cells were placed on the prepared percoll gradient and centrifuged at 4°C (300g, 20 min). DRGs were gathered from the neuron richest layer of the gradient (between 35% and 60%) and centrifuged (3 min, 120 g) and dispersed in NBA culture medium. Obtained cells were seeded on poly-L-lysine (1.8 mg/cm², 2h at RT) and laminin (40 ng/mm², overnight at 37°C) coated glass-bottomed petri dishes (35 mm diameter). After 2 h of incubation (37°C, 5% CO₂) petri dishes were washed to get rid of unadhered cells and remnants, and fresh medium was added.

2.2.2.2. Determination of the cellular uptake by ICP-MS analysis

DRGs were cultured on petri dishes in 4×10^2 cells/petri. The total volume of each petri dish was 1 mL and 90% of this volume was adjusted to be the culture medium. Gold nanoparticles were added to each petri in different concentrations (0.5 $\mu\text{g/mL}$, 5 $\mu\text{g/mL}$, 50 $\mu\text{g/mL}$) and after 4 h of incubation with cells, the cell culture media were discarded and cells were washed with PBS three times. Following that, in order to dissolve gold nanoparticles, 1 mL of aqua regia solution (HCl: HNO_3 , 3:1) was added to each petri and cells were left for lysis for 1 h. Obtained mixture of each petri was transferred to 1.5 mL Eppendorf tube and analyzed by Inductively Coupled Mass Spectrophotometry (ICP-MS) (PerkinElmer) to determine the amount of gold.

2.2.2.3. Imaging the cellular biodistribution of gold nanoparticles by confocal microscope

To determine the cellular distribution of gold nanoparticles in DRG neurons LSCM microscope was used. Gold nanoparticles were added in 5 $\mu\text{g/mL}$ concentration to each petri dish and cells were imaged under LSCM microscope. Cells were imaged by using 40x water objective and their viability was controlled by using the incubator system of the microscope. In the first step, excitation and emission wavelengths were determined and it was noticed to eliminate the noises by using control group petri dishes. No fluorescent dye was used during confocal microscope examinations and the imaging procedure totally relied on the luminescence of the gold nanoparticles at the specific wavelength.

2.2.2.4. Imaging of the nanoparticle incubated cells by two-photon microscope

Imaging parameters were adjusted to infra-red laser wavelength of 810 nm, laser intensity of 5% and gain master of 700 which are specific detection parameters for Alexa 488 dye. After optimizing the parameters of the system, gold nanoparticles were tracked by means of a deeping ceramic objective for 30 min. In order to image viable cells, the infrared red laser of the two-photon microscope was directed to LSCM microscope and cells were monitored for 2 h using water objective. During the imaging procedure, the wavelength of the infrared laser was optimized for all the nanoparticles.

2.2.2.5. Toxicity studies of gold nanoparticles

Toxicity of nanoparticles was evaluated by two different methods and on two different cell types. In the first method, in order to evaluate the effect of nanoparticles on cell viability, three different concentrations (0.5 µg/mL, 5 µg/mL, 50 µg/mL) were defined. For each petri dish, 400 DRG cells were seeded and after 2 h of incubation, nanoparticle concentrations were added. Subsequently, propidium iodide (7.5 µL per dish) was added and cell viability was evaluated for next 3 days. Cell viability was quantified in the certain time intervals (2 h, 24 h, 48 h, 72 h) using a laser scanning confocal microscope (Zeiss LSM 780 confocal microscope). Propidium iodide does not have any adverse effect on cell viability, and nuclei of dead cells are stained red by this procedure. Following equation was used to quantify the cell viability for each time point:

$$\text{Cell viability \%} = \frac{(\text{Number of initial live cells}) - (\text{Red light emitting number of cells})}{\text{Number of initial live cells}} \times 100$$

Additionally, for all the nanoparticle groups cell morphologies were evaluated under Hoffman modulation contrast microscope (Zeiss).

In the second method, L929 fibroblastic cells were cultured in cell culture medium (DMEM, 10% FBS, 1% L-glutamine, and 0.1% penicillin-streptomycin) and seeded at a density of 1×10^4 cells/well in a 96-well culture plate and incubated for 24 h. After 24 h, different concentrations of synthesized gold nanoparticles (5, 20, 50, 100, 150, and 200 µg/mL) were added and incubated further for 24 h. Then the media were discarded, and after the addition of MTT dye (0.5 mg/mL) the mixture was incubated for 4 h. To dissolve the formazan precipitate, 100 µL of dimethyl sulfoxide (DMSO) was added to each well, and the absorbance was measured at 570 nm using a microplate reader. The results were expressed as the mean percentage of cell viability relative to the control group. Untreated cells were used as the control group and cells treated with DMSO were the positive control.

2.2.2.6. Immunocytochemical studies

Any potential effect of synthesized gold nanoparticles on components of neural cell skeletons (β -III tubulin and neurofilament 200 kDa) was evaluated by immunostaining of the cells. After 2 h of the culture period, gold nanoparticles in 5

µg/mL were added to the culture medium and ICC staining was carried out following to 48 h incubation with nanoparticles.

The culture medium of each petri was removed and washed twice with PBS. After fixation of the cells with 4% PFA for 15 min, cells were washed with PBS again. Following the blocking procedure with goat blocking solution for 30 min, primary antibodies (mouse anti β -III tubulin, chicken anti-NF 200 IgG antibody) were added and incubated overnight at 4°C. The next day, petri dishes were washed three times with PBS and secondary antibodies (Alexa 488 goat-anti-mouse IgG and Alexa 568 goat-anti chicken IgG) were added. After 3 h of incubation time, petri dishes were washed three times with PBS again. Finally, DAPI was added to each petri and cells were imaged under laser scanning confocal microscope (LSCM).

2.2.3. *In Vitro* and *In Vivo* Gene Delivery Studies

2.2.3.1. Determination of optimal siRNA conjugation ratio

To determine the optimal siRNA loading ratio, different AuNP-PEI/eEF-2K siRNA w/w ratios (0.25, 0.5, 1, 1.5, 2, 2.5, 3, 5, and 7) were prepared. siRNA loading was achieved by adding the calculated amount of siRNA to the nanoparticle solution, pipetting at least 10 times, and incubating for 15 min. The loading efficiency was analyzed by gel electrophoresis experiments. To this end, 20 µL of each sample was mixed with 4 µL of 6× loading buffer. Agarose gel (2%) containing 5 µg/mL ethidium bromide was prepared, and 2 µL of the mixture was loaded onto the agarose gel. Electrophoresis was performed under 120 V electrical potential for 15 min, and bands were visualized at a wavelength of 254 nm. Also, in order to verify the results, nanoparticles were centrifuged at 7000 g for 30 min, and the absorbance of the obtained supernatant was measured at a wavelength of 260 nm.

2.2.3.2. siRNA design and *in vitro* gene-knockdown studies

eEF-2K siRNA (5'-GCCAACCAGUACUACCAAA-3') and control siRNA (5'-AAUUCUCCGAACGUGUCACGU-3') were custom synthesized [35]. siRNAs were conjugated with AuNP-PEI nanoparticles in a predetermined 3:1 ratio and confirmed by gel electrophoresis studies. MDA-MB-231 cells (1×10^4) were seeded in 96-well plates, and the following day the AuNP-PEI/eEF-2K siRNA nano-formulation was added in 50 nM eEF-2K siRNA. Cells were incubated for 72 h for cell survival and target knockdown studies by western blot analysis.

Western blot analysis was performed based on a previously published study [35]. Briefly, after the treated cells were washed twice in ice-cold PBS they were lysed at 4°C, and the protein concentration was determined by using the Bradford assay, and western blotting was performed. Membranes were blocked with 5% dry milk or BSA and probed with the following primary antibodies: eEF-2K, p-EF2 (Thr-56), EF2, p-Src (Tyr-416), Src, p-p38, and p-ERK. Detection was performed by using horseradish peroxidase-conjugated anti-rabbit or anti-mouse secondary antibody. ChemiGlow detection reagents were used for chemiluminescence detection. Visualization of the blots and quantification were performed by a FluorChem 8900 imager and a densitometer using the Alpha Imager application program (Alpha Innotech), respectively. β -Actin expression was monitored by using mouse anti- β -actin (primary) and donkey anti-mouse (secondary) antibodies.

2.2.3.3. Development of orthotopic xenograft tumor model in mice

All *in vivo* studies were conducted according to a protocol approved by the MD Anderson Institutional Animal Care and Use Committee. *In vivo* studies were performed on 5-week-old athymic female *nu/nu* mice (n=5) (procured from the Department of Experimental Radiation Oncology at MD Anderson Cancer Center, Houston, TX). An orthotopic xenograft tumor model of MDA-MB-231 cells was developed by injecting cells (2×10^6 cells) into the right middle mammary fat pad of each mouse. After 2 weeks, when tumor size reached about 3-5 mm, siRNA therapy was initiated.

2.2.3.4. Injection of prepared nano-formulation and tumor analysis

Each mouse was intravenously injected once a week with AuNP-PEI/control siRNA or AuNP-PEI/eEF-2K siRNA at a siRNA concentration of 8 μ g/mouse for 4 weeks. Tumor volumes were measured weekly to determine the tumor growth. After 4 weeks, mice were euthanized with CO₂, and tumor tissues were removed and analyzed by Western blot.

2.2.4. Development of Doxorubicin and eEF-2K siRNA Conjugated Gold Nanoparticles for Combinational Therapy Approach

2.2.4.1. Preparation of doxorubicin and eEF-2K siRNA conjugated gold nanoparticles

In the first step, doxorubicin was thiolated with 2-iminothiolane through the NH₂ group of the doxorubicin. To do so, a stock solution of doxorubicin was prepared in 344.84 µM concentration and 2-iminothilane was added to the stock solution in 653.93 µM concentration. The reaction was continued for 1 h at room temperature while mildly stirring.

After the thiolation step, gold nanoparticles in 200 µg/mL concentration was mixed with the doxorubicin solution in 1.5 µM concentration. Then, the available surface on the nanoparticles was conjugate with PEI in 0.005% (v/v %) concentration and stirred. Finally, eEF-2K siRNA in the final concentration of 50 nM was added and incubated with doxorubicin and PEI conjugated gold nanoparticles for 1 h at room temperature. To increase, the stability of the nanoformulation both at *in vitro* and *in vivo* conditions, thiolated PEG was added in 0.0003% (v/v %) concentration and stirred for 15 min.

Prepared nanoformulation was analyzed with HPLC, in order to prove the conjugation of doxorubicin to the surface of gold nanoparticles. Also, the size and zeta potential of the final nanoformulation were analyzed with Zetasizer Nano ZS instrument.

2.2.4.2. In vitro evaluation of the doxorubicin conjugated gold nanoparticles in MDA-MB-231 cells

MDA-MB-231 cells were culture as mentioned above and were seeded on 96 well plates. To determine the IC₅₀ value different concentrations (0,1, 0.2, 0.4, 0.8, 1.6, 3.2, 6.4 and 12.8 µM) of doxorubicin were added and cells were incubated for 72 h. After 72 h, the MTT assay was performed and the IC₅₀ value was calculated.

After determining the IC₅₀ value, doxorubicin conjugated gold nanoparticles were prepared in the related concentration and their effect on the cell viability of MDA-MB-231 cells was evaluated after 72 h by doing MTT assay.

2.2.4.3. In vitro evaluation of the doxorubicin and eEF-2K siRNA conjugated gold nanoparticles in MDA-MB-231 and MDA-MB-436 cells

Cells were collected and about 1000 cells were seeded into 96-well plates. MTS assay was used for the evaluation of the efficiency of the developed nanotherapeutics. Cells were treated with nanoparticles in different doxorubicin concentrations (0.1 μ M and 0.25 μ M) for 72 h and cell proliferation was determined. Then 20 μ L of MTS solution was added to each well and plates were incubated at 37°C for 4 h. The absorbance was measured by using a microplate reader at the wavelength of 490 nm.

2.2.5. Statistical Analysis

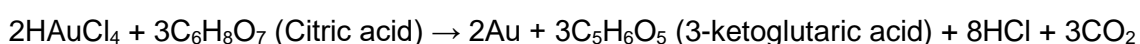
All data are reported as means \pm SD, and statistical analysis was performed using the one-way analysis of variance (ANOVA), two-tailed and paired Student's t-test. A p value <0.05 was considered as statistically significant.

3. RESULTS AND DISCUSSION

3.1. Synthesis of Gold Nanoparticles

3.1.1. Determining the Optimal Synthesis Method

For a long time since its development by John Turkevich, the Turkevich method has been the standard method of synthesizing gold nanoparticles with different sizes [125]. During the synthesis process, the reduction of gold atoms from Au^{+3} state to Au^0 happens and gold nuclei are formed according to the following reaction.



In the absence of the reducing agent gold atoms in the solution are in the form of Au^{+3} . By the introduction of reducing agent zero state (Au^0) gold atoms are formed in the solution. Formation of the gold atoms continues up to a point of supersaturation in which the concentration of atoms exceeds saturation. At this point, particles are formed and act as nucleation sites for following binding of dissolved gold atoms and growth of the nanoparticles (Figure 5) [129].

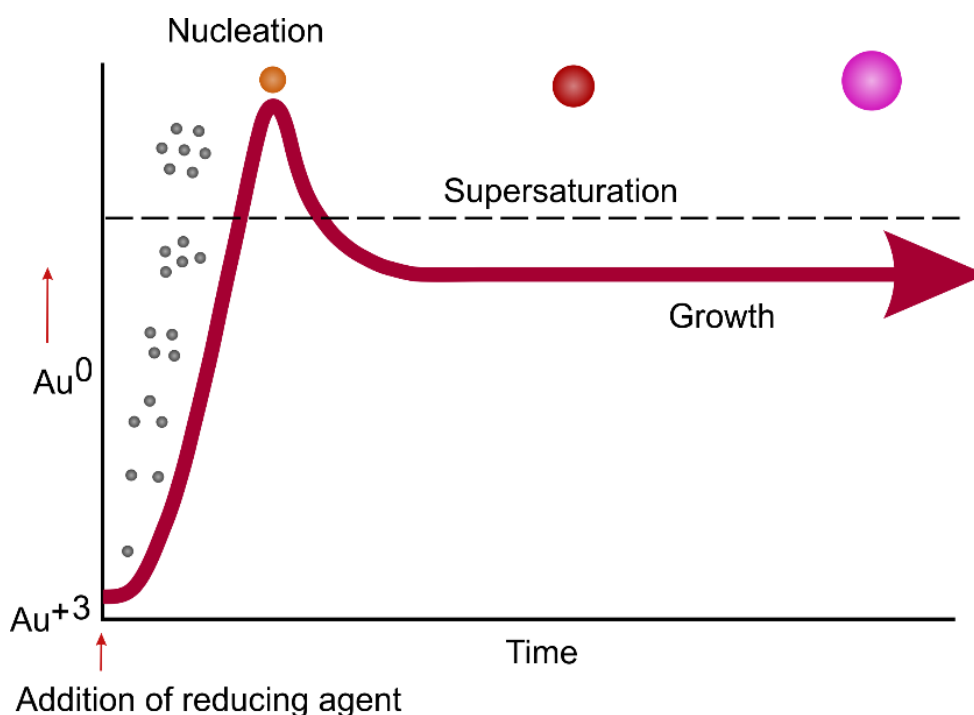


Figure 5. Mechanism of synthesizing gold nanoparticles [129].

As mentioned above nucleation and growth process is very important and should be optimized in order to synthesize highly monodisperse gold nanoparticles. During the synthesis process, it was found that Turkevich method is only suitable for synthesizing gold nanoparticles between 15-25 nm size ranges. But it should be noticed that gold nanoparticles synthesized with conventional Turkevich method were polydisperse with two peaks (Peak 1: 22.53 nm, Peak 2: 4008 nm) and had a polydispersity index (PDI) of 0.21 (Figure 6). Therefore, in this thesis, we modified the conventional method and synthesized nanoparticles were in the size range of 19 nm and had a PDI of 0.05 (Figure 6). By comparing the results, it is obvious that gold nanoparticles synthesized with modified Turkevich method were highly monodisperse.

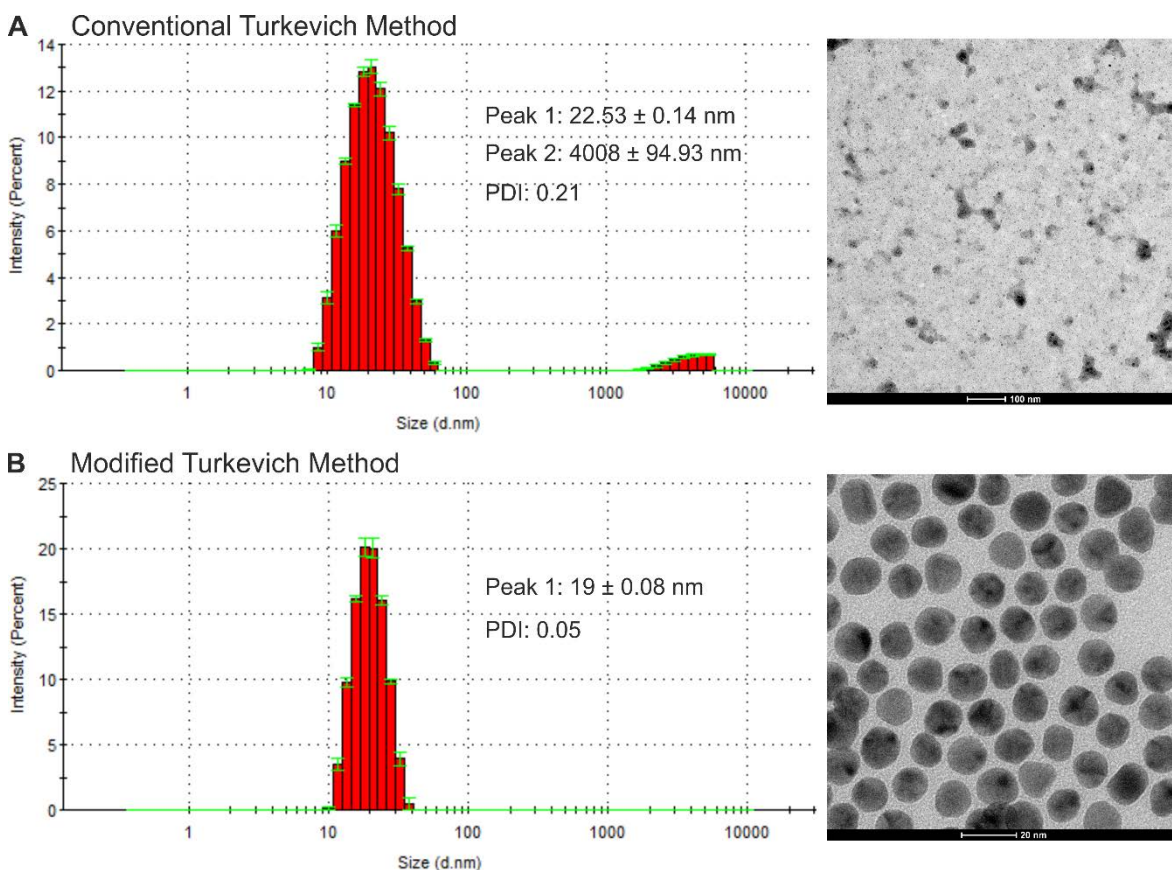


Figure 6. Characteristics of synthesized gold nanoparticles. A) Nanoparticles synthesized with conventional Turkevich method. B) Nanoparticles synthesized with modified Turkevich method.

To synthesize larger gold nanoparticles with the size of about 50 nm, two different methods (Turkevich method and Seeding-Growth method) were used and compared. It was found the Turkevich method is not suitable for the synthesis of gold nanoparticles above 20 nm size range and synthesized gold nanoparticles had two peaks (Peak 1: 50.14 nm, Peak 2: 3.77 nm) with the PDI of 0.55 (Figure 7). For larger size nanoparticles ($50 \geq$), by increasing the size polydispersity index of the nanoparticles increased as well. On the other hand, gold nanoparticles which were synthesized by seeding-growth method had a narrow size distribution (Peak 1: 50.07 nm) with the PDI of 0.05 (Figure 7). So, it can be seen that nanoparticles synthesized with seeding-growth method were highly monodisperse and this method was used for following production of gold nanoparticles with about 50 nm.

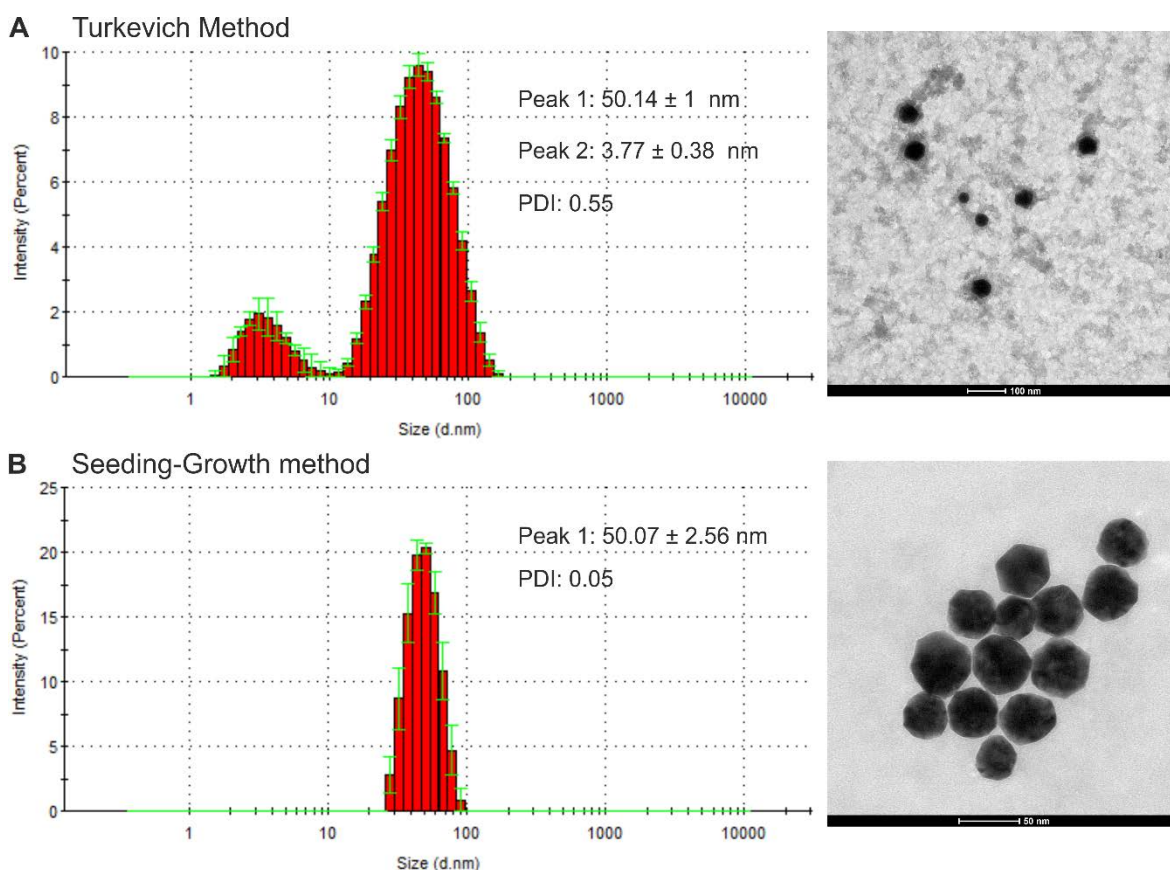


Figure 7. Characteristics of synthesized larger gold nanoparticles. A) Nanoparticles synthesized with conventional Turkevich method. B) Nanoparticles synthesized with the seeding-growth method.

3.2. Surface Modification of Gold Nanoparticles with Polyethylenimine

3.2.1. Synthesis of Citrate Capped Gold Nanoparticles in Different Size Ranges

Synthesis of gold nanoparticles was carried out in six different sizes with and without PEI functionalization as shown in table 1. Gold nanoparticles with the size of 19 nm (AuNP₁₉) were synthesized with high monodispersity by the modified Turkevich method and these nanoparticles were used as seed nanoparticles to synthesize larger nanoparticles (Figure 8 and Figure 9 A). In the Turkevich method, HAuCl₄ and trisodium citrate dehydrate concentrations play a fundamental role in the development of highly monodisperse gold nanoparticles with narrow size distribution. By adjusting these two parameters as mentioned above, we were able to synthesize seed nanoparticles with low PDI (0.05).

Table 1. Properties of synthesized gold nanoparticle groups.

Nanoparticles	Rounded Z-Average (nm)	Polydispersity index	Peak SPR Wavelength (nm)	Zeta potential (mV)
AuNP ₁₉ *	19 ± 0.02	0.05	519	-36.4
PEI/AuNP ₂₃	23 ± 0.03	0.19	532	+28.2
AuNP ₄₅	45 ± 0.3	0.05	527	-32.5
PEI/AuNP ₄₈	48 ± 0.2	0.05	527	+45.6
AuNP ₇₆	76 ± 0.2	0.07	548	-29.8
PEI/AuNP ₈₂	82 ± 0.3	0.05	548	+45.0

*Subscript represents the size of nanoparticles

By using the seed gold nanoparticles, larger gold nanoparticles (AuNP₄₅, AuNP₇₆) were synthesized by seeding-growth method (Figure 8 and Figure 9 C, E). As a significant rule in the seeding-growth method, highly monodisperse seed

nanoparticles will result in larger gold nanoparticles with narrow size distribution and low PDI. It can be seen from SEM images that synthesized nanoparticles had a uniform shape and narrow size distribution. Likewise, larger gold nanoparticles were highly monodisperse with the polydispersity index (PDI) of 0.05 (Table 1 and Figure 8). Gold nanoparticles in their specific size have their own specific SPR peak and the spectrum changes with any change in the size of nanoparticles. Thus, as it is shown in figure 8 B the shifts in the spectrum prove the gold nanoparticles with different sizes.

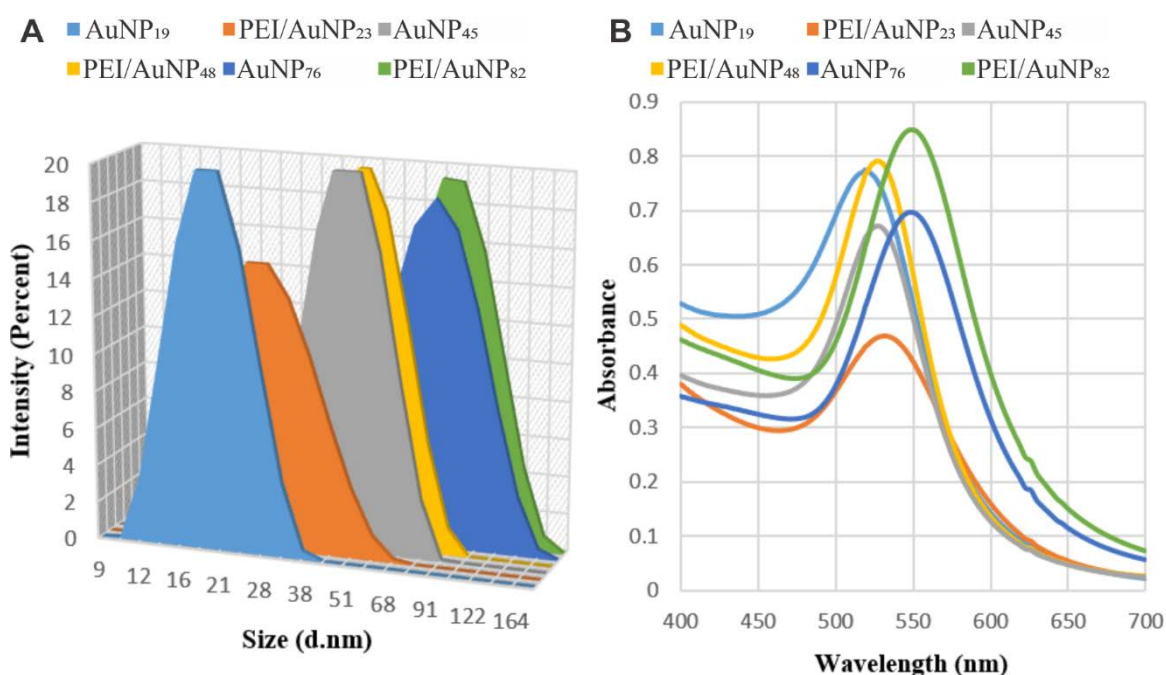


Figure 8. Characteristics of synthesized gold nanoparticles. A) Size distribution of the nanoparticles showing the shifts in size after PEI modification B) UV-visible spectrum of nanoparticles showing the shifts in the spectrum after PEI modification.

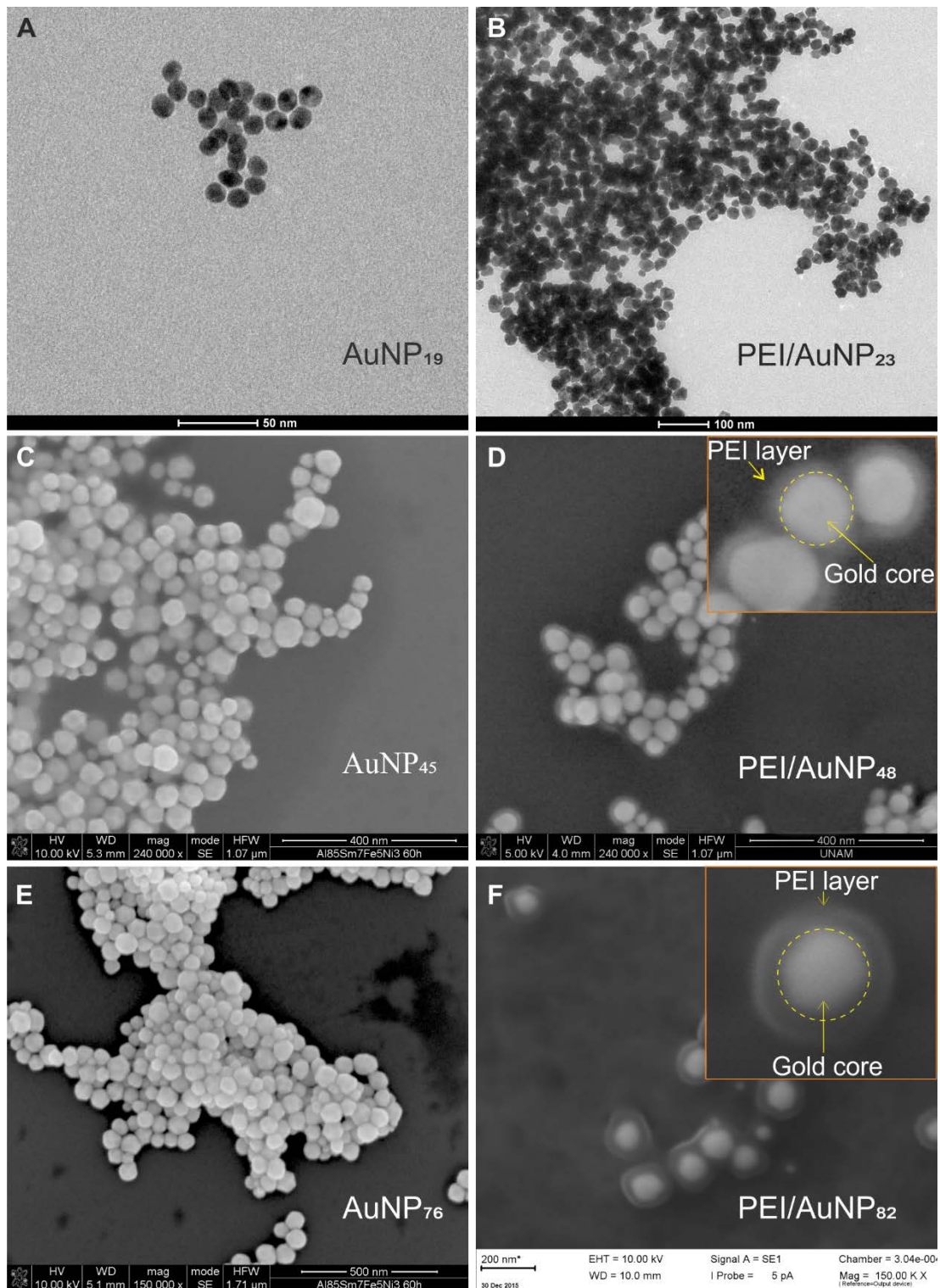


Figure 9. Transmission electron microscope (TEM) and scanning electron microscope (SEM) images of gold nanoparticles showing the morphology, size and PEI coating. A) AuNP₁₉ (Seed gold nanoparticles). B) PEI/AuNP₂₃ nanoparticles. C) AuNP₄₅ nanoparticles. D) PEI/AuNP₄₈ nanoparticles. E) AuNP₇₆ nanoparticles. F) PEI/AuNP₈₂ nanoparticles.

3.2.2. Polyethylenimine Modification of Gold Nanoparticles in Different Size Ranges

Recently, gold nanoparticles are of much interest due to either their ease of synthesis or their easy functionalization by different chains and chemical groups like; amine, carboxyl, hydroxyl, etc. In this regard, functionalization of gold nanoparticles with amine (-NH₂) containing polymers is still a challenging task as electrostatic interactions between negatively charged gold nanoparticles and positively charged polyelectrolytes can lead to irreversible aggregation of gold nanoparticles. Polymers such as; chitosan [130], polyethyleneimine (PEI) [122] and poly(L-lysine) [131] which have many amine groups in their structure are great candidates for this purpose. Among the mentioned polymers, PEI has been widely used for gene delivery applications and because of that functionalization of gold nanoparticles with PEI has garnered much attention. Generally, amine-functionalized nanoparticles are considered as the gold standard in gene delivery studies for the delivery of oligonucleotides like siRNA [124] and DNA [132]. Negatively charged oligos can be easily conjugated to the surface of PEI-functionalized gold nanoparticles. Also, as it was noticed during the experiments PEI functionalization increases the gold nanoparticles stability inside the cell culture medium.

To date, methods such as; reduction of HAuCl₄/PEI solution by sodium borohydride (NaBH₄), direct reduction of chloroauric acid (HAuCl₄) by PEI at room temperature, thermal reduction of HAuCl₄/PEI solution [133], reduction of thiolated PEI (PEI-SH)/HAuCl₄ solution by NaBH₄ [134, 135], and surface modification with 11-mercaptoundecanoic acid (MUA) to stabilize 18 nm gold nanoparticles for following PEI functionalization [123] have been used for the functionalization of gold nanoparticles with PEI. However, by examining the transmission electron microscope images, it was clear that none of these methods have yielded highly monodisperse PEI coated gold nanoparticles. The main handicap for the low quality of PEI modified gold nanoparticles is the sensitivity of gold colloids to positively charged polymers and the imposed aggregation of nanoparticles upon polyelectrolyte addition.

Here in this thesis, two different methods were examined for the preparation of PEI-functionalized gold nanoparticles. In our developed method, PEI functionalization

was carried out after the seeding-growth process as mentioned in the methods section (Figure 10). It was found that the stability of gold nanoparticles after the seeding-growth process was higher and nanoparticles could stand the addition of PEI and charge change without any sign of aggregation. Developed PEI-functionalized gold nanoparticles (PEI/AuNP₄₈, PEI/AuNP₈₂) were highly monodisperse with the PDI of 0.05 (Table 1). Very precise shifts in the size distribution graph and UV-visible spectrum of the nonfunctionalized (AuNP₄₅, AuNP₇₆) and functionalized (PEI/AuNP₄₈, PEI/AuNP₈₂) nanoparticles were all proving the binding of PEI to the surface of gold nanoparticles (Figure 8 A and B). Also, another compelling proof is the change in the zeta potential values from negative to positive (from -32.5 for AuNP₄₅ to +45.6 for PEI/AuNP₄₈ and from -29.8 for AuNP₇₆ to + 45 for PEI/AuNP₈₂). Additionally, SEM images in figure 9 D and F are clearly showing the uniform surface functionalization with PEI (PEI layer ~ 4-6 nm) without any aggregation.

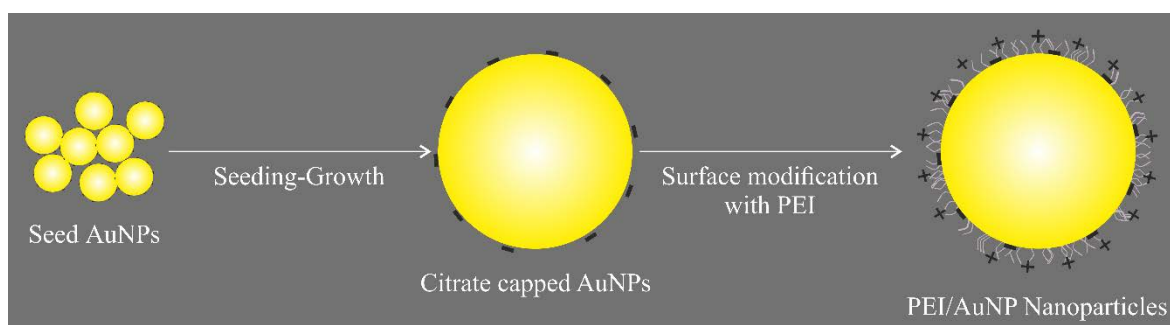


Figure 10. Seeding-growth and functionalization of gold nanoparticles surface with PEI.

In order to compare the results with previous methods, PEI functionalization was also carried out by conventional direct reduction of H₂AuCl₄ with PEI [133]. In this method, PEI is directly added to the H₂AuCl₄ solution in 0.015% concentration and stirred at RT for 1 week. It was found that the prepared PEI functionalized gold nanoparticles (PEI/AuNP₂₃) were very polydisperse with PDI of 0.19 (Table 1). Also, size distribution graph of the nanoparticles was very broad which is another indicator of the low quality of the sample (Figure 8 A). As it is shown by TEM image in figure 9 B, most of the nanoparticles were in the aggregated form and complete aggregation of the nanoparticles happened during a one-month period. However,

PEI functionalized gold nanoparticles prepared by our developed method were stable even after one year.

As a result, PEI functionalization of gold nanoparticles after seeding-growth process yields highly monodisperse surface modified nanoparticles with high stability, which increased the shelf life of gold nanoparticles to more than 1 year. With the proposed method, PEI functionalized gold nanoparticles in desired size ranges and zeta potentials can be prepared precisely with a thin layer of PEI, without any unwanted changes in size and polydispersity.

3.3. Cellular Biodistribution and Imaging Potential of Gold Nanoparticles

3.3.1. Effect of Gold Nanoparticles on Cell Morphology

Cellular biodistribution and imaging studies were carried out in dorsal root ganglion sensory neurons (DRG) as these cells are known to be very difficult to transfect. Morphology of the DRG neurons after 2 h was spherical without any axon or neurite elongation with small satellite cells around the cell bodies of the neurons (Figure 11 A1). Neurite elongations, axons and synaptic connections between neuronal cells were visible after 24 h (Figure 11 A2). It should be noticed that DRG neurons are postmitotic cells and do not have the ability of proliferation. On the other hand, glial cells can divide and increase their number.

In order to evaluate the effect of gold nanoparticles on cell morphology they were added in two different concentrations (5 µg/mL, 50 µg/mL) and their effects on cells were evaluated at two time points (24 h and 48 h) by using Hoffman microscope (Figure 11 B1-B2). For low concentration (5 µg/mL) no significant effect was observed on the cells, however, for high concentration (50 µg/mL), PEI/AuNP₂₃ nanoparticles adversely affected the normal spherical cell morphology. It can be explained by the high amount of PEI which is used in the conventional method of surface modification (Figure 11 E1 and E2). Also, by close inspection of the images, it was found that citrate capped gold nanoparticles (AuNP₁₉ and AuNP₄₅) had a relatively fast excretion rate (Figure 11 C1, C2 and G1, G2). For PEI/AuNP₂₃, aggregates were visible for low concentration as well that is in close relation to the low stability and fast excretion of these nanoparticles by cells. On the other hand, there was no sign of aggregation in the medium for gold nanoparticles functionalized by our developed (PEI/AuNP₄₈ and PEI/AuNP₈₂) which can be explained by their high uptake rate, late excretion and high stability (Figure 11 H1-I2 and L1-M2).

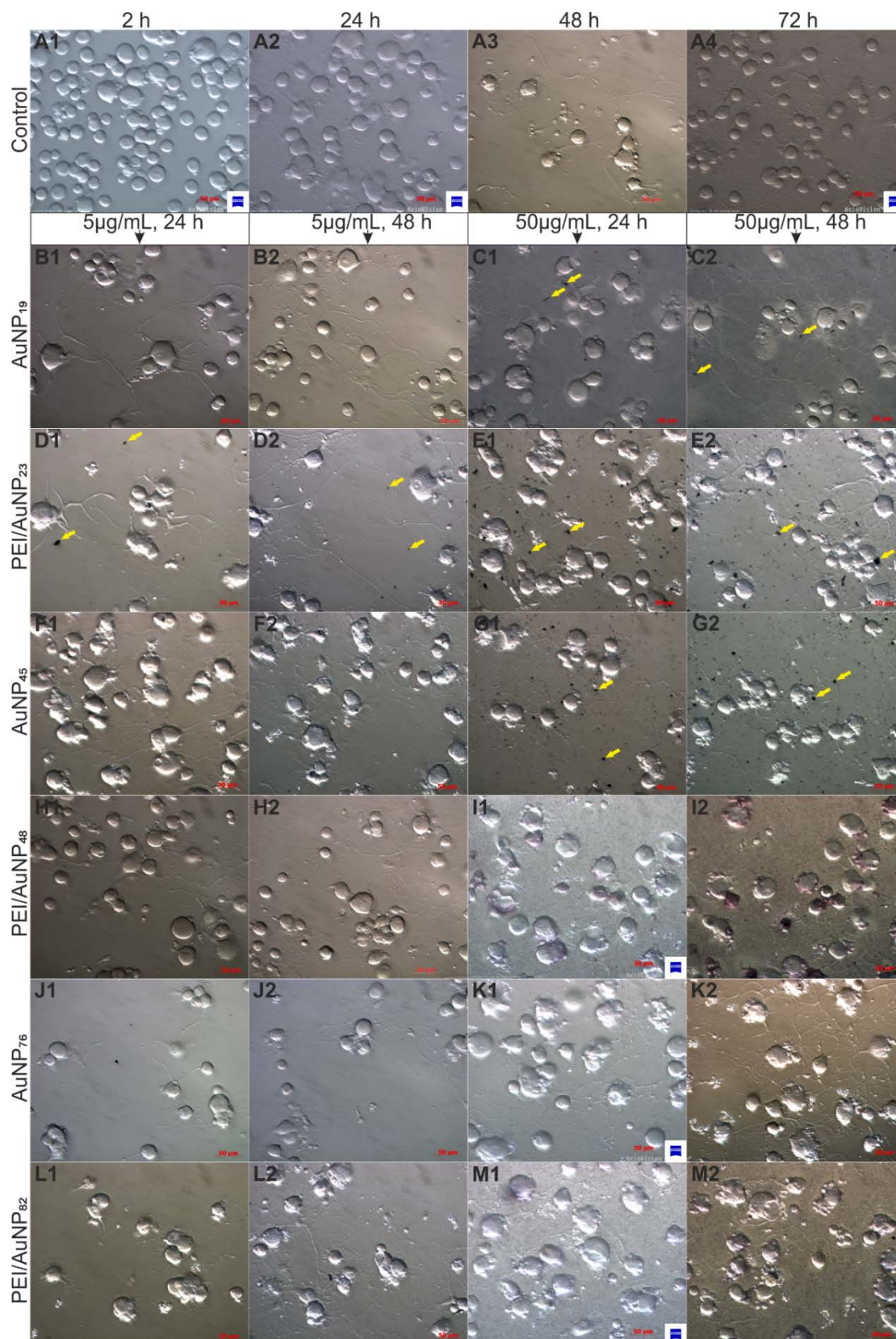


Figure 11. Hoffman modulation contrast microscope images of the DRG neurons before and after incubation with different gold nanoparticle groups. Yellow arrows are showing the nanoparticle aggregates.

As it has been previously reported by Chithrani and Chan [136], the uptake and excretion of nanoparticles are size-dependent. It has been reported that smaller NPs have a faster exocytosis rate with a higher percentage than large NPs. For instance, according to previously published results exocytosis of 14 nm NPs was two times faster and higher than NPs with 74 nm size range. They studied the excretion of nanoparticles over 8 h period and found that the fraction of exocytosed nanoparticles were 0.4, 0.2, 0.1 for 14 nm, 50 nm and 74 nm nanoparticles, respectively. Also, it has been reported by other groups that factors such as; surface charge, ligand and shape of the nanoparticles are very significant factors in determining their rate of excretion [137]. Similarly, it has been mentioned by Oh and Park [138] that positively charged nanoparticles have a predilection to stay longer in the cell. This statement explains the reason why PEI-functionalized gold nanoparticles with larger sizes tended to stay longer in the cell and even after 48 h there was no sign of aggregates.

3.3.2. Effect of Gold Nanoparticles on Cell Viability

The toxicity of gold nanoparticles has long been investigated and the particles found to be nontoxic [139-142]. However, some studies have suggested that AuNPs with the size of 5 nm may exert some cytotoxic effects while nanoparticles above this size were nontoxic [143]. For the accurate assessment of cell viability, only DRG neurons were counted and glial cells were just ignored. For cells in time zero cell viability was accepted to be 100%. Any adverse effect on the cell viability was determined by detecting the cells stained with propidium iodide. Gold nanoparticles in three different concentrations (0.5 $\mu\text{g/mL}$, 5 $\mu\text{g/mL}$, 50 $\mu\text{g/mL}$) were incubated with cells and cell viability was evaluated at four different time points (2 h, 24 h, 48 h, 72 h) (Figure 12). There was not any significant toxicity associated with the lowest concentration (0.5 $\mu\text{g/mL}$) for all the nanoparticle groups. For moderate concentration (5 $\mu\text{g/mL}$) decrease in cell viability was noticed for AuNP₄₅ (Figure 12 B). For high concentration (50 $\mu\text{g/mL}$) a dose dependent decrease happened for AuNP₄₅, AuNP₇₆, and PEI/AuNP₈₂, however, it should be noticed that all the nanoparticle groups had a cell viability of above 80% which is considered to be non-toxic (Figure 12 C).

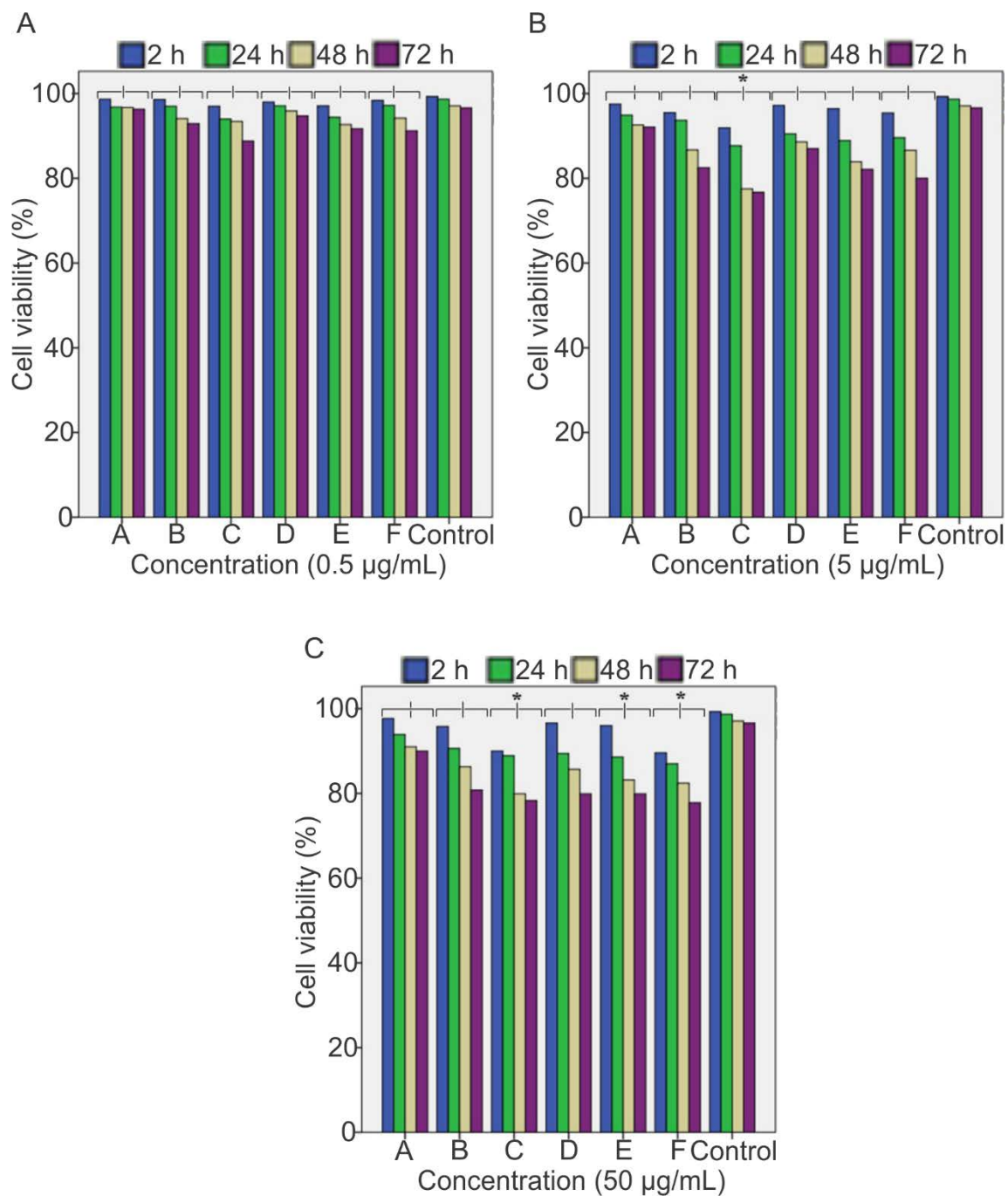


Figure 12. Cell viability studies showing the effect of gold nanoparticles on cells at different concentrations and time intervals. A) 0.5 µg/mL. B) 5 µg/mL. C) 50 µg/mL. Samples are labelled as; (A) AuNP₁₉, (B) PEI/AuNP₂₃, (C) AuNP₄₅, (D) PEI/AuNP₄₈, (E) AuNP₇₆, (F) PEI/AuNP₈₂.

It is known that molecular weight and concentration of PEI are two very important factors that play a critical role in cellular cytotoxicity and transfection. However, at higher molecular weights and concentrations both the imposed toxicity and transfection increase accordingly [144, 145]. By our developed functionalization procedure only a trivial amount of low molecular weight (2000 MW) PEI (0.005%) is used and according to the cell viability test, even at high concentrations, functionalized nanoparticles were considered to be non-toxic.

We also investigated the toxicity of both 51 nm citrate capped gold nanoparticles and 54 nm PEI-functionalized gold nanoparticles on standard L929 fibroblast cells at different concentrations (5, 20, 50, 100, 150, and 200 $\mu\text{g/mL}$). It was found that cell viability was over 75% for both citrate capped and PEI-functionalized gold nanoparticles even at the highest concentration (200 $\mu\text{g/mL}$), which was not due to the toxicity of gold nanoparticles but rather was a dose-dependent toxicity (Figure 13 A and B). It should be noted that the concentrations above 50 $\mu\text{g/mL}$ were not even used during the *in vivo* studies and were tested just to demonstrate that synthesized gold nanoparticles were nontoxic even at the highest concentrations.

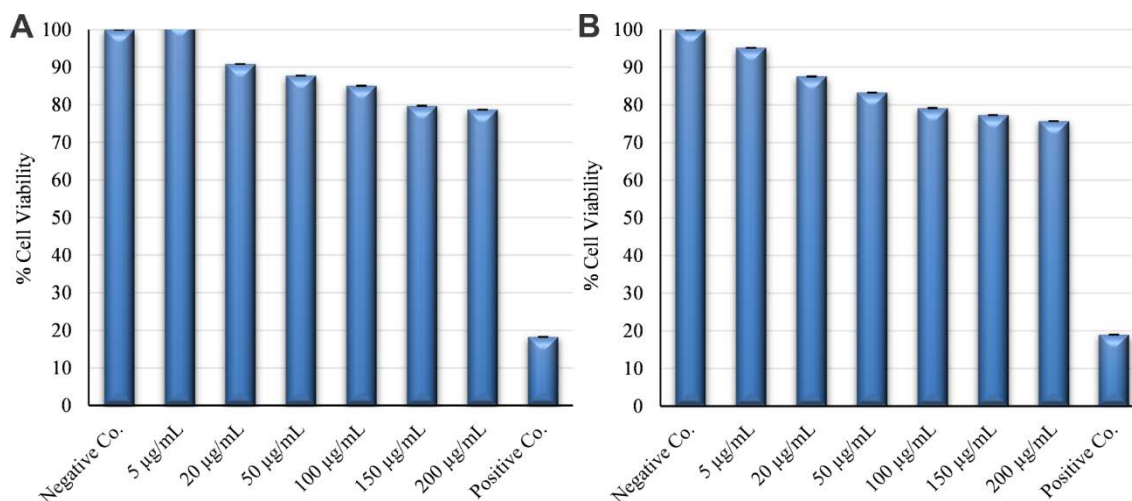


Figure 13. Toxicity of citrate capped and PEI-functionalized gold nanoparticles on L929 fibroblast cells. A) Cell viability by the treatment with 51 nm citrate capped gold nanoparticles. B) Cell viability for 54 nm PEI-functionalized gold nanoparticles. DMSO was used as a positive control for cell viability.

3.3.3. Effect of Gold Nanoparticles on Neural Cell Skeleton

In order to investigate any potential toxic effects in detail, ICC staining was performed and the expression of neural cell skeleton components such as; β -III tubulin and NF 200 filaments was imaged. In this regard, gold nanoparticles in 5 $\mu\text{g}/\text{mL}$ concentration were incubated with the DRG cells for 48 h (Figure 14). It was found that for all the nanoparticles except PEI/AuNP₂₃, there was not any adverse effect on cell skeleton components. However, about the cells incubated with PEI/AuNP₂₃, NF 200 filament (associated with the red color) was adversely affected (Figure 14 C1-C3). This unfavorable effect can be explained by the method of synthesis which relies on the direct reduction of HAuCl_4 with PEI, in which to obtain nanoparticles with smaller sizes the higher amount of PEI is needed which in turn increases the toxicity.

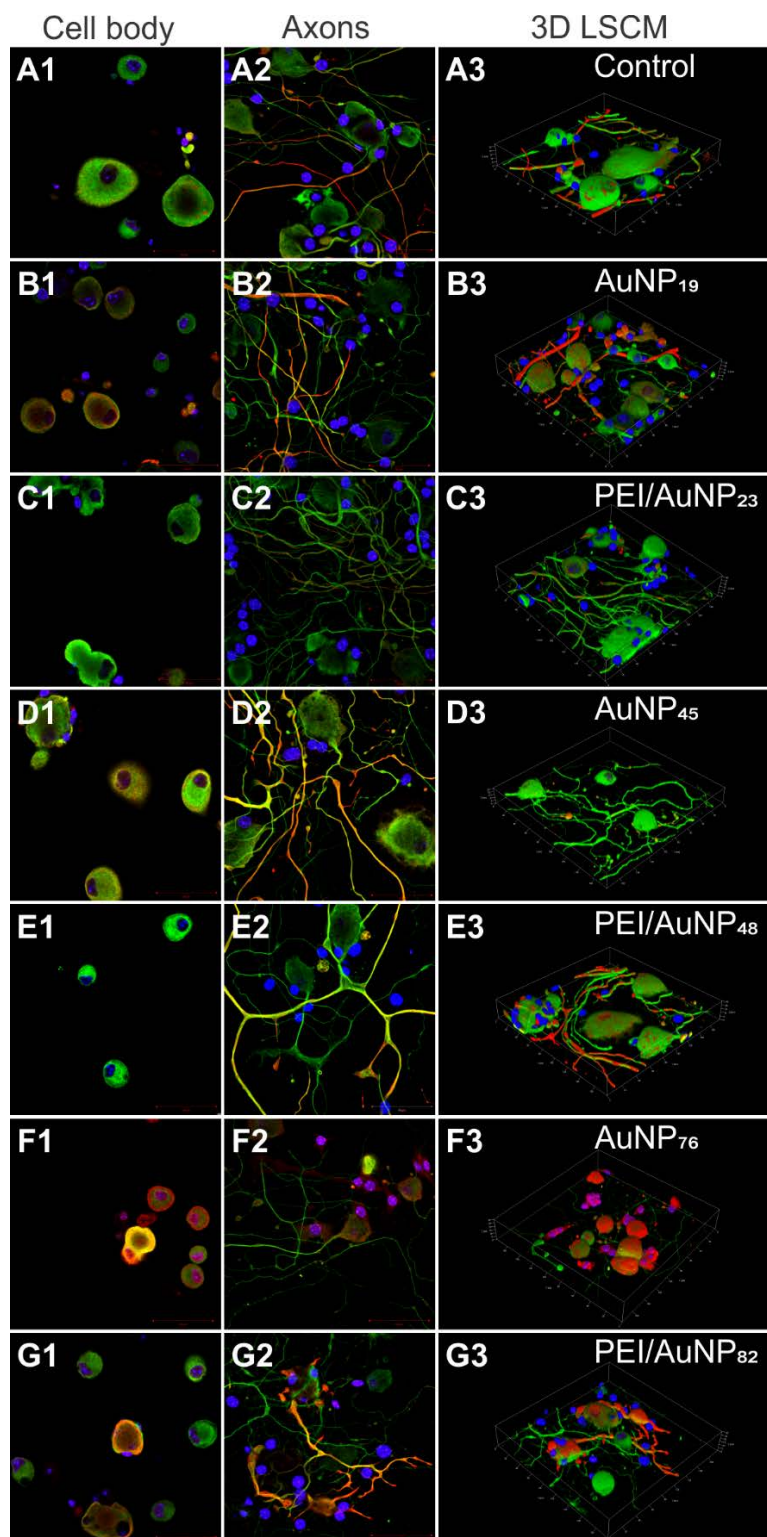


Figure 14. Effect of citrate capped and PEI-functionalized gold nanoparticles on DRG neural cell skeleton. A1-A3) Control. B1-B3) AuNP₁₉ nanoparticles. C1-C3) PEI/AuNP₂₃ nanoparticles. D1-D3) AuNP₄₅ nanoparticles. E1-E3) PEI/AuNP₄₈ nanoparticles. F1-F3) AuNP₇₆ nanoparticles. G1-G3) PEI/AuNP₈₂ nanoparticles. Images were taken by using 40x objective.

3.3.4. Cellular Uptake of Gold nanoparticles

The amount of internalized gold nanoparticles was determined by analyzing the cell lysates with ICP-MS instrument. DRG cells were cultured for 24 h, and then they were incubated with gold nanoparticles for 4 h. As mentioned above nanoparticles excretion happens in 24 h, so cell uptake studies were carried out after 4 h of incubation with nanoparticles. The amounts of internalized gold nanoparticles are shown in table 2. By inspecting the results it is obvious that the size of nanoparticles plays a key role in their uptake and with the increase in the size of the nanoparticles the uptake amount of the nanoparticles increases as well. Uptake of the gold nanoparticles in 50 µg/mL concentration increased from 10.34 % for AuNP₁₉ to 41.34 % and 34.26 % for AuNP₄₅ and AuNP₇₆, respectively. This result coincides with the results obtained by Gao et al. [146]. They stated that wrapping time, which is described as how a membrane encloses a particle, is very important in the cellular uptake of gold nanoparticles and it changes in correlation with the size of the nanoparticle. They mentioned that the wrapping time for the nanoparticles with the size of 55 nm was minimum and this led to a higher uptake rate of the 55 nm nanoparticles. On the other hand, it has been discussed that the free energy of smaller nanoparticles will not be sufficient to thoroughly wrap the nanoparticles by the membrane which will result in the prevention of endocytosis assisted cellular uptake of the nanoparticles [136].

Table 2. Uptake amounts of gold nanoparticles (%) in DRG neurons.

	AuNP concentration (0.5 µg/mL)	AuNP concentration (5 µg/mL)	AuNP concentration (50 µg/mL)
AuNP ₁₉	18%	17.6%	10.34%
PEI/AuNP ₂₃	22%	20.4%	16.32%
AuNP ₄₅	10.6%	17.6%	41.34%
PEI/AuNP ₄₈	30%	22.8%	53.58%
AuNP ₇₆	42%	29.2%	34.26%
PEI/AuNP ₈₂	50%	44%	71.1%

**Subscript represents the size of nanoparticles*

As it is reported in table 2, in compare to citrate capped gold nanoparticles for all the concentrations cellular uptakes of PEI functionalized gold nanoparticles were higher. For high concentration, the difference in the uptake of nanoparticles was at the significant level ($p < 0.05$). Comparing the results for AuNP₇₆ and PEI/AuNP₈₂, it was found that the cellular uptake of the nanoparticles doubled (from 34.26% to 71.1%) with PEI functionalization. It can be noticed that for PEI-functionalized gold nanoparticles nearly half of the amounts of nanoparticles entered into the cells. So, it can be concluded that the surface modification of gold nanoparticles can affect their cellular uptake which in the case of DRG neurons that are known to be very difficult to transfect, the uptake amount was almost doubled for PEI functionalized gold nanoparticles. These results can also be proved by the optical measurement images which showed the rapid and complete uptake for larger gold nanoparticles and latest excretion time for the PEI-functionalized gold nanoparticles [147]. Taking into account that uptake studies were carried out on DRG neurons which are postmitotic cells and the transfection is literally difficult in these cells, achieved results are far better than existing approaches.

3.3.5. Imaging the Cellular Biodistribution of Gold Nanoparticles by Confocal Microscope

Cellular biodistribution of gold nanoparticles was monitored by real time imaging with laser scanning confocal microscope without using any fluorescent dye. Following 30 min incubation of the cells with gold nanoparticles, imaging was carried out for 2 h under LSCM microscope in five different modes of imaging (classical mode, T-PMT mode, 3D mode, time series mode and tile scan mode). After testing various excitation and emission parameters it was found the excitation value of 490 nm and emission value of 525 nm were optimal imaging parameters. These parameters are the same as the standard parameters for Alexa 488 dye. In order to eliminate the noise/autofluorescence phenomena stemming from the high intensity of the laser, all the adjustments were carried out on control group cells with no visible signal to provide no noise/no autofluorescence condition (Figure 15 A1 and A2).

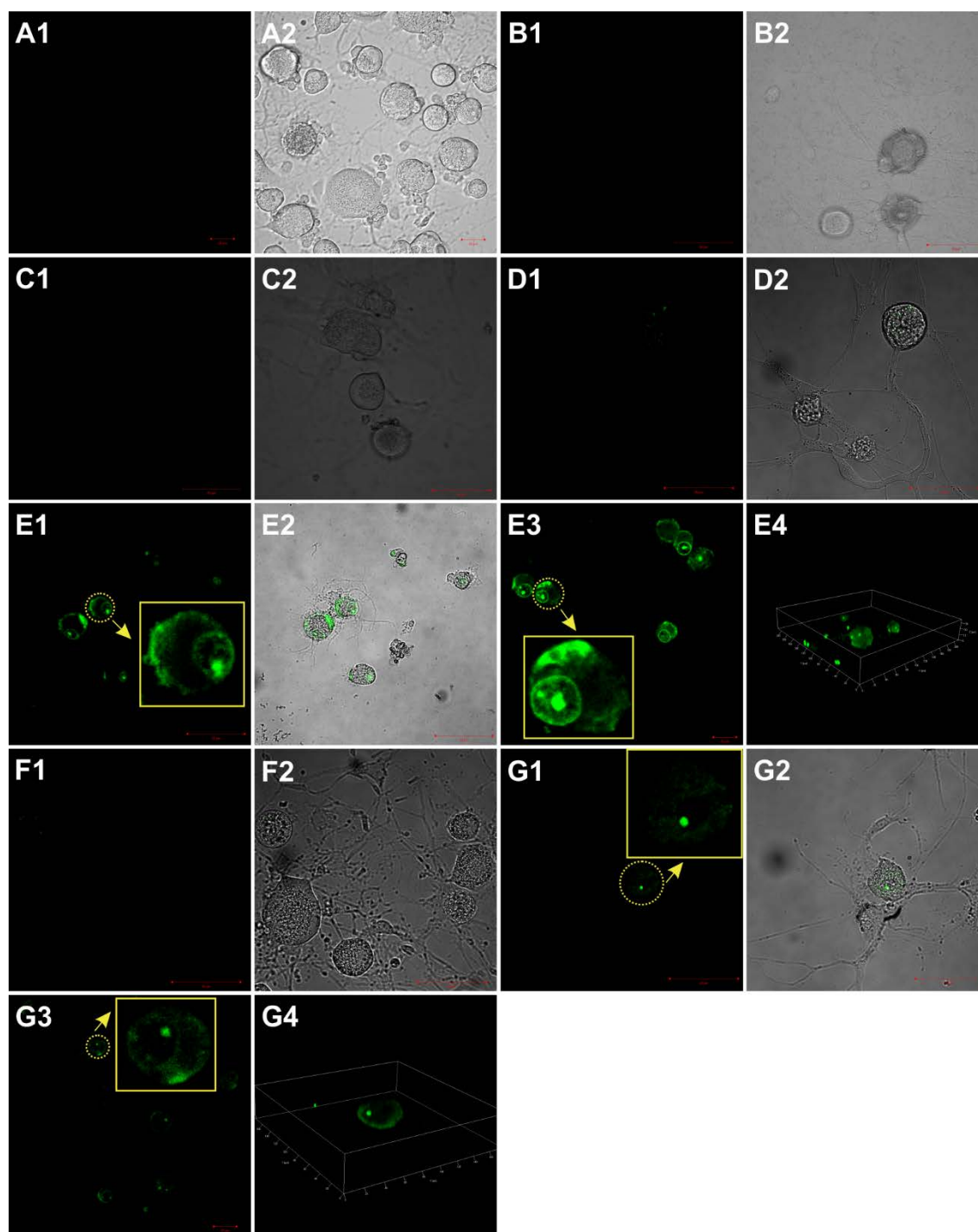


Figure 15. Imaging gold nanoparticles incubated cells with laser scanning confocal microscope. (a1, a2) Control. (b1, b2) AuNP₁₉. (c1, c2) PEI/AuNP₂₃. (d1, d2) AuNP₄₅. (e1-e4) PEI/AuNP₄₈. (f1, f2) AuNP₇₆. (g1-g4) PEI/AuNP₈₂. Images in T-PMT mode have a gray background.

As for control group, there was not any obtained signal for AuNP₁₉ and PEI/AuNP₂₃ and we were not able to image the cells with the small gold nanoparticles (Figure 15 B1-C2). As the size of gold nanoparticles increased visible signal were obtained, however, the obtained signal was too weak for citrate capped gold nanoparticles (AuNP₄₅ and AuNP₇₆) and consequently the resolution of the obtained images was very low (Figure 15 D and F). Klein et al. [148], have also mentioned before that gold nanoparticles of over 40 nm size range can be imaged under the confocal microscope but however, this signal is too weak to provide a clear image of the cell. On the other hand, image resolution attained from PEI-functionalized gold nanoparticles (PEI/AuNP₄₈ and PEI/AuNP₈₂) was a lot higher and much stronger signals were obtained without any noise (Figure 15 E and G). Also, by looking at the images of the cells incubated with PEI/AuNP₄₈ and PEI/AuNP₈₂ it is easy to accurately determine the cellular localization of nanoparticles. Cellular biodistribution of PEI-functionalized gold nanoparticles (PEI/AuNP₄₈) was better visualized by time-lapse images which beginning from the fifth minute of incubation, were taken every five minutes (Figure 16). By evaluating the images, it was found that during the initial period of incubation nanoparticles were near the cell membrane and after entrance, they distributed in the cytoplasm over time and finally strong signals were received from the cell nucleolus which showed the localization of PEI-functionalized gold nanoparticles in this small compartment.

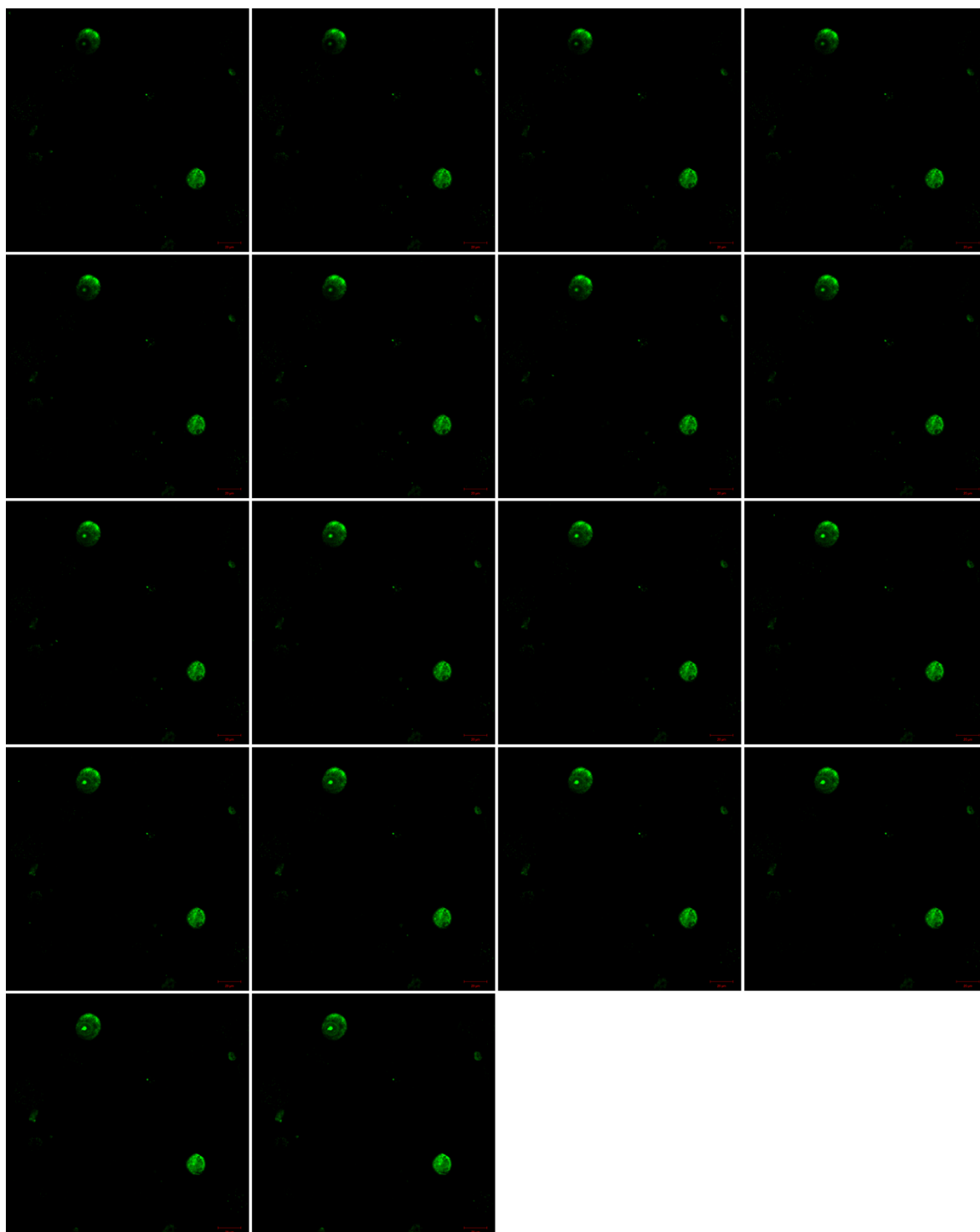


Figure 16. Times series mode imaging of the PEI/AuNP₄₈ nanoparticles. Images were taken by using 40x objective and they were taken with 5 min intervals.

3.3.6. Nucleolar Localization of PEI-Functionalized Gold Nanoparticles

From the tile scan and maximum intensity projection images in figure 17, it can be seen that all the cells in the petri dish were clearly visualized by PEI/AuNP₄₈ nanoparticles and obtained results can be referred to every single cell in the petri dish (Figure 17 A and B). The magnified image in figure 17 C shows that apart from the imaging of the cells in whole, PEI-functionalized gold nanoparticles can be used as delivery agents for nucleolar targeting in cells. The high signal intensity inside the nucleolus proves the nanoparticles amassing inside the nucleolus and implies that these nanoparticles pass through the cell nucleus and move towards the cell nucleolus which finally, before being excreted by different cellular mechanisms localize in this small compartment of the cell.

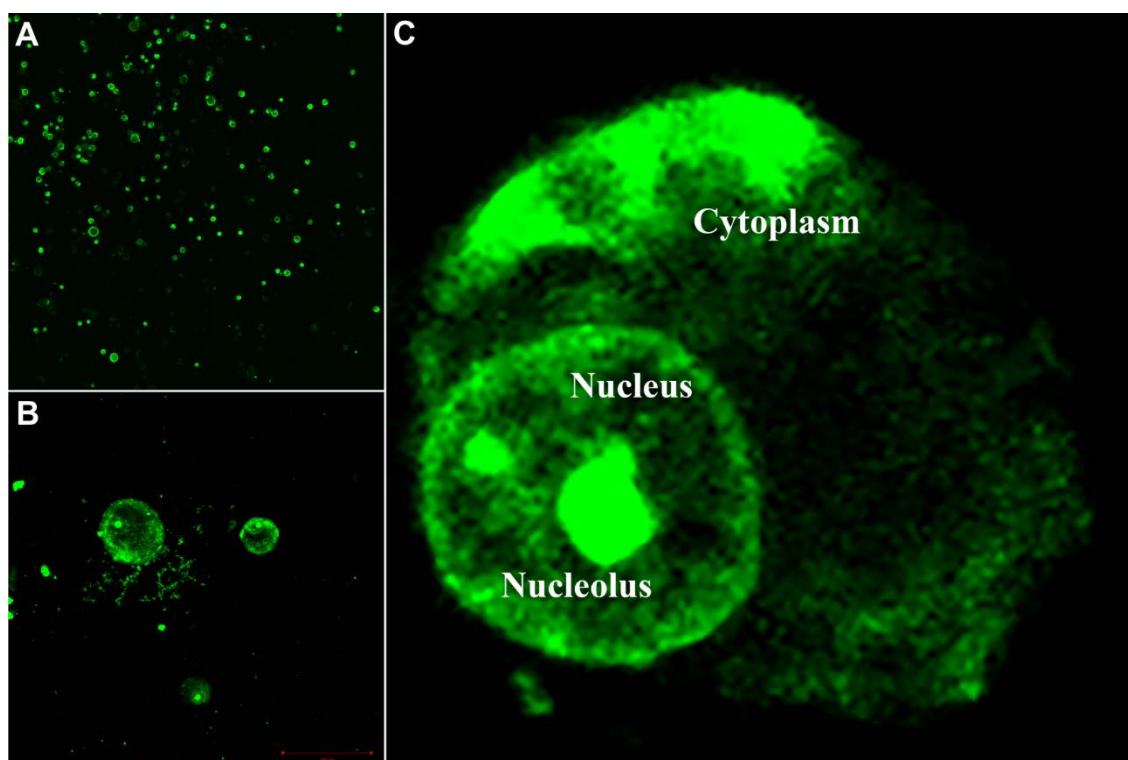


Figure 17. Nucleolar localization of PEI-functionalized gold nanoparticles. A) Tile scan mode. B) Maximum intensity projection mode. C) Magnified confocal image.

Imaging the cells after 24 h of incubation with PEI-functionalized nanoparticles showed that nanoparticle aggregates were excreted from the cell and there was not any obtained signal from the cells. Nevertheless, after washing the cells and

incubating the nanoparticles (PEI/AuNP₄₈ and PEI/AuNP₈₂) with cells, strong signals were obtained from the cell nucleolus (Figure 18). It should be noticed that all the obtained signals and luminescence are actually specific emissions originated from the localized surface plasmon resonance of the gold nanoparticles in the specific size range.

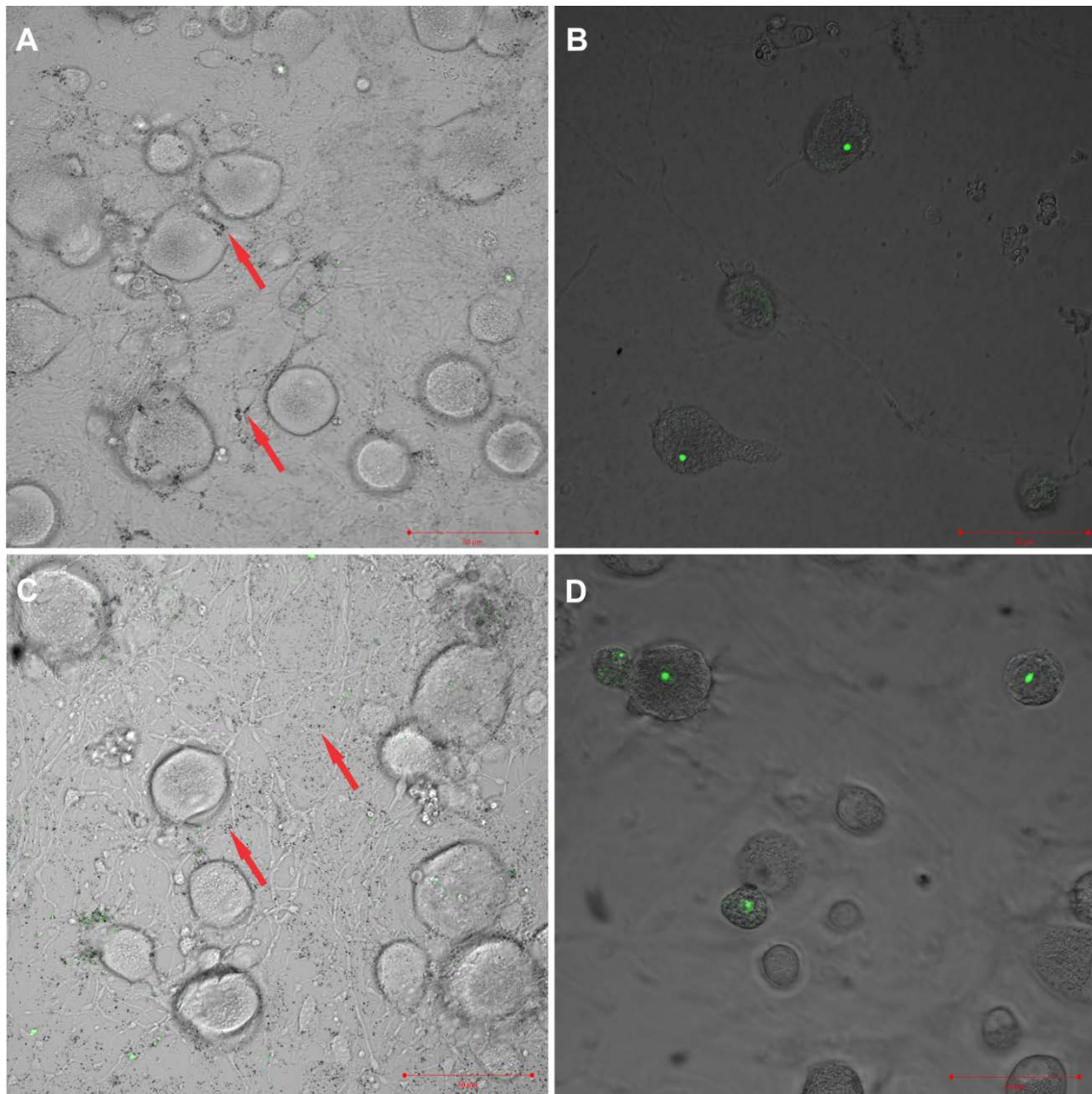


Figure 18. Washing and re-incubation of the cells with PEI-functionalized gold nanoparticles. A) DRG cells after 24 h of incubation with PEI/AuNP₄₈ nanoparticles. B) Re-incubation of the cells with PEI/AuNP₄₈ nanoparticles. C) DRG cells after 24 h of incubation with PEI/AuNP₈₂. D) Re-incubation of the cells with PEI/AuNP₈₂ nanoparticles. Excreted nanoparticle aggregates are shown with red arrows. Images were taken by using 40x objective.

To summarize, as it has been reported before, gold nanoparticles with the sizes over 40 nm can be visualized under the confocal microscope [148]. Here in this thesis, by functionalizing the gold nanoparticles with PEI and imaging by confocal microscope it was found for the first time that PEI-functionalized gold nanoparticles can enter to cell nucleolus irrespective of their size. Evaluation of the cellular biodistribution of these nanoparticles by LSCM microscope clarified that both PEI/AuNP₄₈ and PEI/AuNP₈₂ with the z-averages of 48 nm and 82 nm respectively, localized in the nucleolus of the DRG neurons. This is in contrast to citrate capped gold nanoparticles which were not undergone any surface functionalization (AuNP₄₅ and AuNP₇₆ with the z-averages of 45 nm and 76 nm respectively) only localized in the cytoplasm (Figure 19). These results correct the previous information which emphasized that only gold nanoparticles of small sizes can localize to cell nucleus [149].

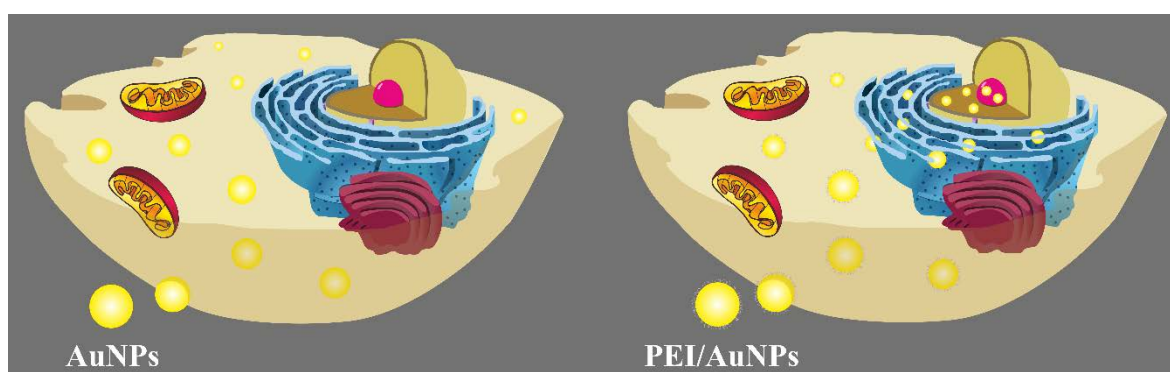


Figure 19. Cellular biodistribution of unfunctionalized citrate capped gold nanoparticles and PEI-functionalized gold nanoparticles.

Emission signal for unfunctionalized citrate capped gold nanoparticles was so weak however, the signal strength for PEI-functionalized gold nanoparticles was a lot higher, in a way that the cellular biodistribution of gold nanoparticles was clearly visible in the cytoplasm, nucleus and nucleolus. This result is in accordance with the uptake results which showed the high uptake rate for PEI-functionalized gold nanoparticles. The high resolution of the images and improved detection sensitivity by PEI-functionalized gold nanoparticles are reasoned to be related to both the

higher uptake rate of these nanoparticles which results in higher cumulative signal and also increased LSPR peak intensity with PEI functionalization (Figure 8 B). Owing to the higher signal intensity and not photo-bleachable properties of PEI-functionalized gold nanoparticles it was possible to track them inside the cell without any time limitation which constraints the use of fluorescent dyes. This advantage which is brought by these nanoparticles provided the time lapse imaging applicable which in turn showed the gradual increase in the signal intensity in the cell nucleolus over time. Again, by taking advantage of this properties it was possible to record the cellular biodistribution in a video format which showed that how fast is the entrance of nanoparticles and it occurs within 10 min by the distribution of nanoparticles in the cytoplasm, passing through the nucleus and eventually entering to the cell nucleolus.

Bearing in mind how difficult it is to transfect post-mitotic neurons [150], high uptake amount and nucleolar localization of surface functionalized gold nanoparticles potentiate the importance of PEI-functionalized gold nanoparticles as a delivery vehicle for the delivery of oligonucleotides and drugs to the cell nucleolus.

3.3.7. Imaging Gold Nanoparticle Incubated Cells by IR Irradiation

After incubating the PEI-functionalized gold nanoparticles with cells imaging was carried out under IR irradiation by using a two-photon microscope (Zeiss) (Figure 20). It was performed to prove the accuracy of cellular biodistribution and also show that imaging can be fulfilled under IR irradiation which is harmless and has a great tissue penetration. Imaging adjustments were as; the infra-red laser wavelength of 810 nm laser intensity of 5%, 700 gain master and a specific detector for Alexa 488. Two-photon microscope does not contain any incubator system and because of that cells were imaged for 30 min. Before imaging starts, adjustments were performed on control group cells to eliminate any potential noise or autofluorescence. It was found that the specific detector for Alexa 488 dye is an optimal parameter for imaging. In accordance with the LSCM results, it was found that the signal strength for PEI/AuNP₄₈ and PEI/AuNP₈₂ was the highest. It was also observed that glial cells and satellite cells were more saturated with nanoparticles. Image resolution for PEI/AuNP₈₂ was higher than PEI/AuNP₄₈ because of the LSPR peak of PEI/AuNP₈₂ which was in the infrared region. More detailed studies were carried out for cells incubated with PEI/AuNP₈₂ and it was found that likewise, the results obtained with

LSCM microscope, with the two-photon microscope the typical nucleolus saturation with PEI/AuNP₈₂ nanoparticles was observable too (Figure 20 C). Imaging with two-photon microscope underlined the fact that PEI/AuNP₄₈ and PEI/AuNP₈₂ can be used for in vivo imaging with IR irradiation. With high penetration capability of IR laser in tissues, these nanoparticles can be used in theranostic studies for real-time monitoring of the cells in vivo. Also, the obtained results confirmed the previous results and once again proved that the PEI-functionalized gold nanoparticles can enter to cell nucleolus.

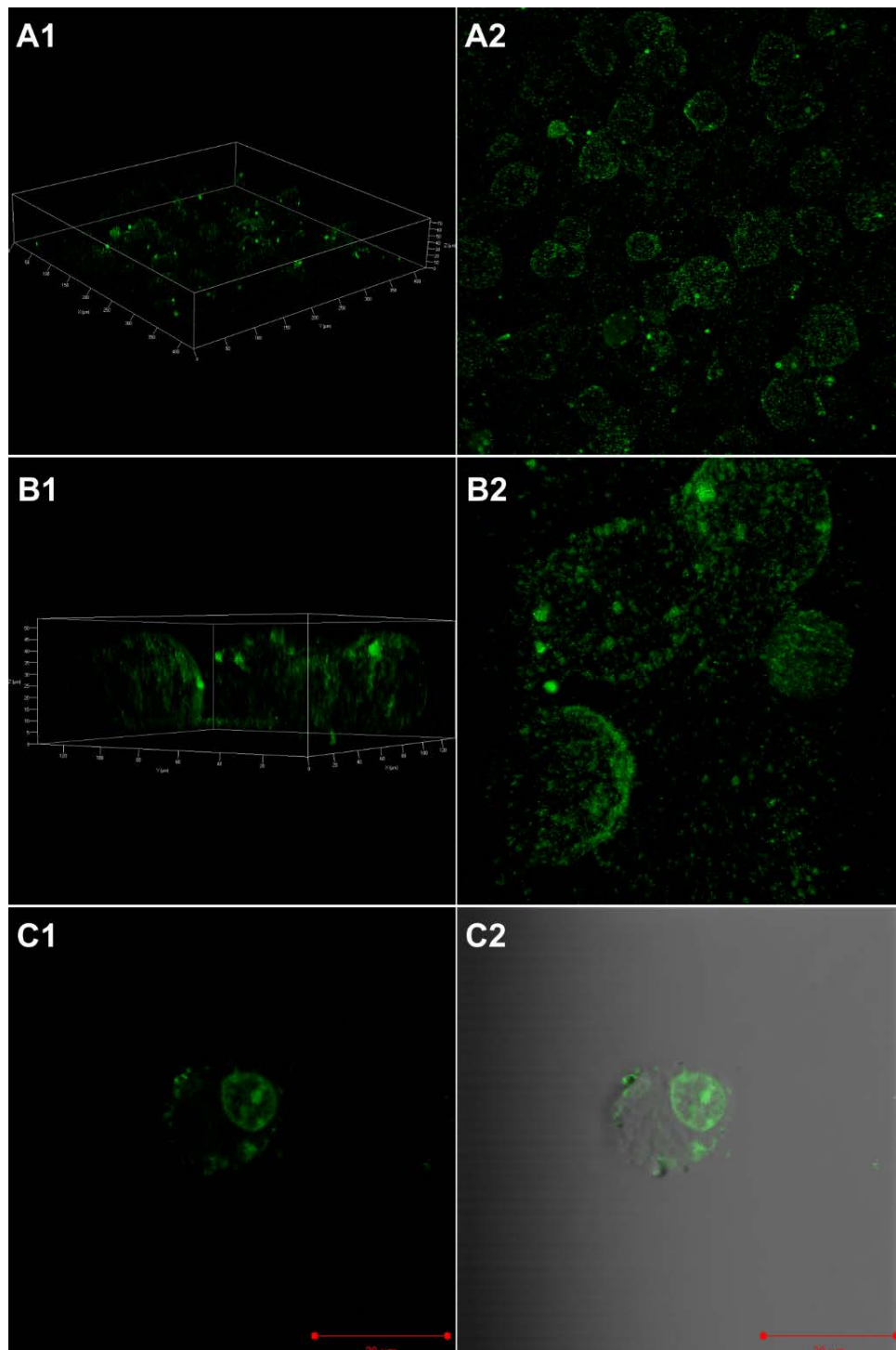


Figure 20. Imaging the cells incubated with PEI/AuNP₈₂ nanoparticles under the two-photon microscope. A1, A2) 3D and maximum intensity projection images (magnification: 20x). B1, B2) 63x magnification. C1, C2) Single cell imaging with two-photon and T-PMT modes (magnification:63x).

3.3.8. Potential Mechanism for Nucleolar Localization

Many different strategies have been proposed for the localization in the cell nucleus such as; the breakdown of the nuclear membrane during mitosis [151], interaction of PEI with the nuclear membrane and fusion with the nuclear envelope [152], the role of the intracellular components such as microtubules [153] and entering through nuclear pores [147, 154]. However, comparing the size of nuclear pores (25 nm) with the size of large complexes like plasmid/PEI (150 nm) that enter to the nucleus and also nuclear localization in post-mitotic cells overrule some of these theories [147]. Our new hypothesis underlines the importance of 5S ribosomal RNA for nucleolar delivery of PEI-functionalized gold nanoparticles to the cell nucleolus. It is generally known that the assembly of ribosomes is carried out in the nucleolus. On the other hand, 5S rRNA which is transcribed outside the nucleolus should be brought to the nucleolus by ribosomal L5 protein [155]. So, here it is hypothesized that the electrostatic interaction of negatively charged 5s rRNA with the positively charged PEI-functionalized gold nanoparticles facilitates the transportation of nanoparticles by L5 protein to the cell nucleolus.

3.4. Gene-Knockdown Studies by siRNA/Gold Nanotherapeutics for Triple Negative Breast Cancer Therapy

3.4.1. Properties of PEI-Functionalized Gold Nanoparticles as eEF-2K siRNA Carriers

As mentioned above, siRNAs can be attached to the gold nanoparticle surface via thiol linkage [121] or conjugated to the polyelectrolyte-modified surface [122]. However, adding polyelectrolytes such as PEI can cause irreversible aggregation of gold nanoparticles. Thus, gold nanoparticles should be stabilized with 11-mercaptoundecanoic acid and then modified with PEI [122]. However, this extra step can lead to partial aggregation of gold nanoparticles as well. To overcome these problems and develop AuNP-based siRNA nanoparticles, we synthesized PEI-functionalized gold nanoparticles (AuNP-PEI) after the seeding-growth step (Figure 21).

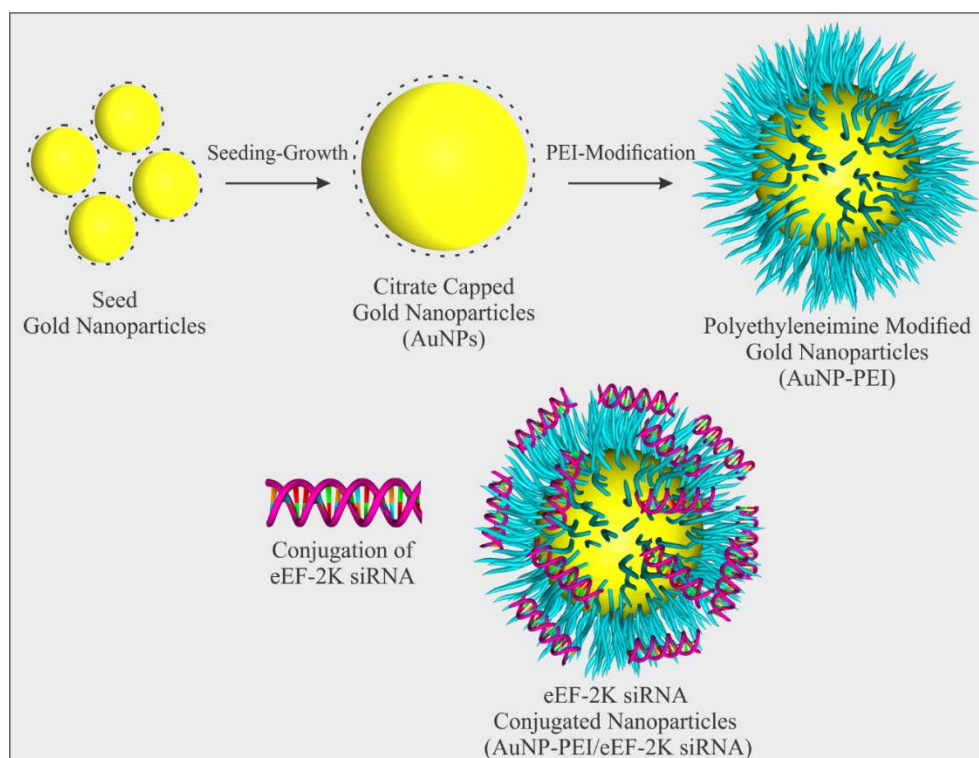


Figure 21. Schematic representation of AuNP-PEI and eEF-2K siRNA conjugation.

In the first step, seed AuNPs with a hydrodynamic diameter of 21 ± 2 nm and polydispersity index (PDI) of 0.05 were synthesized (Figure 22 A). Synthesized nanoparticles were highly monodisperse and had a zeta potential of -55.8 ± 7 mV and LSPR peak of 519 nm (Figure 22 B and Figure 23 A, B). In the second step, seed AuNPs were grown and AuNPs with a hydrodynamic diameter of 51 ± 0.3 nm and PDI of 0.05 were synthesized. These newly synthesized nanoparticles were also highly monodisperse with a zeta potential of -32.6 ± 0.36 mV, LSPR peak of 528 nm, and optical density (OD) of 0.23835 (Figure 22 B and Figure 23 C). The concentration of synthesized AuNPs was found to be 50 $\mu\text{g}/\text{mL}$ by ICP-MS analysis.

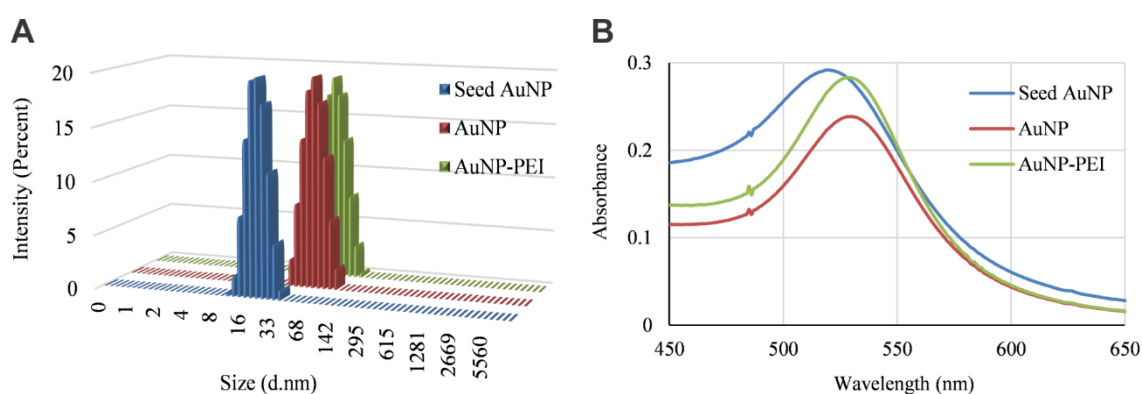


Figure 22. Characterization of synthesized AuNP-PEI nanoparticles. A) Size distribution of synthesized nanoparticles. B) LSPR peak reveals shifts indicating an increase in size and surface modification of AuNP-PEI.

We found that AuNPs after the seeding-growth step were highly stable against polyelectrolyte addition, and no aggregation was observed after directly adding PEI to the gold nanoparticle solution. Thus, AuNP-PEI nanoparticles with a hydrodynamic diameter of 54 ± 0.45 nm and PDI of 0.06 were prepared and used (Figure 22 A and Figure 23 D). AuNP-PEI nanoparticles were highly monodisperse with a zeta potential value of $+39.3 \pm 0.34$ mV and LSPR peak of 528 nm. All these results along with the related OD (0.28315) that was greater than for AuNPs (Figure 22 B), indicated that AuNP-PEI nanoparticles were successfully synthesized and modified.

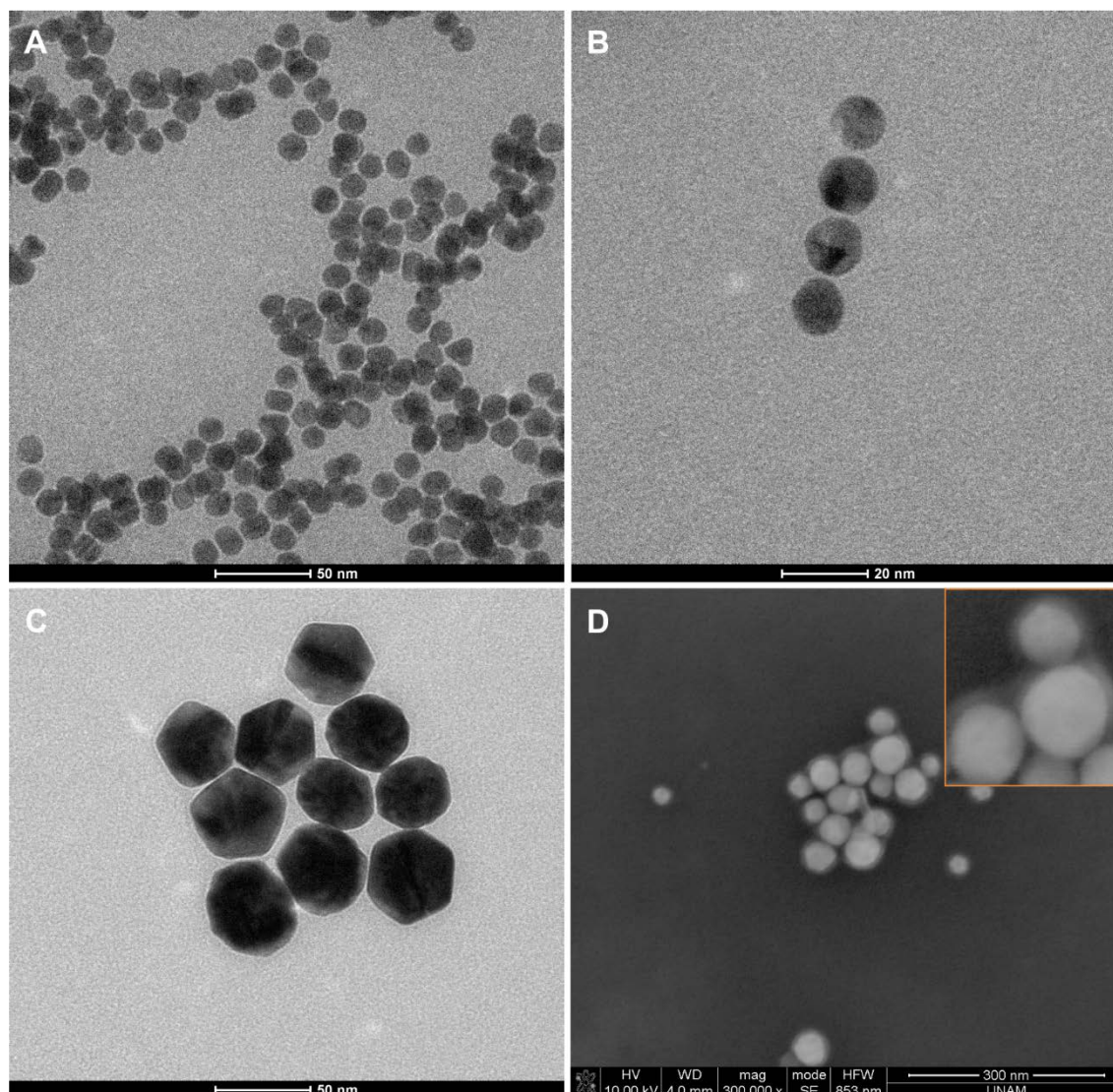


Figure 23. Transmission electron microscope (TEM) and scanning electron microscope (SEM) images of synthesized gold nanoparticles. A, B) TEM images of synthesized seed gold nanoparticles. C) TEM image of AuNPs after seeding-growth step. D) SEM image of PEI-functionalized gold nanoparticles (AuNP-PEI).

Despite the fact that gold nanoparticles are very sensitive to polyelectrolyte addition and tend to aggregate, their homogeneous surface modification with PEI was achieved after seeding-growth of the nanoparticles. PEI in different molecular weights, especially 25000 MW, has been widely used during gene delivery studies, but it is known to be toxic [156]. So, in this study, a lower molecular weight of PEI (2000 MW) in a very low concentration (0.005%, v/v) was used to modify the surface of AuNPs with a thin layer of PEI. We found that the AuNP-PEI:siRNA ratio of 3 was

optimal for siRNA conjugation to nanoparticles and that prepared nano-formulations were stable in terms of their shelf life. One of the most important factors about nanoparticles in cancer therapy is their size. As is known, small nanoparticles (<5 nm) are eliminated by kidneys, whereas nanoparticles in the size range of 10-20 nm tend to accumulate mostly in the liver, and larger nanoparticles (100-200 nm) accumulate in both the liver and spleen [157-159]. Therefore, in this study, special attention was given to preparing nano-formulations within the size range of 50-60 nm for safe and increased eEF-2K siRNA delivery into the tumors.

3.4.2. Conjugation of eEF-2K siRNA to PEI-Functionalized Gold Nanoparticles

To find the optimal gold nanoparticle and siRNA conjugation ratio, we prepared various AuNP-PEI:siRNA nano-formulations in different w/w ratios (0.25, 0.5, 1, 1.5, 2, 2.5, 3, 5, and 7). Gel electrophoresis analysis revealed that siRNAs (100 µg/mL) were fully captured for the AuNP-PEI:eEF-2K siRNA w/w ratio of 0.5 or above. As shown in figure 24 A, when comparing the results with positive and negative controls, eEF-2K siRNA was efficiently loaded at the ratio above 0.25. On the other hand, the stability of prepared formulations was better for the ratio of 1.5 and above. In contrast, the ratios below 1.5 were unstable and tended to precipitate over time (Figure 24 B) and may negatively affect the shelf life of the therapeutics. However, the precipitation of the nanoparticles was reversible and upon shaking the samples they were easily dispersed (Figure 24 C). Precipitation of nanoparticles is in close relation to the change in zeta potential.

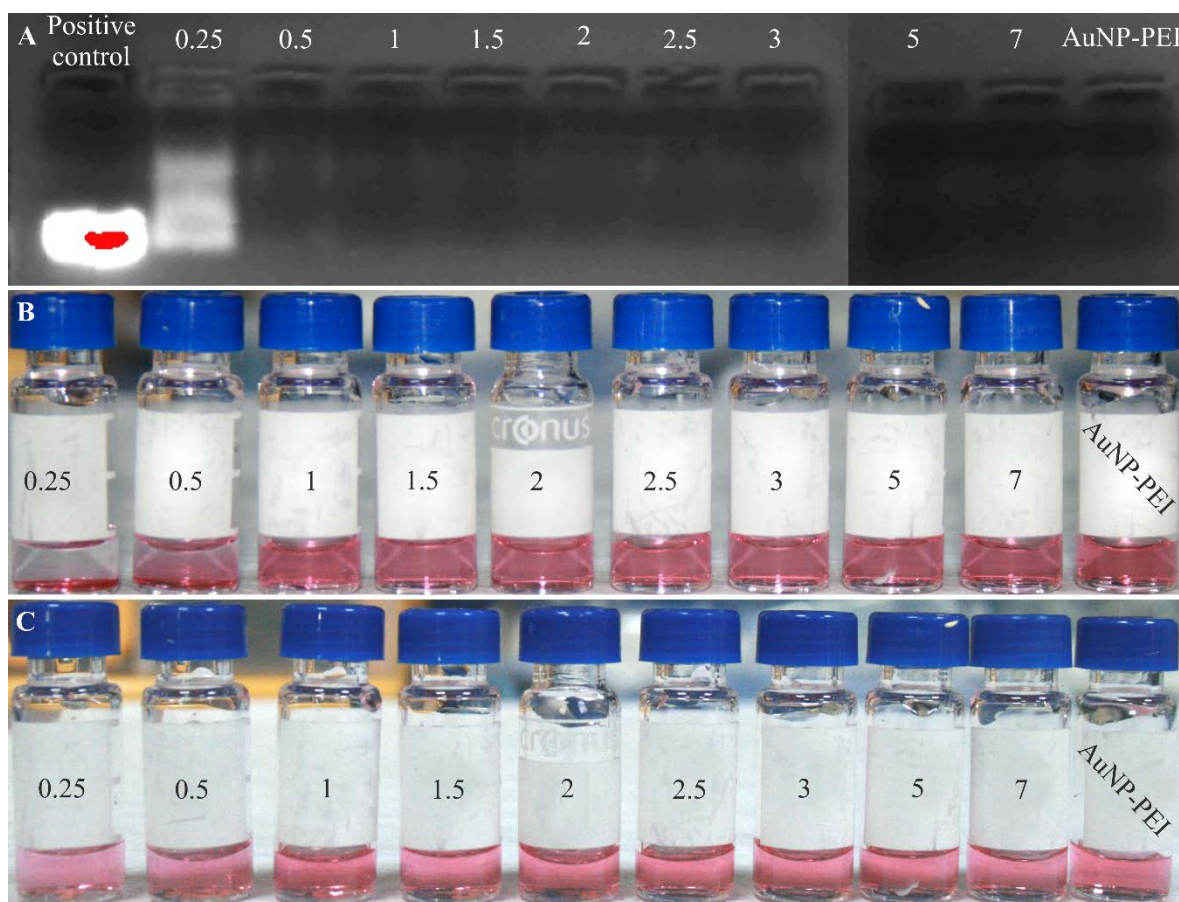


Figure 24. Analysis of various AuNP-PEI:siRNA conjugation ratios and stability tests. A) Gel electrophoresis analysis of different AuNP-PEI:eEF-2K siRNA conjugation ratios. B) Stability of various AuNP-PEI:siRNA ratios over 1 h period. C) Re-dispersing of the precipitated nanoparticles by shaking them. Positive control is only siRNA alone without AuNP-PEI nanoparticles. Negative control consists of AuNP-PEI nanoparticles without any siRNA conjugation.

Moreover, for more precise analysis, prepared nano-formulations were centrifuged and supernatant absorbances were measured at an oligonucleotide specific wavelength of 260 nm (Figure 25). Results showed that complete siRNA conjugation to nanoparticles occurred at the ratio of 3 or above. Further LSPR peak characterization proved that the ratios below 1.5 were associated with shifts in peaks, indicating instability and aggregation (Figure 26).

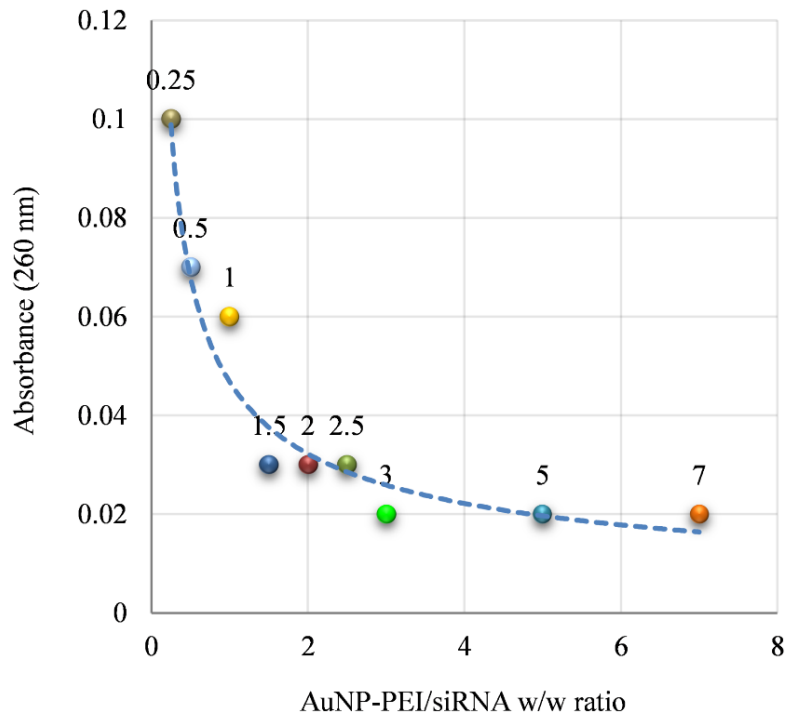


Figure 25. UV-visible spectrophotometric analysis of the various AuNP-PEI:siRNA ratios.

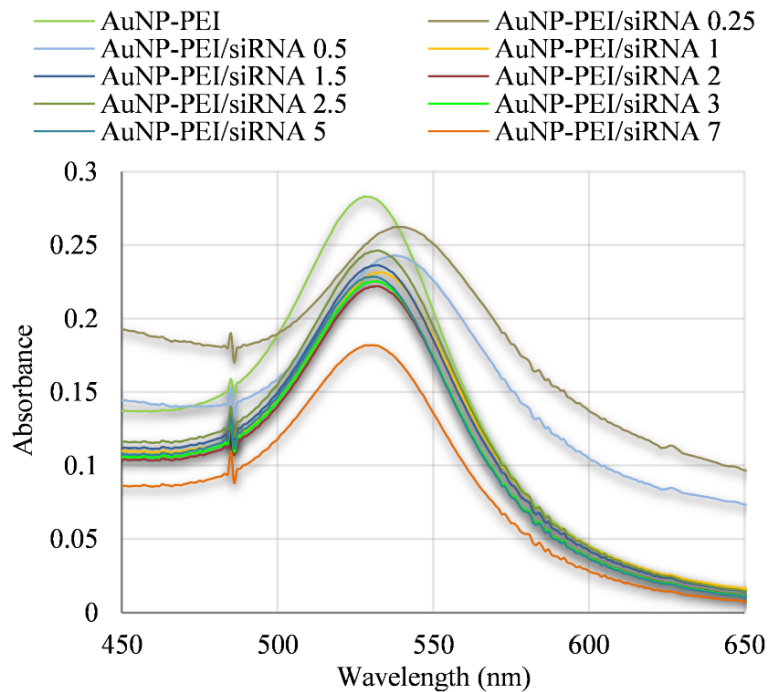


Figure 26. LSPR peaks of various AuNP-PEI:siRNA ratios.

Size analysis of nano-formulations also showed the aggregation state of the nanoparticles for ratios below 1.5 (Figure 27). However, through extensive analysis, we found that monodisperse nano-formulation with reasonable PDI was achieved by the ratio of 3 or above (Table 3). As a result, a ratio of 3 was selected as the optimal AuNP-PEI:siRNA ratio and a AuNP-PEI/eEF-2K siRNA nano-formulation (58 nm) with a PDI of 0.1 and zeta potential of +27 mV was used for the following gene knockdown studies.

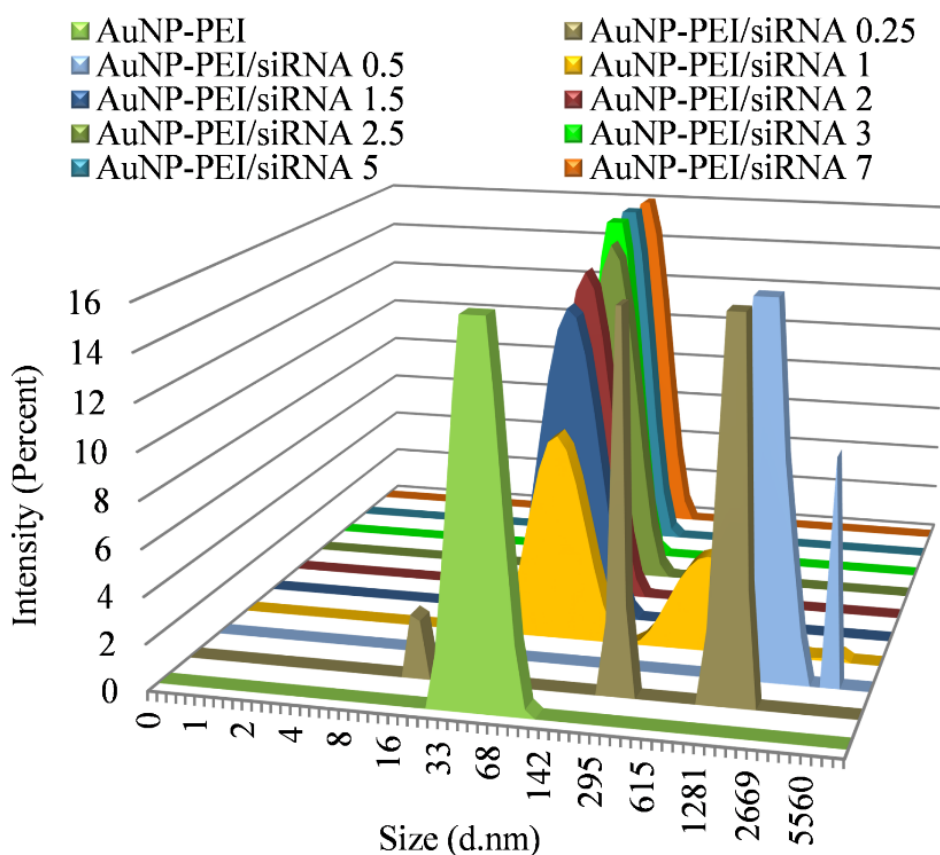


Figure 27. Size distribution of AuNP-PEI/eEF-2K siRNA nanoparticles at different ratios.

Table 3. Effect of different AuNP-PEI:siRNA ratios on size, polydispersity index (PDI), and zeta potential values.

AuNP-PEI:siRNA w/w ratios	Hydrodynamic diameter (nm)	PDI	Zeta potential (mV)
0.25	1121 ± 722.6	0.30	+9.59 ± 0.54
0.50	2064 ± 464.2	0.36	+18.2 ± 1.35
1.00	73.19 ± 0.58	0.46	+26.8 ± 0.40
1.50	66.40 ± 0.72	0.14	+27.8 ± 0.60
2.00	63.72 ± 0.31	0.13	+28.3 ± 1.47
2.50	74.11 ± 0.84	0.11	+25.2 ± 2.25
3.00	57.99 ± 0.70	0.10	+27.3 ± 1.40
5.00	57.05 ± 0.55	0.10	+29.1 ± 0.20
7.00	59.36 ± 0.42	0.11	+27.7 ± 0.34

Zeta potential values indicate the marked change of zeta potential from negative values for AuNPs to positive values for AuNP-PEI nanoparticles (Figure 28). The stability of the nano-formulations correlated with the zeta potential of nanoparticles. Zeta potentials for 0.25 and 0.5 ratios were very low and close to the neutral charge, ranging between -10 and +10, and tended to precipitate over time. However, zeta potentials for other ratios were in the preferred range and were very stable over time.

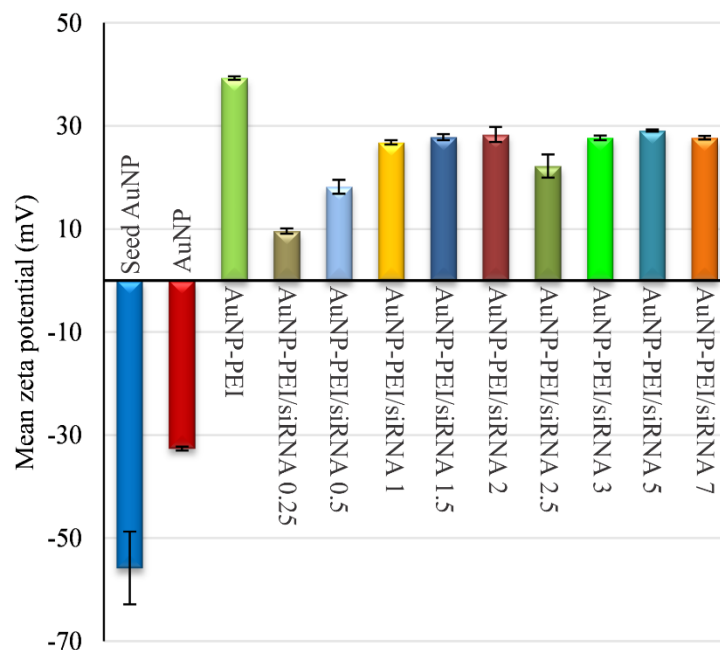


Figure 28. Zeta potential values of synthesized nanoparticles and prepared nanoformulations at different ratios.

3.4.3. *In Vitro* Down-Regulation of eEF-2K by AuNP-PEI/eEF-2K siRNA

We first evaluated *in vitro* eEF-2K knockdown by AuNP-PEI/eEF-2K siRNA nanoformulation in MDA-MB-231 TNBC cells. As shown in Figure 29, AuNP-PEI/eEF-2K siRNA successfully downregulated eEF-2K and inhibited phosphorylation of its downstream substrate, EF2 protein. Also, the activity/phosphorylation (Try416) of Src, which has been strongly implicated in cell motility, invasion, metastasis, growth, and progression of breast cancer [160], was inhibited. *In vitro* studies also indicated that AuNP-PEI/eEF-2K siRNA formulation with only 50 nM siRNA concentration induced target downregulation as well as the commercially available transfection reagent (HiPerFect), which is known to have high transfection efficacy but cannot be used due to its positive charge and toxicity in *in vivo* animal models.

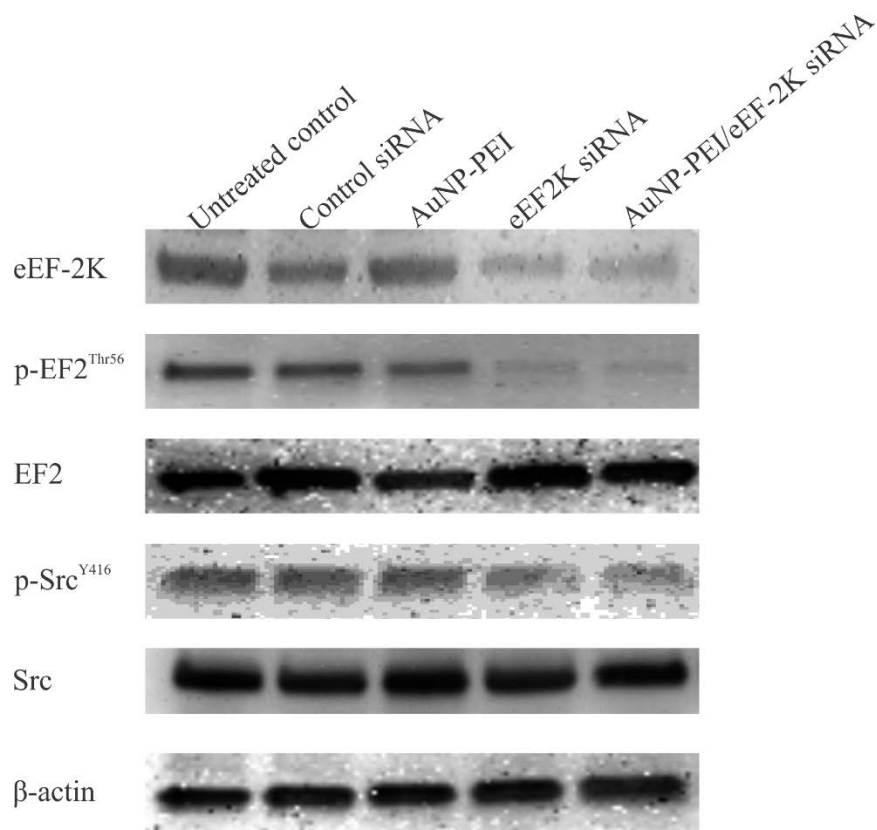


Figure 29. AuNP-PEI/eEF-2K siRNA nano-formulation effectively downregulates eEF-2K in MDA-MB-231 TNBC cells and inhibits phosphorylation of its downstream target EF2 *in vitro*.

3.4.4. Effective *In Vivo* Target Knockdown and Growth Inhibition in a TNBC Tumor Model

We next evaluated the effects of AuNP-PEI/eEF-2K siRNA nano-formulation in *in vivo* studies in terms of target knockdown and antitumor efficacy. Once-a-week injection of AuNP-PEI/eEF-2K siRNA (8 μ g per mouse) also demonstrated successful downregulation of eEF-2K compared with control groups treated with AuNP-PEI/control siRNA nano-formulation (Figure 30). AuNP-PEI/eEF-2K siRNA treatment also resulted in complete inhibition of EF2 phosphorylation in tumors. Likewise, the phosphorylation of ERK-MAPK, which is also very important for cell proliferation, cell survival, and metastasis [161], was markedly inhibited (Figure 30). Activation of MAPK-p38 [162], did not change in the tumors after EF2K inhibition.

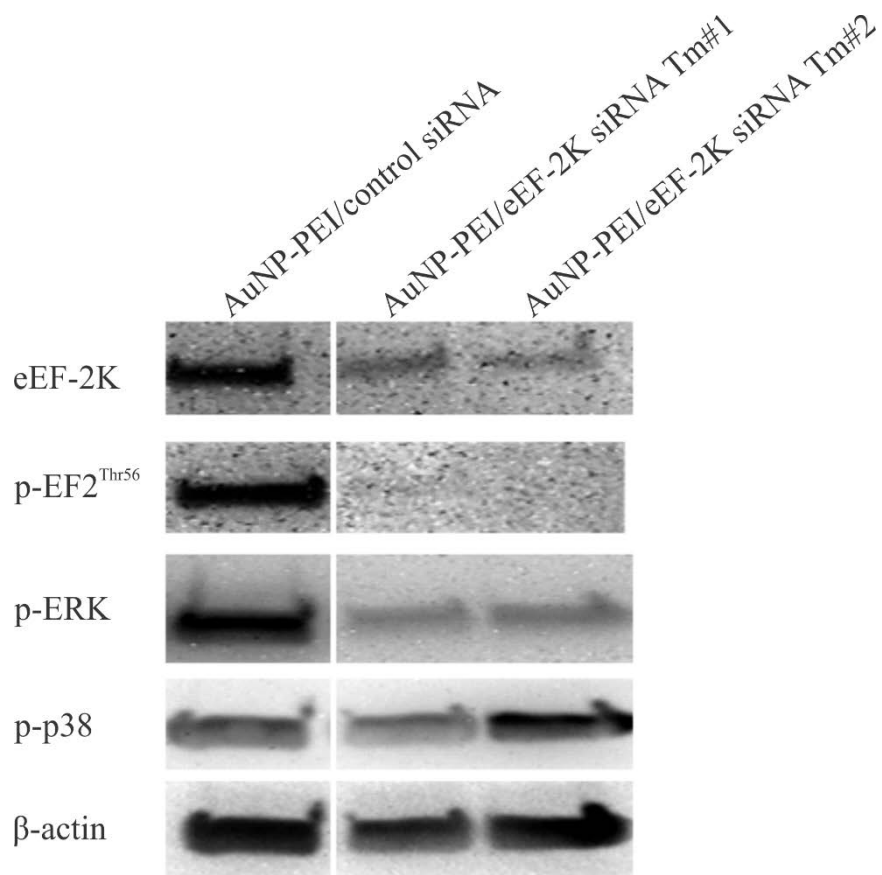


Figure 30. *In vivo* gene knockdown studies by systemically (intravenously, n=5) injected AuNP-PEI/eEF-2K siRNA nano-formulation shows effective eEF-2K downregulation along with the inhibition of EF2 phosphorylation.

It is important to note that many gene knockdown studies with nanoparticles are performed under *in vitro* conditions that differ completely from the *in vivo* tumor microenvironment. Thus, *in vivo* testing is critical to assess the effectiveness of nanoparticles because many factors such as nonspecific binding of serum proteins and elimination by the reticuloendothelial system may reduce efficacy. Also, the better loading capacity of nanoparticles and protection from nucleases are important and may help reduce the siRNA dose. In the current study, significant tumor inhibition (~90 %) was achieved by only one intravenous injection of AuNP-PEI/eEF-2K siRNA per week at a relatively low dose of 8 $\mu\text{g}/\text{mouse}$ (0.3 mg/kg), which is below the limit of any potential toxicity and can be applied in the clinic and is 10-70 fold lower than for previously published studies. This could be related to siRNA protection from serum components and passive targeting by AuNP-PEI/eEF-2K

siRNA nano-formulation in the previously reported size range of 50-60 nm [120]. As a result of all these molecular effects, remarkable target downregulation and inhibition of tumor growth were achieved by AuNP-PEI/eEF-2K siRNA (Figure 31). It is important to note that all these effects were achieved by using a very low concentration of eEF-2K siRNA nanoparticles, which is very important in bringing this therapeutic approach to the clinic. In addition to highly effective siRNA capturing ability, the size of the AuNP-PEI/eEF-2K siRNA nano-formulation (approximately 60 nm) could have played a significant role in its *in vivo* effects.

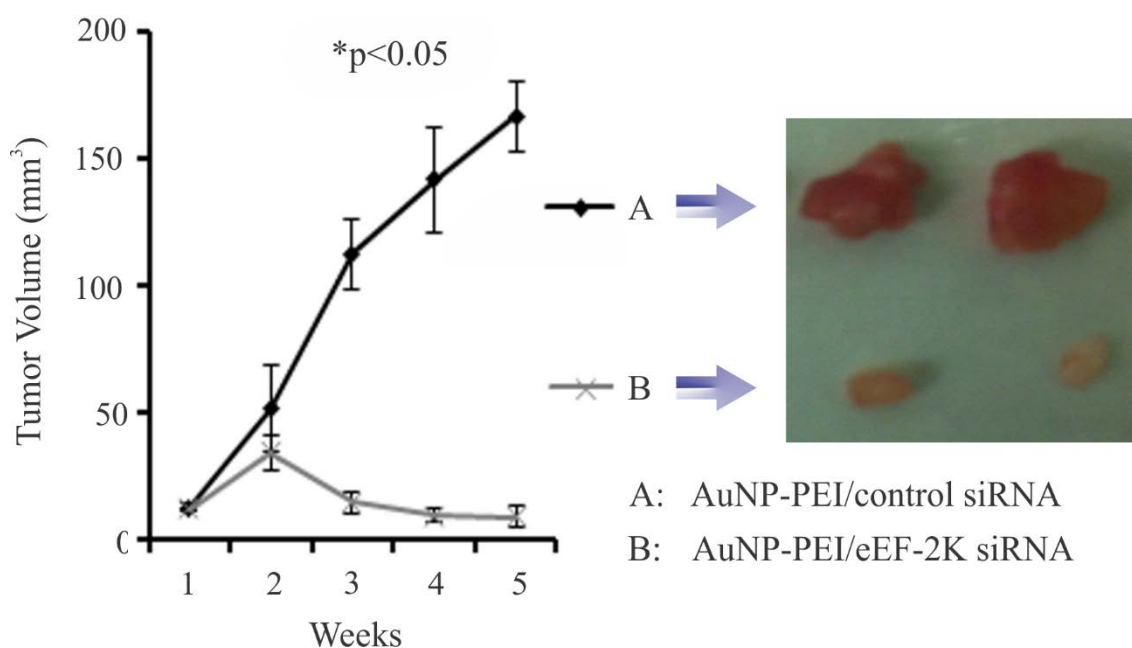


Figure 31. Inhibition of tumor growth was observed during the 4 weeks of intravenous treatment with AuNP-PEI/eEF-2K siRNA nano-formulation (once-a-week injection with 8 μ g of siRNA per mouse, n=5) in the MDA-MB-231 TNBC orthotopic xenograft tumor model. A and B indicate treatment with AuNP-PEI/control-siRNA and AuNP-PEI/eEF-2K-siRNA, respectively.

eEF-2K has been recently shown as a potential molecular target that plays a key role in TNBC tumor growth and progression by upregulating pro-tumorigenic signaling pathways, including cyclin D1, c-Myc, c-Src/FAK, and PI3K/Akt [35, 47]. However due to the unsolved crystal structure of protein, currently there is no specific inhibitor of eEF-2K identified. Thus, siRNA based-target silencing has been considered as a potential strategy for targeting the gene. *In vivo* eEF-2K downregulation by nano-liposomal siRNA impairs its activity and leads to inhibition of tumor growth [7]. Nevertheless, in this prior study effective knockdown of eEF-2K by liposomal siRNA was achieved by twice-weekly injection, whereas in our study once-a-week injection of AuNP-PEI/siRNA was enough to achieve potent downregulation of EF2K and better antitumor efficacy in the TNBC model.

3.5. Doxorubicin Conjugated siRNA Therapeutics for Combinational Therapy

3.5.1. Characterization of Doxorubicin and eEF-2K siRNA Conjugated Gold Nanoparticles

Doxorubicin as a potent cancer drug for TNBC therapy. It has an amine (NH_2) group which can attach to the surface of negatively charged gold nanoparticles. However, this interaction will not be strong enough to preserve the molecule until its final destination in the tumor site. So, in this thesis it was aimed to thiolate the doxorubicin through its NH_2 group by using a highly selective chemical agent 2-iminothiolane which reacts with primary amines (—NH_2) to add sulfhydryl (—SH) groups while preserving charge properties of the original amino group. Thiolation is carried out by adding a small spacer arm (8.1 angstroms) with a free sulfhydryl group at the end of it (Figure 32).

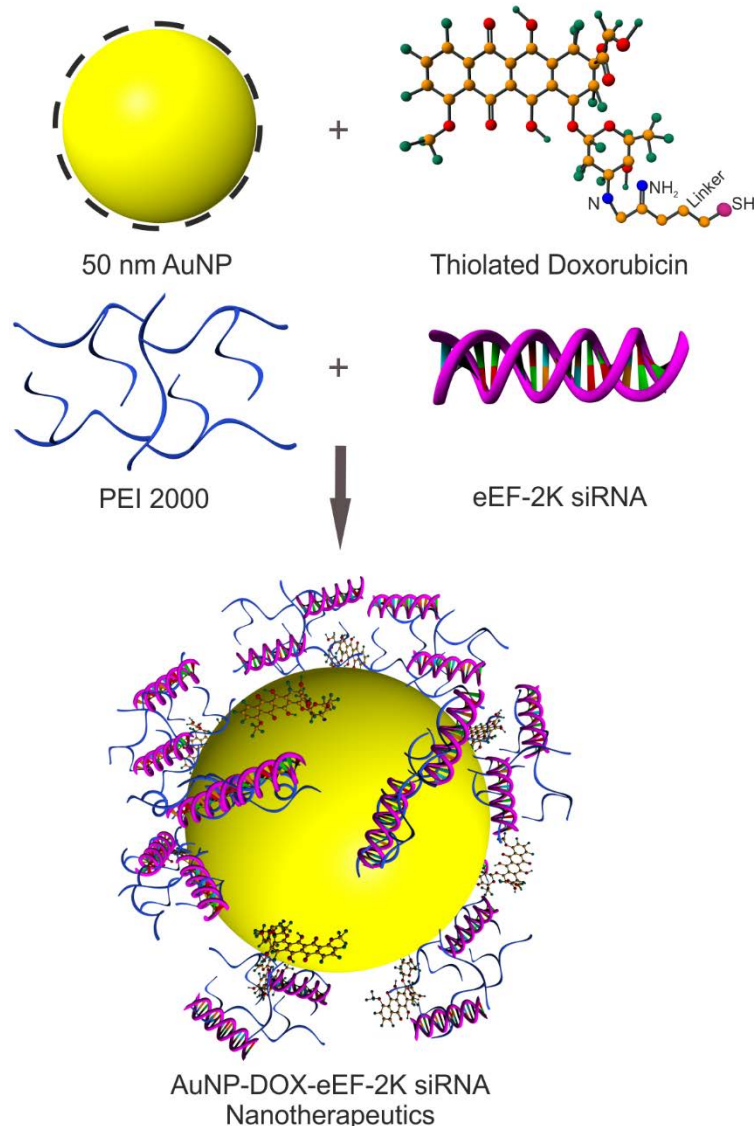


Figure 32. Preparation steps of the doxorubicin and eEF-2K siRNA conjugated gold nanoparticles (AuNP-DOX-eEF-2K siRNA) as combinational nanotherapeutics.

Thiolation of doxorubicin helped to reach to a maximum conjugation concentration of 1.2 μM . Also, gold nanoparticles were conjugated with PEI to capture siRNA. In this way, a complex nanotherapeutics bearing both doxorubicin and eEF-2K siRNA was prepared (Figure 32). To increase the *in vitro* and *in vivo* stability of the final nanotherapeutics, the remaining empty surface of the nanoparticles was conjugated with thiolated PEG. Size characterization results showed that the size of gold nanoparticles (50.45 nm) increased to 68.62 nm for final nanotherapeutics bearing both doxorubicin and eEF-2K siRNA (Figure 33). Also, the zeta potential of gold nanoparticles changed from -37.4 mV for citrate capped gold nanoparticles to +22.9

mV for the final doxorubicin and eEF-2K siRNA conjugated combinational nanotherapeutics.

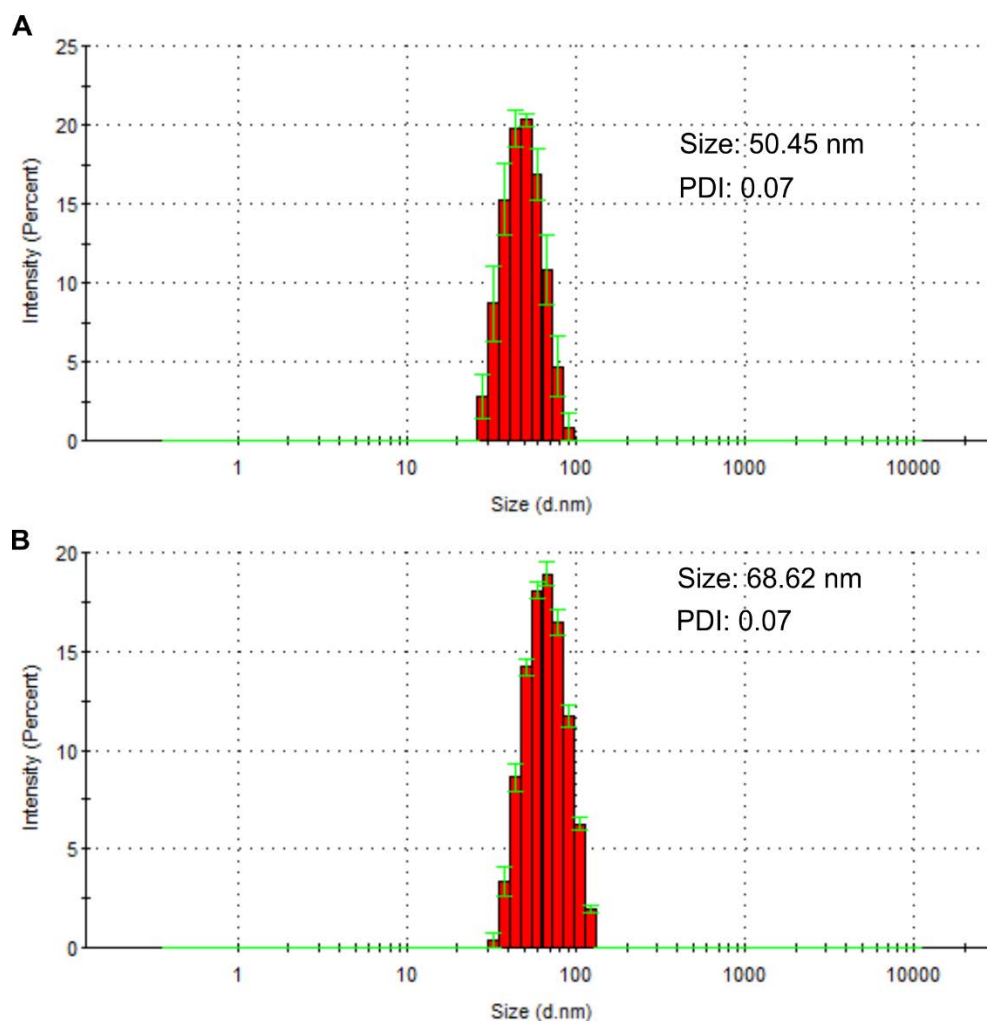


Figure 33. Size distribution graph of; A) citrate capped gold nanoparticles and B) Doxorubicin and eEF-2K siRNA conjugated gold nanoparticles.

3.5.2. Effect of Doxorubicin Conjugated Gold Nanoparticles on the Cell Viability of MDA-MB-231 Cells

In order to determine the optimum concentration for doxorubicin, MTT assay was performed after testing different doxorubicin concentrations (0.1, 0.2, 0.4, 0.8, 1.6, 3.2, 6.4, 12.8 μM) and the IC_{50} value was found to be 0.2 $\mu\text{g}/\text{mL}$ (Figure 34). All the following studies were carried out in 0.2 μM doxorubicin concentration.

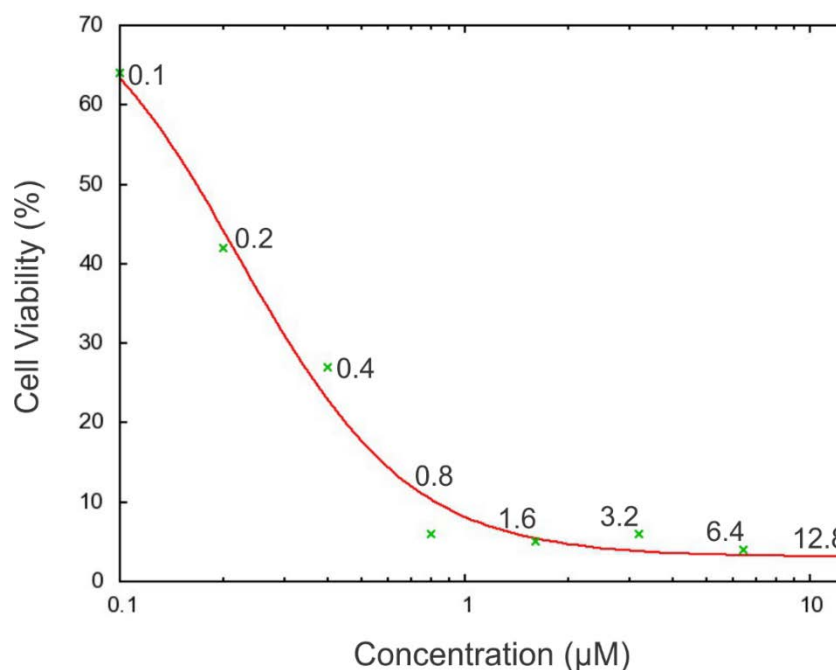


Figure 34. Cell viability assay showing the concentration dependent decrease of the cell viability in MDA-MB-231 cells after doxorubicin treatment. The IC_{50} value of doxorubicin was found to be 0.2 μM after 48 h.

In the following experiments, it was aimed to evaluate the effect of doxorubicin conjugated gold nanoparticles (AuNP-PEG-PEI-DOX) on MDA-MB-231 cells and compare its effect on cell viability with the unconjugated doxorubicin. As shown in figure 35, It was found that the same effect can be achieved by doxorubicin conjugated gold nanoparticles as it was for unconjugated doxorubicin. The statistical analysis showed that there was no significant difference in decreased cell viability between doxorubicin conjugated gold nanoparticles and unconjugated doxorubicin and about 50 % of cell viability was decreased.

Also, as it can be seen in figure 35, there was no toxic effect associated with the citrate capped gold nanoparticles (AuNP) and PEG/PEI functionalized gold nanoparticles (AuNP-PEG-PEI).

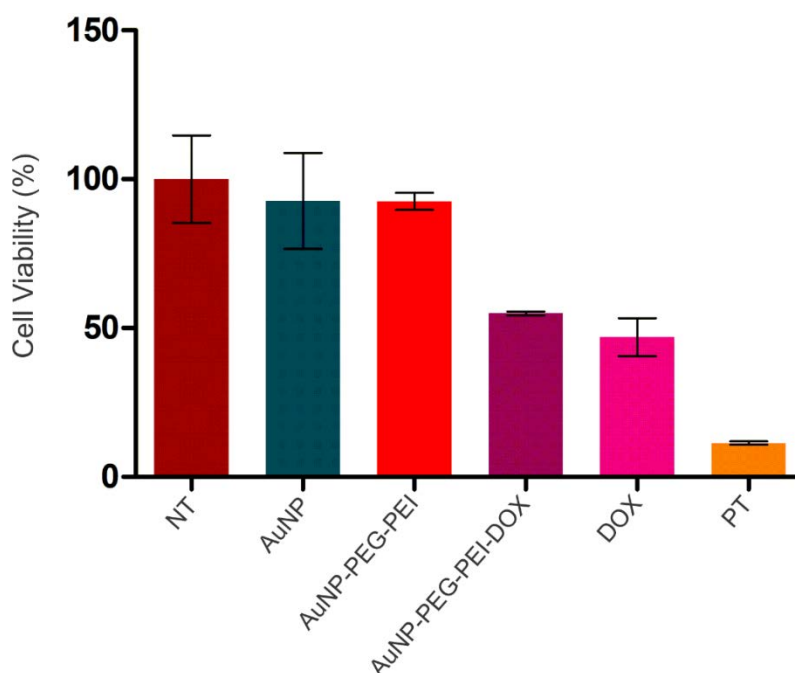


Figure 35. Cell viability assay showing the effect of doxorubicin conjugated gold nanoparticles (AuNP-PEG-PEI-DOX) and unconjugated doxorubicin (DOX) on MDA-MB-231 cells after 72 h.

3.5.3. Effect of Combinational Therapy with Doxorubicin and eEF-2K siRNA Conjugated Gold Nanoparticles on the Cell Viability of MDA-MB-231 Cells

As it was aimed before, it was intended to achieve lower than 50 % cell viability by using combinational therapy approach with both eEF-2K siRNA and doxorubicin. It was found that in compare to doxorubicin conjugated gold nanoparticles, developed eEF-2K siRNA and doxorubicin conjugated gold nanoparticles decreased the cell viability significantly in MDA-MB-436 cells (Figure 36 A). The same results were achieved with MDA-MB-231 cells and developed nanotherapeutics (AuNP-DOX-eEF-2K siRNA) decreased the cell viability significantly in compare to sole

doxorubicin conjugated gold nanoparticles (Figure 36 B). Studies were carried out with two concentrations of doxorubicin (0.1 μM and 0.25 μM) and with constant 50 nM concentration of eEF-2K siRNA. Cell viability decreased from 70% for AuNP-DOX with 0.1 μM concentration to 30% for AuNP-DOX-eEF-2K with the same doxorubicin concentration. As it is shown in figures 36 A and B for both of the doxorubicin concentrations developed combinational nanotherapeutics successfully decreased the cell viability in compare to sole doxorubicin conjugated gold nanoparticles. However, these results need to be proved by further in vivo studies in the future.

As a result, in this thesis, we showed that siRNA/gold nanoparticle conjugates down regulate eEF-2K significantly and reduce tumor volume about 90% in 4 weeks by one injection/week (0.3 mg/kg). Thus, we can say that developed nanotherapeutic was highly effective for TNBC therapy. In addition to this, combination therapy with doxorubicin can decrease side effects of chemotherapeutic by lowering the dose of doxorubicin. As mentioned above this needs further evaluation by in vivo studies.

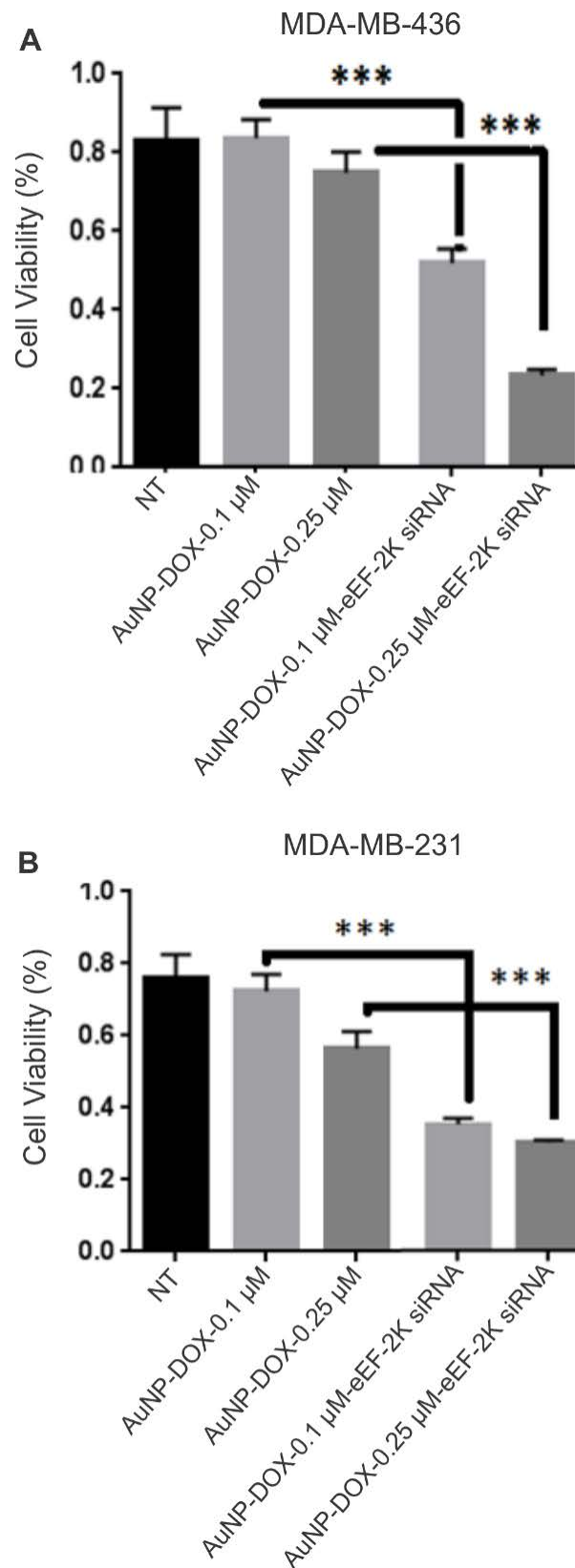


Figure 36. MTS assay comparing the effect of combinational nanotherapeutics (AuNP-DOX-eEF-2K siRNA) and doxorubicin conjugated gold nanoparticles (AuNP-DOX) on; A) MDA-MB-436 cells, and B) MDA-MB-231 cells.

CONCLUSION

In this thesis, it was aimed to develop siRNA/gold nanoparticle based for triple negative breast cancer therapy. In this respect, highly monodisperse gold nanoparticles were synthesized in different size ranges and by using a new method surface of the nanoparticles was functionalized with PEI. It was found that the surface of gold nanoparticles can be functionalized with polyethylenimine after seeding-growth of the nanoparticles without any adverse effect on the high monodispersity of the sample and in a very low PEI concentration. Moreover, these PEI-functionalized gold nanoparticles showed a high uptake rate in postmitotic dorsal root ganglion neurons which are widely known to be very difficult cell types to transfect. Also, for the first time in literature, it was shown PEI-functionalized gold nanoparticles of over 40 nm size range can be easily tracked under both confocal and two-photon microscopes with a very high resolution. This real-time tracking ability of the nanoparticles helped to correct the previous knowledge about gold nanoparticles and prove that PEI-functionalized gold nanoparticles can enter to cell nucleolus even in large nanoparticle size ranges and they tend to localize in the nucleolus. This is the first time that a very potent gene delivery vehicle with no toxicity, high monodispersity, high uptake rate and imaging capability is prepared and can be used for the treatment of neurodegenerative diseases or cancer.

By using characterized PEI-functionalized gold nanoparticles highly monodisperse AuNP-PEI/eEF-2K siRNA nanotherapeutics with a size of about 60 nm were developed. It was found that this carrier system is highly effective in delivering siRNA into tumor tissues and successfully downregulated the proto-oncogenic target eEF-2K at a low siRNA concentration and resulted in the abatement of the tumor growth in TNBC. Also *in vivo* results showed the passive targeting of the proto-oncogenic target eEF-2K gene at low siRNA concentrations. In this regard, *in vivo* once-a-week systemic intravenous treatment with AuNP-PEI/eEF-2K siRNA led to a remarkable antitumor activity in a TNBC model. Thus, these data indicate that eEF-2K plays an important role in TNBC tumor growth and its inhibition by AuNP-PEI/eEF-2K siRNA nanotherapeutics can be successfully used to target eEF-2K or other potential target genes *in vivo* and AuNP-PEI-based oligonucleotide therapeutics can be utilized for the development of targeted therapies.

Finally, by developing a combinational nanotherapeutics bearing both doxorubicin chemotherapeutic and eEF-2K siRNA outstanding results were obtained *in vitro*. The combinational nanotherapeutics were able to decrease the cell viability better than sole doxorubicin chemotherapeutic. This fascinating result showed that eEF-2K plays a very key role in the cell survival and its inhibition results in a more prominent decrease in the cell viability in combination with doxorubicin chemotherapeutic drug. This is the first time in literature that a potent combinational nanotherapeutic is developed for TNBC therapy. The more elaborate *in vivo* studies will be carried out in the future to show even more prominent results as these nanotherapeutics are able to passively target both eEF-2K siRNA and doxorubicin to the tumor site. The achieved results will be fascinating in compare to unconjugated doxorubicin which tends to distribute in all over the body.

In conclusion, given our findings, a potent gold nanoparticle based nanotherapeutics for TNBC therapy with the potential of entering the clinic was proposed by this study. Apart from the gene delivery application, this nanoformulation could be used in theranostic applications because gold nanoparticles can be easily imaged by both infrared light based imaging systems and computed tomography.

REFERENCES

- [1] American Cancer Society, Cancer Facts & Figures 2016. Atlanta: American Cancer Society, **2016**.
- [2] Santen, R. J., Benign Breast Disease in Women, in *Endotext*, L. J. De Groot *et al.*, Eds. South Dartmouth (MA): MDText.com, Inc., **2000**.
- [3] Blows, F. M., Driver, K. E., Schmidt, M. K., Broeks, A., van Leeuwen, F. E., Wesseling, J., Cheang, M. C., Gelmon, K., Nielsen, T. O., Blomqvist, C., Heikkila, P., Heikkinen, T., Nevanlinna, H., Akslen, L. A., Begin, L. R., Foulkes, W. D., Couch, F. J., Wang, X., Cafourek, V., Olson, J. E., Baglietto, L., Giles, G. G., Severi, G., McLean, C. A., Southey, M. C., Rakha, E., Green, A. R., Ellis, I. O., Sherman, M. E., Lissowska, J., Anderson, W. F., Cox, A., Cross, S. S., Reed, M. W., Provenzano, E., Dawson, S. J., Dunning, A. M., Humphreys, M., Easton, D. F., Garcia-Closas, M., Caldas, C., Pharoah, P. D., Huntsman, D., Subtyping of breast cancer by immunohistochemistry to investigate a relationship between subtype and short and long term survival: a collaborative analysis of data for 10,159 cases from 12 studies, *PLoS Med*, 7, 5, e1000279, **2010**.
- [4] Vallejos, C. S., Gomez, H. L., Cruz, W. R., Pinto, J. A., Dyer, R. R., Velarde, R., Suazo, J. F., Neciosup, S. P., Leon, M., de la Cruz, M. A., Vigil, C. E., Breast cancer classification according to immunohistochemistry markers: subtypes and association with clinicopathologic variables in a peruvian hospital database, *Clin Breast Cancer*, 10, 4, 294-300, **2010**.
- [5] Weigelt, B., Baehner, F. L., Reis-Filho, J. S., The contribution of gene expression profiling to breast cancer classification, prognostication and prediction: a retrospective of the last decade, *J Pathol*, 220, 2, 263-80, **2010**.
- [6] Perou, C. M., Sorlie, T., Eisen, M. B., van de Rijn, M., Jeffrey, S. S., Rees, C. A., Pollack, J. R., Ross, D. T., Johnsen, H., Akslen, L. A., Fluge, O., Pergamenschikov, A., Williams, C., Zhu, S. X., Lonning, P. E., Borresen-

- Dale, A.-L., Brown, P. O., Botstein, D., Molecular portraits of human breast tumours, *Nature*, 406, 6797, 747-752, **2000**.
- [7] Sørli, T., Perou, C. M., Tibshirani, R., Aas, T., Geisler, S., Johnsen, H., Hastie, T., Eisen, M. B., van de Rijn, M., Jeffrey, S. S., Thorsen, T., Quist, H., Matese, J. C., Brown, P. O., Botstein, D., Lønning, P. E., Børresen-Dale, A.-L., Gene expression patterns of breast carcinomas distinguish tumor subclasses with clinical implications, *Proceedings of the National Academy of Sciences*, 98, 19, 10869-10874, **2001**.
- [8] Dai, X., Li, T., Bai, Z., Yang, Y., Liu, X., Zhan, J., Shi, B., Breast cancer intrinsic subtype classification, clinical use and future trends, *Am J Cancer Res*, 5, 10, 2929-43, **2015**.
- [9] Vallejos, C. S., Gómez, H. L., Cruz, W. R., Pinto, J. A., Dyer, R. R., Velarde, R., Suazo, J. F., Neciosup, S. P., León, M., de la Cruz, M. A., Vigil, C. E., Breast Cancer Classification According to Immunohistochemistry Markers: Subtypes and Association With Clinicopathologic Variables in a Peruvian Hospital Database, *Clin Breast Cancer*, 10, 4, 294-300, **2010**.
- [10] Sorlie, T., Tibshirani, R., Parker, J., Hastie, T., Marron, J. S., Nobel, A., Deng, S., Johnsen, H., Pesich, R., Geisler, S., Demeter, J., Perou, C. M., Lonning, P. E., Brown, P. O., Borresen-Dale, A. L., Botstein, D., Repeated observation of breast tumor subtypes in independent gene expression data sets, *Proc Natl Acad Sci U S A*, 100, 14, 8418-23, **2003**.
- [11] Brenton, J. D., Carey, L. A., Ahmed, A. A., Caldas, C., Molecular classification and molecular forecasting of breast cancer: ready for clinical application?, *J Clin Oncol*, 23, 29, 7350-60, **2005**.
- [12] O'Brien, K. M., Cole, S. R., Tse, C. K., Perou, C. M., Carey, L. A., Foulkes, W. D., Dressler, L. G., Geradts, J., Millikan, R. C., Intrinsic breast tumor subtypes, race, and long-term survival in the Carolina Breast Cancer Study, *Clin Cancer Res*, 16, 24, 6100-10, **2010**.

- [13] Fan , C., Oh , D. S., Wessels , L., Weigelt , B., Nuyten , D. S. A., Nobel , A. B., van't Veer , L. J., Perou , C. M., Concordance among Gene-Expression–Based Predictors for Breast Cancer, *New England Journal of Medicine*, 355, 6, 560-569, **2006**.
- [14] Ho-Yen, C., Bowen, R. L., Jones, J. L., Characterization of basal-like breast cancer: an update, *Diagnostic Histopathology*, 18, 3, 104-111, **2012**.
- [15] Rakha, E. A., Putti, T. C., Abd El-Rehim, D. M., Paish, C., Green, A. R., Powe, D. G., Lee, A. H., Robertson, J. F., Ellis, I. O., Morphological and immunophenotypic analysis of breast carcinomas with basal and myoepithelial differentiation, *J Pathol*, 208, 4, 495-506, **2006**.
- [16] Carey, L., O'Shaughnessy, J., O'Shaughnessy, J., Hoadley, K., Khambata-Ford, S., Horak, C., Xu, L., Awad, M., Brickman, D., Muller, S., Donato, J., Asmar, L., Stiljeman, I., Ebbert, M., Bernard, P., Perou, C., Potential Predictive Markers of Benefit from Cetuximab in Metastatic Breast Cancer: An Analysis of Two Randomized Phase 2 Trials, *Cancer Research*, 69, 24 Supplement, 2014-2014, **2009**.
- [17] Carey, L., Winer, E., Viale, G., Cameron, D., Gianni, L., Triple-negative breast cancer: disease entity or title of convenience?, *Nat Rev Clin Oncol*, 7, 12, 683-92, **2010**.
- [18] van de Rijn, M., Perou, C. M., Tibshirani, R., Haas, P., Kallioniemi, O., Kononen, J., Torhorst, J., Sauter, G., Zuber, M., Köchli, O. R., Mross, F., Dieterich, H., Seitz, R., Ross, D., Botstein, D., Brown, P., Expression of Cytokeratins 17 and 5 Identifies a Group of Breast Carcinomas with Poor Clinical Outcome, *The American Journal of Pathology*, 161, 6, 1991-1996, **2002**.
- [19] Tsutsui, S., Ohno, S., Murakami, S., Hachitanda, Y., Oda, S., Prognostic value of epidermal growth factor receptor (EGFR) and its relationship to the estrogen receptor status in 1029 patients with breast cancer, *Breast Cancer Res Treat*, 71, 1, 67-75, **2002**.

- [20] Kreike, B., van Kouwenhove, M., Horlings, H., Weigelt, B., Peterse, H., Bartelink, H., van de Vijver, M. J., Gene expression profiling and histopathological characterization of triple-negative/basal-like breast carcinomas, *Breast Cancer Res*, 9, 5, R65, **2007**.
- [21] Rakha, E. A., El-Sayed, M. E., Green, A. R., Lee, A. H., Robertson, J. F., Ellis, I. O., Prognostic markers in triple-negative breast cancer, *Cancer*, 109, 1, 25-32, **2007**.
- [22] Bostrom, P., Soderstrom, M., Palokangas, T., Vahlberg, T., Collan, Y., Carpen, O., Hirsimaki, P., Analysis of cyclins A, B1, D1 and E in breast cancer in relation to tumour grade and other prognostic factors, *BMC Res Notes*, 2, 140, **2009**.
- [23] Westfall, M. D., Pietenpol, J. A., p63: Molecular complexity in development and cancer, *Carcinogenesis*, 25, 6, 857-64, **2004**.
- [24] Herschkowitz, J. I., He, X., Fan, C., Perou, C. M., The functional loss of the retinoblastoma tumour suppressor is a common event in basal-like and luminal B breast carcinomas, *Breast Cancer Research*, 10, 5, R75, **2008**.
- [25] Viale, G., Rotmensz, N., Maisonneuve, P., Bottiglieri, L., Montagna, E., Luini, A., Veronesi, P., Intra, M., Torrisi, R., Cardillo, A., Campagnoli, E., Goldhirsch, A., Colleoni, M., Invasive ductal carcinoma of the breast with the "triple-negative" phenotype: prognostic implications of EGFR immunoreactivity, *Breast Cancer Res Treat*, 116, 2, 317-28, **2009**.
- [26] Foulkes, W. D., Germline BRCA1 mutations and a basal epithelial phenotype in breast cancer, *J. Natl Cancer Inst.*, 95, 1482-1485, **2003**.
- [27] Turner, N., Tutt, A., Ashworth, A., Hallmarks of 'BRCAness' in sporadic cancers, *Nat. Rev. Cancer*, 4, 814-819, **2004**.
- [28] Ashworth, A., A synthetic lethal therapeutic approach: poly(ADP) ribose polymerase inhibitors for the treatment of cancers deficient in DNA double-strand break repair, *J. Clin. Oncol.*, 26, 3785-3790, **2008**.

- [29] Carey, L. A., The triple negative paradox: primary tumor chemosensitivity of breast cancer subtypes, *Clin. Cancer Res.*, 13, 2329-2334, **2007**.
- [30] Troester, M. A., Cell-type-specific responses to chemotherapeutics in breast cancer, *Cancer Res.*, 64, 4218-4226, **2004**.
- [31] Harris, L. N., Molecular subtypes of breast cancer in relation to paclitaxel response and outcomes in women with metastatic disease: results from CALGB 9342, *Breast Cancer Res.*, 8, R66, **2006**.
- [32] Tan, D. S. P., Triple negative breast cancer: molecular profiling and prognostic impact in adjuvant anthracycline-treated patients, *Breast Cancer Res. Treat.*, 111, 27-44, **2008**.
- [33] Kennedy, R. D., Quinn, J. E., Mullan, P. B., Johnston, P. G., Harkin, D. P., The role of BRCA1 in the cellular response to chemotherapy, *J. Natl Cancer Inst.*, 96, 1659-1668, **2004**.
- [34] Hait, W. N., Wu, H., Jin, S., Yang, J. M., Elongation factor-2 kinase: Its role in protein synthesis and autophagy, *Autophagy*, 2, 4, 294-296, **2006**.
- [35] Tekedereli, I., Alpay, S. N., Tavares, C. D., Cobanoglu, Z. E., Kaoud, T. S., Sahin, I., Sood, A. K., Lopez-Berestein, G., Dalby, K. N., Ozpolat, B., Targeted silencing of elongation factor 2 kinase suppresses growth and sensitizes tumors to doxorubicin in an orthotopic model of breast cancer, *Plos One*, 7, 7, e41171, **2012**.
- [36] Ryazanov, A. G., Shestakova, E. A., Natapov, P. G., Phosphorylation of elongation factor 2 by EF-2 kinase affects rate of translation, *Nature*, 334, 6178, 170-3, **1988**.
- [37] Marin, P., Nastiuk, K. L., Daniel, N., Girault, J. A., Czernik, A. J., Glowinski, J., Nairn, A. C., Premont, J., Glutamate-dependent phosphorylation of elongation factor-2 and inhibition of protein synthesis in neurons, *J Neurosci*, 17, 10, 3445-54, **1997**.

- [38] Parmer, T. G., Ward, M. D., Yurkow, E. J., Vyas, V. H., Kearney, T. J., Hait, W. N., Activity and regulation by growth factors of calmodulin dependent protein kinase III (elongation factor 2-kinase) in human breast cancer, *British Journal of Cancer*, 79, 1, 59-64, **1999**.
- [39] Katz, E., Willner, I., Integrated nanoparticle-biomolecule hybrid systems: synthesis, properties, and applications, *Angew Chem Int Ed Engl*, 43, 45, 6042-108, **2004**.
- [40] Browne, G. J., Proud, C. G., A novel mTOR-regulated phosphorylation site in elongation factor 2 kinase modulates the activity of the kinase and its binding to calmodulin, *Mol Cell Biol*, 24, 7, 2986-97, **2004**.
- [41] Wang, X., Li, W., Williams, M., Terada, N., Alessi, D. R., Proud, C. G., Regulation of elongation factor 2 kinase by p90(RSK1) and p70 S6 kinase, *EMBO J*, 20, 16, 4370-9, **2001**.
- [42] Parmer, T. G., Ward, M. D., Yurkow, E. J., Vyas, V. H., Kearney, T. J., Hait, W. N., Activity and regulation by growth factors of calmodulin-dependent protein kinase III (elongation factor 2-kinase) in human breast cancer, *Br J Cancer*, 79, 1, 59-64, **1999**.
- [43] Cheng, Y., Li, H., Ren, X., Niu, T., Hait, W. N., Yang, J., Cytoprotective effect of the elongation factor-2 kinase-mediated autophagy in breast cancer cells subjected to growth factor inhibition, *PLoS One*, 5, 3, e9715, **2010**.
- [44] Wu, H., Yang, J. M., Jin, S., Zhang, H., Hait, W. N., Elongation factor-2 kinase regulates autophagy in human glioblastoma cells, *Cancer Res*, 66, 6, 3015-23, **2006**.
- [45] Riis, B., Rattan, S. I., Clark, B. F., Merrick, W. C., Eukaryotic protein elongation factors, *Trends Biochem Sci*, 15, 11, 420-4, **1990**.
- [46] Smith, E. M., Proud, C. G., cdc2–cyclin B regulates eEF2 kinase activity in a cell cycle- and amino acid-dependent manner, *The EMBO Journal*, 27, 7, 1005-1016, **2008**.

- [47] Shahbazi, R., Ozpolat, B., Ulubayram, K., Oligonucleotide-based theranostic nanoparticles in cancer therapy, *Nanomedicine (Lond)*, 11, 10, 1287-308, **2016**.
- [48] Summerton, J., Morpholino antisense oligomers: the case for an RNase H-independent structural type, *Biochim Biophys Acta*, 1489, 1, 141-58, **1999**.
- [49] Corey, D. R., Abrams, J. M., Morpholino antisense oligonucleotides: tools for investigating vertebrate development, *Genome Biol*, 2, 5, REVIEWS1015, **2001**.
- [50] Inoue, S., Patil, R., Portilla-Arias, J., Ding, H., Konda, B., Espinoza, A., Mongayt, D., Markman, J. L., Elramsisy, A., Phillips, H. W., Black, K. L., Holler, E., Ljubimova, J. Y., Nanobiopolymer for direct targeting and inhibition of EGFR expression in triple negative breast cancer, *PLoS One*, 7, 2, e31070, **2012**.
- [51] Sekhon, H. S., London, C. A., Sekhon, M., Iversen, P. L., Devi, G. R., c-MYC antisense phosphosphorodiamidate morpholino oligomer inhibits lung metastasis in a murine tumor model, *Lung Cancer*, 60, 3, 347-54, **2008**.
- [52] Fire, A., Xu, S., Montgomery, M. K., Kostas, S. A., Driver, S. E., Mello, C. C., Potent and specific genetic interference by double-stranded RNA in *Caenorhabditis elegans*, *Nature*, 391, 6669, 806-11, **1998**.
- [53] Elbashir, S. M., Harborth, J., Lendeckel, W., Yalcin, A., Weber, K., Tuschl, T., Duplexes of 21-nucleotide RNAs mediate RNA interference in cultured mammalian cells, *Nature*, 411, 6836, 494-498, **2001**.
- [54] Resnier, P., Montier, T., Mathieu, V., Benoit, J. P., Passirani, C., A review of the current status of siRNA nanomedicines in the treatment of cancer, *Biomaterials*, 34, 27, 6429-43, **2013**.
- [55] Guo, W., Chen, W., Yu, W., Huang, W., Deng, W., Small interfering RNA-based molecular therapy of cancers, *Chin J Cancer*, 32, 9, 488-93, **2013**.

- [56] Watts, J. K., Deleavey, G. F., Damha, M. J., Chemically modified siRNA: tools and applications, *Drug Discovery Today*, 13, 19-20, 842-55, **2008**.
- [57] Reischl, D., Zimmer, A., Drug delivery of siRNA therapeutics: potentials and limits of nanosystems, *Nanomedicine*, 5, 1, 8-20, **2009**.
- [58] Winter, J., Jung, S., Keller, S., Gregory, R. I., Diederichs, S., Many roads to maturity: microRNA biogenesis pathways and their regulation, *Nature Cell Biology*, 11, 3, 228-234, **2009**.
- [59] Gandhi, N. S., Tekade, R. K., Chougule, M. B., Nanocarrier mediated delivery of siRNA/miRNA in combination with chemotherapeutic agents for cancer therapy: current progress and advances, *J Control Release*, 194, 238-56, **2014**.
- [60] Cai, Y., Yu, X., Hu, S., Yu, J., A brief review on the mechanisms of miRNA regulation, *Genomics Proteomics Bioinformatics*, 7, 4, 147-54, **2009**.
- [61] Diaz, M. R., Vivas-Mejia, P. E., Nanoparticles as Drug Delivery Systems in Cancer Medicine: Emphasis on RNAi-Containing Nanoliposomes, *Pharmaceuticals (Basel)*, 6, 11, 1361-80, **2013**.
- [62] Cullen, B. R., RNAi the natural way, *Nat Genet*, 37, 11, 1163-5, **2005**.
- [63] Lee, Y., Ahn, C., Han, J., Choi, H., Kim, J., Yim, J., Lee, J., Provost, P., Radmark, O., Kim, S., Kim, V. N., The nuclear RNase III Drosha initiates microRNA processing, *Nature*, 425, 6956, 415-9, **2003**.
- [64] Zhang, H. D., Kolb, F. A., Brondani, V., Billy, E., Filipowicz, W., Human Dicer preferentially cleaves dsRNAs at their termini without a requirement for ATP, *Embo Journal*, 21, 21, 5875-5885, **2002**.
- [65] Lee, Y., Jeon, K., Lee, J. T., Kim, S., Kim, V. N., MicroRNA maturation: stepwise processing and subcellular localization, *Embo Journal*, 21, 17, 4663-4670, **2002**.
- [66] Cullen, B. R., Transcription and processing of human microRNA precursors, *Molecular Cell*, 16, 6, 861-865, **2004**.

- [67] Yi, R., Qin, Y., Macara, I. G., Cullen, B. R., Exportin-5 mediates the nuclear export of pre-microRNAs and short hairpin RNAs, *Genes & Development*, 17, 24, 3011-3016, **2003**.
- [68] Lund, E., Guttinger, S., Calado, A., Dahlberg, J. E., Kutay, U., Nuclear export of microRNA precursors, *Science*, 303, 5654, 95-98, **2004**.
- [69] Lee, Y. S., Nakahara, K., Pham, J. W., Kim, K., He, Z., Sontheimer, E. J., Carthew, R. W., Distinct roles for *Drosophila* Dicer-1 and Dicer-2 in the siRNA/miRNA silencing pathways, *Cell*, 117, 1, 69-81, **2004**.
- [70] Rao, D. D., Vorhies, J. S., Senzer, N., Nemunaitis, J., siRNA vs. shRNA: similarities and differences, *Adv Drug Deliv Rev*, 61, 9, 746-59, **2009**.
- [71] Ozpolat, B., Sood, A. K., Lopez-Berestein, G., Nanomedicine based approaches for the delivery of siRNA in cancer, *J Intern Med*, 267, 1, 44-53, **2010**.
- [72] Ozcan, G., Ozpolat, B., Coleman, R. L., Sood, A. K., Lopez-Berestein, G., Preclinical and clinical development of siRNA-based therapeutics, *Adv Drug Deliv Rev*, 87, 108-19, **2015**.
- [73] Draz, M. S., Fang, B. A., Zhang, P., Hu, Z., Gu, S., Weng, K. C., Gray, J. W., Chen, F. F., Nanoparticle-mediated systemic delivery of siRNA for treatment of cancers and viral infections, *Theranostics*, 4, 9, 872-92, **2014**.
- [74] Nayerossadat, N., Maedeh, T., Ali, P. A., Viral and nonviral delivery systems for gene delivery, *Adv Biomed Res*, 1, 27, **2012**.
- [75] Huang, Y., Liu, X., Dong, L., Liu, Z., He, X., Liu, W., Development of viral vectors for gene therapy for chronic pain, *Pain Res Treat*, 2011, 968218, **2011**.
- [76] Gardlik, R., Palffy, R., Hodosy, J., Lukacs, J., Turna, J., Celec, P., Vectors and delivery systems in gene therapy, *Med Sci Monit*, 11, 4, RA110-21, **2005**.
- [77] Katare, D. P., Aeri, V., Progress in gene therapy: A Review, *IJTPR*, 1, 33-41, **2010**.

- [78] Anson, D. S., The use of retroviral vectors for gene therapy-what are the risks? A review of retroviral pathogenesis and its relevance to retroviral vector-mediated gene delivery, *Genet Vaccines Ther*, 2, 1, 9, **2004**.
- [79] Bushman, F. D., Retroviral integration and human gene therapy, *J Clin Invest*, 117, 8, 2083-6, **2007**.
- [80] Laufs, S., Gentner, B., Nagy, K. Z., Jauch, A., Benner, A., Naundorf, S., Kuehlcke, K., Schiedlmeier, B., Ho, A. D., Zeller, W. J., Fruehauf, S., Retroviral vector integration occurs in preferred genomic targets of human bone marrow-repopulating cells, *Blood*, 101, 6, 2191-8, **2003**.
- [81] Fox, J. L., US authorities uphold suspension of SCID gene therapy, *Nat Biotechnol*, 21, 3, 217, **2003**.
- [82] Hacein-Bey-Abina, S., Von Kalle, C., Schmidt, M., McCormack, M. P., Wulffraat, N., Leboulch, P., Lim, A., Osborne, C. S., Pawliuk, R., Morillon, E., Sorensen, R., Forster, A., Fraser, P., Cohen, J. I., de Saint Basile, G., Alexander, I., Wintergerst, U., Frebourg, T., Aurias, A., Stoppa-Lyonnet, D., Romana, S., Radford-Weiss, I., Gross, F., Valensi, F., Delabesse, E., Macintyre, E., Sigaux, F., Soulier, J., Leiva, L. E., Wissler, M., Prinz, C., Rabbitts, T. H., Le Deist, F., Fischer, A., Cavazzana-Calvo, M., LMO2-associated clonal T cell proliferation in two patients after gene therapy for SCID-X1, *Science*, 302, 5644, 415-9, **2003**.
- [83] Thrasher, A. J., Gaspar, H. B., Baum, C., Modlich, U., Schambach, A., Candotti, F., Otsu, M., Sorrentino, B., Scobie, L., Cameron, E., Blyth, K., Neil, J., Abina, S. H., Cavazzana-Calvo, M., Fischer, A., Gene therapy: X-SCID transgene leukaemogenicity, *Nature*, 443, 7109, E5-6; discussion E6-7, **2006**.
- [84] Marshall, E., Gene therapy death prompts review of adenovirus vector, *Science*, 286, 5448, 2244-5, **1999**.
- [85] Raper, S. E., Chirmule, N., Lee, F. S., Wivel, N. A., Bagg, A., Gao, G. P., Wilson, J. M., Batshaw, M. L., Fatal systemic inflammatory response

- syndrome in a ornithine transcarbamylase deficient patient following adenoviral gene transfer, *Mol Genet Metab*, 80, 1-2, 148-58, **2003**.
- [86] Teramoto, S., Ishii, T., Matsuse, T., Crisis of adenoviruses in human gene therapy, *Lancet*, 355, 9218, 1911-2, **2000**.
- [87] Cideciyan, A. V., Hauswirth, W. W., Aleman, T. S., Kaushal, S., Schwartz, S. B., Boye, S. L., Windsor, E. A., Conlon, T. J., Sumaroka, A., Roman, A. J., Byrne, B. J., Jacobson, S. G., Vision 1 year after gene therapy for Leber's congenital amaurosis, *N Engl J Med*, 361, 7, 725-7, **2009**.
- [88] Balague, C., Zhou, J., Dai, Y., Alemany, R., Josepfs, S. F., Andreason, G., Hariharan, M., Sethi, E., Prokopenko, E., Jan, H. Y., Lou, Y. C., Hubert-Leslie, D., Ruiz, L., Zhang, W. W., Sustained high-level expression of full-length human factor VIII and restoration of clotting activity in hemophilic mice using a minimal adenovirus vector, *Blood*, 95, 3, 820-8, **2000**.
- [89] Trobridge, G. D., Foamy virus vectors for gene transfer, *Expert Opin Biol Ther*, 9, 11, 1427-36, **2009**.
- [90] Liu, W., Liu, Z., Liu, L., Xiao, Z., Cao, X., Cao, Z., Xue, L., Miao, L., He, X., Li, W., A novel human foamy virus mediated gene transfer of GAD67 reduces neuropathic pain following spinal cord injury, *Neurosci Lett*, 432, 1, 13-8, **2008**.
- [91] Goss, J. R., Harley, C. F., Mata, M., O'Malley, M. E., Goins, W. F., Hu, X., Glorioso, J. C., Fink, D. J., Herpes vector-mediated expression of proenkephalin reduces bone cancer pain, *Ann Neurol*, 52, 5, 662-5, **2002**.
- [92] Lachmann, R. H., Efstathiou, S., The use of herpes simplex virus-based vectors for gene delivery to the nervous system, *Mol Med Today*, 3, 9, 404-11, **1997**.
- [93] Federici, T., Kutner, R., Zhang, X. Y., Kuroda, H., Tordo, N., Boulis, N. M., Reiser, J., Comparative analysis of HIV-1-based lentiviral vectors bearing lyssavirus glycoproteins for neuronal gene transfer, *Genet Vaccines Ther*, 7, 1, **2009**.

- [94] Gomez, C. E., Najera, J. L., Krupa, M., Esteban, M., The poxvirus vectors MVA and NYVAC as gene delivery systems for vaccination against infectious diseases and cancer, *Curr Gene Ther*, 8, 2, 97-120, **2008**.
- [95] Mecsas, J., Sugden, B., Replication of plasmids derived from bovine papilloma virus type 1 and Epstein-Barr virus in cells in culture, *Annu Rev Cell Biol*, 3, 87-108, **1987**.
- [96] Kishida, T., Shin-Ya, M., Imanishi, J., Mazda, O., "Application of EBV-based artificial chromosome to genetic engineering of mammalian cells and tissues," in *IEEE International Symposium on Micro-NanoMechatronics and Human Science*, 2005, 2005, pp. 133-138: IEEE.
- [97] Audouy, S. A., de Leij, L. F., Hoekstra, D., Molema, G., In vivo characteristics of cationic liposomes as delivery vectors for gene therapy, *Pharm Res*, 19, 11, 1599-605, **2002**.
- [98] Wolff, J. A., Ludtke, J. J., Acsadi, G., Williams, P., Jani, A., Long-term persistence of plasmid DNA and foreign gene expression in mouse muscle, *Hum Mol Genet*, 1, 6, 363-9, **1992**.
- [99] Yang, N. S., Burkholder, J., Roberts, B., Martinell, B., McCabe, D., In vivo and in vitro gene transfer to mammalian somatic cells by particle bombardment, *Proc Natl Acad Sci U S A*, 87, 24, 9568-72, **1990**.
- [100] Heller, L. C., Ugen, K., Heller, R., Electroporation for targeted gene transfer, *Expert Opin Drug Deliv*, 2, 2, 255-68, **2005**.
- [101] Liu, F., Song, Y., Liu, D., Hydrodynamics-based transfection in animals by systemic administration of plasmid DNA, *Gene Ther*, 6, 7, 1258-66, **1999**.
- [102] Kim, H. J., Greenleaf, J. F., Kinnick, R. R., Bronk, J. T., Bolander, M. E., Ultrasound-mediated transfection of mammalian cells, *Hum Gene Ther*, 7, 11, 1339-46, **1996**.

- [103] Plank, C., Schillinger, U., Scherer, F., Bergemann, C., Remy, J. S., Krotz, F., Anton, M., Lausier, J., Rosenecker, J., The magnetofection method: using magnetic force to enhance gene delivery, *Biol Chem*, 384, 5, 737-47, **2003**.
- [104] Son, K. K., Tkach, D., Hall, K. J., Efficient in vivo gene delivery by the negatively charged complexes of cationic liposomes and plasmid DNA, *Biochim Biophys Acta*, 1468, 1-2, 6-10, **2000**.
- [105] Immordino, M. L., Dosio, F., Cattel, L., Stealth liposomes: review of the basic science, rationale, and clinical applications, existing and potential, *Int J Nanomedicine*, 1, 3, 297-315, **2006**.
- [106] Wolfert, M. A., Seymour, L. W., Atomic force microscopic analysis of the influence of the molecular weight of poly(L)lysine on the size of polyelectrolyte complexes formed with DNA, *Gene Ther*, 3, 3, 269-73, **1996**.
- [107] El-Aneed, A., An overview of current delivery systems in cancer gene therapy, *J Control Release*, 94, 1, 1-14, **2004**.
- [108] Wightman, L., Kircheis, R., Rossler, V., Carotta, S., Ruzicka, R., Kursa, M., Wagner, E., Different behavior of branched and linear polyethylenimine for gene delivery in vitro and in vivo, *J Gene Med*, 3, 4, 362-72, **2001**.
- [109] Tang, M. X., Szoka, F. C., The influence of polymer structure on the interactions of cationic polymers with DNA and morphology of the resulting complexes, *Gene Ther*, 4, 8, 823-32, **1997**.
- [110] Fischer, D., Bieber, T., Li, Y., Elsasser, H. P., Kissel, T., A novel non-viral vector for DNA delivery based on low molecular weight, branched polyethylenimine: effect of molecular weight on transfection efficiency and cytotoxicity, *Pharm Res*, 16, 8, 1273-9, **1999**.
- [111] Gao, X., Huang, L., Potentiation of cationic liposome-mediated gene delivery by polycations, *Biochemistry*, 35, 3, 1027-36, **1996**.

- [112] Mehier-Humbert, S., Guy, R. H., Physical methods for gene transfer: improving the kinetics of gene delivery into cells, *Adv Drug Deliv Rev*, 57, 5, 733-53, **2005**.
- [113] Guo, S., Huang, Y., Jiang, Q., Sun, Y., Deng, L., Liang, Z., Du, Q., Xing, J., Zhao, Y., Wang, P. C., Dong, A., Liang, X. J., Enhanced gene delivery and siRNA silencing by gold nanoparticles coated with charge-reversal polyelectrolyte, *ACS Nano*, 4, 9, 5505-11, **2010**.
- [114] Patil, Y., Panyam, J., Polymeric nanoparticles for siRNA delivery and gene silencing, *Int J Pharm*, 367, 1-2, 195-203, **2009**.
- [115] Lin, Q., Chen, J., Zhang, Z., Zheng, G., Lipid-based nanoparticles in the systemic delivery of siRNA, *Nanomedicine (Lond)*, 9, 1, 105-20, **2014**.
- [116] Ozpolat, B., Sood, A. K., Lopez-Berestein, G., Liposomal siRNA nanocarriers for cancer therapy, *Adv Drug Deliv Rev*, 66, 110-6, **2014**.
- [117] Akbarzadeh, A., Rezaei-Sadabady, R., Davaran, S., Joo, S. W., Zarghami, N., Hanifehpour, Y., Samiei, M., Kouhi, M., Nejati-Koshki, K., Liposome: classification, preparation, and applications, *Nanoscale Res Lett*, 8, 1, 102, **2013**.
- [118] Boisselier, E., Astruc, D., Gold nanoparticles in nanomedicine: preparations, imaging, diagnostics, therapies and toxicity, *Chem Soc Rev*, 38, 6, 1759-82, **2009**.
- [119] Ding, Y., Jiang, Z., Saha, K., Kim, C. S., Kim, S. T., Landis, R. F., Rotello, V. M., Gold nanoparticles for nucleic acid delivery, *Mol Ther*, 22, 6, 1075-83, **2014**.
- [120] Sykes, E. A., Chen, J., Zheng, G., Chan, W. C., Investigating the impact of nanoparticle size on active and passive tumor targeting efficiency, *ACS Nano*, 8, 6, 5696-706, **2014**.

- [121] Giljohann, D. A., Seferos, D. S., Prigodich, A. E., Patel, P. C., Mirkin, C. A., Gene regulation with polyvalent siRNA-nanoparticle conjugates, *J Am Chem Soc*, 131, 6, 2072-3, **2009**.
- [122] Guo, S. T., Huang, Y. Y., Jiang, Q. A., Sun, Y., Deng, L. D., Liang, Z. C., Du, Q. A., Xing, J. F., Zhao, Y. L., Wang, P. C., Dong, A. J., Liang, X. J., Enhanced Gene Delivery and siRNA Silencing by Gold Nanoparticles Coated with Charge-Reversal Polyelectrolyte, *Acs Nano*, 4, 9, 5505-5511, **2010**.
- [123] Elbakry, A., Zaky, A., Liebk, R., Rachel, R., Goepferich, A., Breunig, M., Layer-by-Layer Assembled Gold Nanoparticles for siRNA Delivery, *Nano Letters*, 9, 5, 2059-2064, **2009**.
- [124] Song, W. J., Du, J. Z., Sun, T. M., Zhang, P. Z., Wang, J., Gold Nanoparticles Capped with Polyethyleneimine for Enhanced siRNA Delivery, *Small*, 6, 2, 239-246, **2010**.
- [125] Turkevich, J., Stevenson, P. C., Hillier, J., A Study of the Nucleation and Growth Processes in the Synthesis of Colloidal Gold, *Discussions of the Faraday Society*, 11, 55-75, **1951**.
- [126] Frens, G., Controlled Nucleation for Regulation of Particle-Size in Monodisperse Gold Suspensions, *Nature-Physical Science*, 241, 105, 20-22, **1973**.
- [127] Perrault, S. D., Chan, W. C. W., Synthesis and Surface Modification of Highly Monodispersed, Spherical Gold Nanoparticles of 50-200 nm, *Journal of the American Chemical Society*, 131, 47, 17042-17043, **2009**.
- [128] Demir, O., Aysit, N., Onder, Z., Turkel, N., Ozturk, G., Sharrocks, A. D., Kurnaz, I. A., ETS-domain transcription factor Elk-1 mediates neuronal survival: SMN as a potential target, *Biochimica Et Biophysica Acta-Molecular Basis of Disease*, 1812, 6, 652-662, **2011**.
- [129] MRSEC Education Group. Nucleation and Growth Mechanism of Gold Nanoparticles. <http://education.mrsec.wisc.edu/277.htm> (December, **2016**).

- [130] Han, L., Zhao, J., Zhang, X., Cao, W. P., Hu, X. X., Zou, G. Z., Duan, X. L., Liang, X. J., Enhanced siRNA Delivery and Silencing Gold-Chitosan Nanosystem with Surface Charge-Reversal Polymer Assembly and Good Biocompatibility, *Acs Nano*, 6, 8, 7340-7351, **2012**.
- [131] Bogdanov, A. A., Jr., Gupta, S., Koshkina, N., Corr, S. J., Zhang, S., Curley, S. A., Han, G., Gold Nanoparticles Stabilized with MPEG-Grafted Poly(L-lysine): in Vitro and in Vivo Evaluation of a Potential Theranostic Agent, *Bioconjug Chem*, 26, 1, 39-50, **2015**.
- [132] Thomas, M., Klibanov, A. M., Conjugation to gold nanoparticles enhances polyethylenimine's transfer of plasmid DNA into mammalian cells, *Proceedings of the National Academy of Sciences of the United States of America*, 100, 16, 9138-9143, **2003**.
- [133] Mohammed, F. S., Cole, S. R., Kitchens, C. L., Synthesis and Enhanced Colloidal Stability of Cationic Gold Nanoparticles using Polyethyleneimine and Carbon Dioxide, *Acs Sustainable Chemistry & Engineering*, 1, 7, 826-832, **2013**.
- [134] Hu, C., Peng, Q., Chen, F. J., Zhong, Z. L., Zhuo, R. X., Low Molecular Weight Polyethyleneimine Conjugated Gold Nanoparticles as Efficient Gene Vectors, *Bioconjug Chem*, 21, 5, 836-843, **2010**.
- [135] Sharma, A., Tandon, A., Tovey, J. C. K., Gupta, R., Robertson, J. D., Fortune, J. A., Klibanov, A. M., Cowden, J. W., Rieger, F. G., Mohan, R. R., Polyethyleneimine-conjugated gold nanoparticles: Gene transfer potential and low toxicity in the cornea, *Nanomedicine-Nanotechnology Biology and Medicine*, 7, 4, 505-513, **2011**.
- [136] Chithrani, B. D., Chan, W. C. W., Elucidating the Mechanism of Cellular Uptake and Removal of Protein-Coated Gold Nanoparticles of Different Sizes and Shapes, *Nano Letters*, 7, 6, 1542-1550, **2007**.
- [137] Sakhtianchi, R., Minchin, R. F., Lee, K.-B., Alkilany, A. M., Serpooshan, V., Mahmoudi, M., Exocytosis of nanoparticles from cells: Role in cellular

- retention and toxicity, *Advances in Colloid and Interface Science*, 201–202, 18-29, **2013**.
- [138] Oh, N., Park, J. H., Endocytosis and exocytosis of nanoparticles in mammalian cells, *Int J Nanomedicine*, 9 Suppl 1, 51-63, **2014**.
- [139] Alkilany, A. M., Murphy, C. J., Toxicity and cellular uptake of gold nanoparticles: what we have learned so far?, *Journal of Nanoparticle Research*, 12, 7, 2313-2333, **2010**.
- [140] Connor, E. E., Mwamuka, J., Gole, A., Murphy, C. J., Wyatt, M. D., Gold nanoparticles are taken up by human cells but do not cause acute cytotoxicity, *Small*, 1, 3, 325-7, **2005**.
- [141] Shukla, R., Bansal, V., Chaudhary, M., Basu, A., Bhonde, R. R., Sastry, M., Biocompatibility of gold nanoparticles and their endocytotic fate inside the cellular compartment: a microscopic overview, *Langmuir*, 21, 23, 10644-54, **2005**.
- [142] Villiers, C., Freitas, H., Couderc, R., Villiers, M. B., Marche, P., Analysis of the toxicity of gold nano particles on the immune system: effect on dendritic cell functions, *J Nanopart Res*, 12, 1, 55-60, **2010**.
- [143] Coradeghini, R., Gioria, S., García, C. P., Nativo, P., Franchini, F., Gilliland, D., Ponti, J., Rossi, F., Size-dependent toxicity and cell interaction mechanisms of gold nanoparticles on mouse fibroblasts, *Toxicology Letters*, 217, 3, 205-216, **2013**.
- [144] Li, S., Wang, Y., Zhang, J., Yang, W. H., Dai, Z. H., Zhu, W., Yu, X. Q., Biodegradable cross-linked poly(amino alcohol esters) based on LMW PEI for gene delivery, *Mol Biosyst*, 7, 4, 1254-62, **2011**.
- [145] Xie, Q., Xinyong, G., Xianjin, C., Yayu, W., PEI/DNA formation affects transient gene expression in suspension Chinese hamster ovary cells via a one-step transfection process, *Cytotechnology*, 65, 2, 263-71, **2013**.

- [146] Gao, H., Shi, W., Freund, L. B., Mechanics of receptor-mediated endocytosis, *Proc Natl Acad Sci U S A*, 102, 27, 9469-74, **2005**.
- [147] Shahbazi, R., Ozcicek, I., Ozturk, G., Ulubayram, K., Functionalized gold nanoparticles manifested as potent carriers for nucleolar targeting, *Nanotechnology*, 28, 2, 025103, **2017**.
- [148] Klein, S., Petersen, S., Taylor, U., Rath, D., Barcikowski, S., Quantitative visualization of colloidal and intracellular gold nanoparticles by confocal microscopy, *J Biomed Opt*, 15, 3, 036015, **2010**.
- [149] Huang, K. Y., Ma, H. L., Liu, J., Huo, S. D., Kumar, A., Wei, T., Zhang, X., Jin, S. B., Gan, Y. L., Wang, P. C., He, S. T., Zhang, X. N., Liang, X. J., Size-Dependent Localization and Penetration of Ultrasmall Gold Nanoparticles in Cancer Cells, Multicellular Spheroids, and Tumors in Vivo, *Acs Nano*, 6, 5, 4483-4493, **2012**.
- [150] Dib-Hajj, S. D., Choi, J. S., Macala, L. J., Tyrrell, L., Black, J. A., Cummins, T. R., Waxman, S. G., Transfection of rat or mouse neurons by biolistics or electroporation, *Nature Protocols*, 4, 8, 1118-1127, **2009**.
- [151] Grosse, S., Thevenot, G., Monsigny, M., Fajac, I., Which mechanism for nuclear import of plasmid DNA complexed with polyethylenimine derivatives?, *Journal of Gene Medicine*, 8, 7, 845-51, **2006**.
- [152] Godbey, W. T., Wu, K. K., Mikos, A. G., Tracking the intracellular path of poly(ethylenimine)/DNA complexes for gene delivery, *Proc Natl Acad Sci U S A*, 96, 9, 5177-81, **1999**.
- [153] Grandinetti, G., Reineke, T. M., Exploring the mechanism of plasmid DNA nuclear internalization with polymer-based vehicles, *Mol Pharm*, 9, 8, 2256-67, **2012**.
- [154] Modra, K., Dai, S., Zhang, H., Shi, B. Y., Bi, J. X., Polycation-mediated gene delivery: Challenges and considerations for the process of plasmid DNA transfection, *Engineering in Life Sciences*, 15, 5, 489-498, **2015**.

- [155] Ciganda, M., Williams, N., Eukaryotic 5S rRNA biogenesis, *Wiley Interdiscip Rev RNA*, 2, 4, 523-33, **2011**.
- [156] Moghimi, S. M., Symonds, P., Murray, J. C., Hunter, A. C., Debska, G., Szewczyk, A., A two-stage poly(ethylenimine)-mediated cytotoxicity: implications for gene transfer/therapy, *Mol Ther*, 11, 6, 990-995, **2005**.
- [157] De Jong, W. H., Hagens, W. I., Krystek, P., Burger, M. C., Sips, A. J., Geertsma, R. E., Particle size-dependent organ distribution of gold nanoparticles after intravenous administration, *Biomaterials*, 29, 12, 1912-9, **2008**.
- [158] Longmire, M., Choyke, P. L., Kobayashi, H., Clearance properties of nano-sized particles and molecules as imaging agents: considerations and caveats, *Nanomedicine (Lond)*, 3, 5, 703-17, **2008**.
- [159] Blanco, E., Shen, H., Ferrari, M., Principles of nanoparticle design for overcoming biological barriers to drug delivery, *Nat Biotechnol*, 33, 9, 941-51, **2015**.
- [160] Irby, R. B., Yeatman, T. J., Role of Src expression and activation in human cancer, *Oncogene*, 19, 49, 5636-42, **2000**.
- [161] Samatar, A. A., Poulidakos, P. I., Targeting RAS-ERK signalling in cancer: promises and challenges, *Nat Rev Drug Discov*, 13, 12, 928-942, **2014**.
- [162] Hong, B., Li, H., Zhang, M., Xu, J., Lu, Y., Zheng, Y., Qian, J., Chang, J. T., Yang, J., Yi, Q., p38 MAPK inhibits breast cancer metastasis through regulation of stromal expansion, *International Journal of Cancer*, 136, 1, 34-43, **2015**.

CURRICULUM VITAE

Credentials

Name, Surname : Reza SHAHBAZI
Place of birth : Iran
Marital status : Married
E-mail : reza_dr2006@yahoo.com
Address : Department of Nanotechnology and Nanomedicine,
Hacettepe University, Beytepe, Ankara, Turkey

Education

BSc. : Veterinary Laboratory Science, Tabriz University
MSc. : Department of Nanotechnology, University of Anatolia
Ph.D. : Department of Nanotechnology and Nanomedicine,
Hacettepe University

Foreign Languages : Fluent in English and Turkish

Work Experience : Research assistant at Department of Basic
Pharmaceutical Sciences, Hacettepe University

Areas of Experiences : Gene delivery, Nanomedicine, Cancer therapy,
Nanoparticles, oligonucleotide based
Nanotherapeutics, Nanobiomaterials

Projects and Budgets :

Thesis Related Publications

R. Shahbazi, I. Ozcicek, G. Ozturk, and K. Ulubayram, "Functionalized gold nanoparticles manifested as potent carriers for nucleolar targeting," *Nanotechnology*, vol. 28, no. 2, p. 025103, 2017.

R. Shahbazi, B. Ozpolat, and K. Ulubayram, "Oligonucleotide-based theranostic nanoparticles in cancer therapy," *Nanomedicine (Lond)*, vol. 11, no. 10, pp. 1287-308, 2016.

Thesis Related Oral and Poster Presentations

R. Shahbazi, I. Ozcicek, G. Ozturk, and K. Ulubayram, "Gold Nanoparticles Delivery to Cell Nucleolus: The Importance of Surface Coating," BIOMED, Oral presentation, 22-24 October, Antalya, Turkey, 2015.



HACETTEPE UNIVERSITY
GRADUATE SCHOOL OF SCIENCE AND ENGINEERING
THESIS/DISSERTATION ORIGINALITY REPORT

HACETTEPE UNIVERSITY
GRADUATE SCHOOL OF SCIENCE AND ENGINEERING
TO THE DEPARTMENT OF NANOTECHNOLOGY AND NANOMEDICINE

Date: 06/02/2017

Thesis Title / Topic: Development of a Gene-Knockdown Approach Based on siRNA/Gold Nanoparticles for Breast Cancer Therapy

According to the originality report obtained by myself/my thesis advisor by using the *Turnitin* plagiarism detection software and by applying the filtering options stated below on 06/02/2017 for the total of 99 pages including the a) Title Page, b) Introduction, c) Main Chapters, d) Conclusion and e) Bibliography sections of my thesis entitled as above, the similarity index of my thesis is 20 %.

Filtering options applied:

1. Bibliography/Works Cited excluded
2. Quotes included
3. Match size up to 5 words excluded

I declare that I have carefully read Hacettepe University Graduate School of Science and Engineering Guidelines for Obtaining and Using Thesis Originality Reports; that according to the maximum similarity index values specified in the Guidelines, my thesis does not include any form of plagiarism; that in any future detection of possible infringement of the regulations I accept all legal responsibility; and that all the information I have provided is correct to the best of my knowledge.

I respectfully submit this for approval.

06/02/2017
Date and Signature

Name Surname: Reza SHAHBAZI
Student No: N12240517
Department: Nanotechnology and Nanomedicine
Program: Nanotechnology and Nanomedicine
Status: Masters Ph.D. Integrated Ph.D.

ADVISOR APPROVAL

APPROVED

Prof. Dr. Kezban ULUBAYRAM

(Title, Name Surname, Signature)